C.1

STEP TRANSFORM PULSE COMPRESSION AND ITS APPLICATION TO SYNTHETIC APERTURE RADAR SYSTEMS

by

MARK WILLIAM SACK

B.Sc., Electrical Engineering, Queen's University, 1978

A THESIS SUBMITTED IN PARTIAL FULFILMENT OF

THE REQUIREMENTS FOR THE DEGREE OF

MASTER OF APPLIED SCIENCE

in

THE FACULTY OF GRADUATE STUDIES

(Department Of Electrical Engineering)

We accept this thesis as conforming

to the required standard

THE UNIVERSITY OF BRITISH COLUMBIA

April 1983

In presenting this thesis in partial fulfilment of the requirements for an advanced degree at the University of British Columbia, I agree that the Library shall make it freely available for reference and study. I further agree that permission for extensive copying of this thesis for scholarly purposes may be granted by the head of my department or by his or her representatives. It is understood that copying or publication of this thesis for financial gain shall not be allowed without my written permission.

Department of ELECTRICAL ENGINEERING

The University of British Columbia
1956 Main Mall
Vancouver, Canada
V6T 1Y3

Date April 26/83

Abstract

Step transform pulse compression is a matched filtering technique applicable to linear FM signals. A mathematical analysis of the method is developed and its application to the azimuth processing of synthetic aperture radar (SAR) target returns is explored. In particular, several satellite-borne SAR systems are used as examples to compare the performance of this technique to other approaches. Problems peculiar to SAR azimuth processing including FM rate error, range cell migration, and multilook processing are considered. The computation rates, memory requirements, and complexity of the processing algorithms are also evaluated.

The step transform is studied analytically to determine how appropriate choices of processing parameters can be made to achieve acceptable image quality, while minimizing the hardware requirements. A method of range cell migration correction, which can be integrated into the step transform process, is proposed and the corresponding parameter restrictions are derived. The hardware requirements of the step transform for SAR applications, relative to some other pulse compression techniques, are shown to be less dependent on SAR system parameters and more dependent on the step transform processing parameters chosen. A computer simulation program was written to confirm the analytical results.

Table of Contents

List of Tables

List of Figures

Acknowledgement

I would like to thank Dr. M. R. Ito for providing much guidance and encouragement throughout the course of this research. I would also like to thank the people at MacDonald, Dettwiler, and Associates for providing the detailed information on SAR systems and research in the area, much of which is not available in published literature. In particular, the assistance of Dr. Ian Cumming, in reviewing drafts of this paper and providing useful suggestions to improve it, is very much appreciated.

I gratefully acknowledge the financial support of the Natural Sciences and Engineering Research Council in the form of a Postgraduate Scholarship. I also acknowledge the financial assistance of a Teaching Assistantship from the University of British Columbia.

I. INTRODUCTION

The step transform [28] is a technique for pulse compression[1] of linear FM waveforms. It has important applications in radar signal processing where pulse compression techniques are used to achieve the full resolution inherent in the signal. The linear FM or "chirp" signal is in common use in radar systems because it is easy to generate, provides both good resolution and high energy, and is easy to process [31]. In particular, synthetic aperture radar (SAR) signals have a Doppler history which is a linear FM waveform in the azimuth direction. This fact is determined by the physical properties of SAR systems, and so all SAR systems require some form of linear FM pulse compression.

The step transform technique of pulse compression is based on the concept of spectral analysis. In essence, the linear FM signal to be compressed (target return) is multiplied by a reference signal with the same FM rate but opposite slope. The product is a constant frequency signal whose frequency is dependent on the relative positions of the reference and target return signals. A Fourier transform of the product resolves the target return data into the final output image. (Spectral analysis is described in greater detail in Chapter II.)

The step transform is a refinement of this technique which uses a series of short reference ramps. The product is a series

---

[1] Pulse compression is equivalent to matched filtering in radar terminology.

of constant frequency signals of increasing frequency, which are each resolved using an initial Fourier transform whose duration is the same as the short ramp. The output data of these coarse resolution transforms is then reordered and applied to a second fine resolution transform which achieves the full resolution inherent in the signal.

1.1 Objectives

The objective of this thesis is to analyze the step transform method of pulse compression and understand more fully its properties, limitations, and applicability to signal processing problems. Its application to the azimuth processing of SAR signals is of interest and will be examined in detail. Satellite SAR systems present some particularly challenging problems in signal processing and will be the prime application area focussed on. Memory requirements, computation requirements, and control complexity will be examined. Methods of dealing with particular SAR problems such as range cell migration and multi-look processing are described. The effect of errors in the estimation of the FM rate is also examined. An analysis of the performance of the step transform relative to other techniques is presented.

1.2 Structure Of The Thesis

The approach used in the study of the step transform was to develop a basic mathematical understanding of the technique. The concepts demonstrated in this theoretical framework were used to write a computer simulation program which could perform step transform processing on a linear FM signal. At the same time, a basic understanding of SAR systems was developed. The final stage of the research was to examine how the step transform would be used in the SAR azimuth processing problem and to examine its performance relative to some other approaches. Thus, the various issues related to the thesis topic will be addressed in the following manner.

Chapter II describes the commonly used techniques for linear FM pulse compression as applied to azimuth SAR processing, including time-domain convolution, fast convolution, and spectral analysis. Their strengths and weaknesses and common areas of application are discussed. Spectral analysis is presented in some detail.

Chapter III describes the step transform in detail. A mathematical analysis is performed to determine the form of the output for a single point target. Some considerations for choosing the various processing parameters are discussed. In particular, it is shown how aliasing of adjacent targets at the same frequency is prevented by a proper choice of parameters.

Chapter IV examines the considerations used to choose processing parameters in greater detail. The data windows chosen to reduce sidelobe levels can have a significant effect

on the processing requirements. The properties of the windows which particularly affect the step transform technique are described and examples are given for some common windows. Formulae are derived to determine the actual computation rates required. Since most digital SAR systems require multilook processing, the effect of this requirement on the computation rates and other aspects of the step transform is also examined. Finally, a comparison is made between the step transform and bandpass filter spectral analysis.

Chapter V presents the major details of SAR azimuth processing which will allow us to visualize how the step transform fits into this application. The format of the SAR azimuth signal is presented. The effect of the antenna profile on processing of the signal is discussed. The basic formulae which determine the FM rate of the signal and the extent of range cell migration are presented. A simulation program, written to perform the pulse compression operation on a single line of target return data using the step transform, is described.

Chapter VI specifically considers two problems related to the azimuth processing of SAR signals using the step transform, FM rate error and range cell migration. Basic theoretical analysis is supported by results obtained using system parameters for several different SAR systems. The effect of FM rate errors on the image quality is analyzed and simulation results are presented. The ease with which range cell migration corrections are performed is determined largely by the azimuth

pulse compression technique chosen. The performance of the step transform in this regard is examined.

After evaluating all of the above considerations, it will become apparent that there are certain requirements placed on the processing parameters which could potentially conflict with each other. In Chapter VII, all of these considerations are drawn together and lead us to choose processing parameters for some typical SAR systems. Computation rates and memory requirements are evaluated and compared to the equivalent requirements for some other pulse compression techniques. Finally, some comments are made about possible hardware implementations of the step transform.

Chapter VIII presents some conclusions about the strengths and limitations of step transform pulse compression and its applicability to SAR processing.

In addition, there are four appendices which present additional information. Appendix A specifies some data windows which might be used in the step transform process. Appendix B lists the various acronyms, abbreviations, and symbols used in the paper. Appendix C presents the system and processing parameters for the three SAR systems which are used as typical examples of potential step transform applications. Appendix D gives a basic functional specification of the computer simulation program.

II. SURVEY OF PULSE COMPRESSION TECHNIQUES

In this chapter, some commonly used approaches to performing pulse compression on radar signals will be described. Each will be evaluated on the basis of its applicability to the processing of SAR azimuth signals, although some have a much broader range of applications.

One of the major criteria for choosing a particular algorithm is the computation rate required and the control complexity of the algorithm. These are determined to a large extent by the parameters of the particular radar system. Typically, airborne systems have fairly modest computation requirements and do not require complicated corrections for range cell migration (RCM) effects. Therefore the processing algorithm chosen would likely not be the most efficient in terms of the number of floating point operations performed, but would possess a simple control structure.

Satellite SAR systems, on the other hand, require a large computational capacity and must have complicated correction factors applied to obtain acceptable image quality. The high computation rates mean that it may be worthwhile to implement an algorithm with a complex control structure. The gain in computational efficiency may be small on a percentage basis, but is magnified because of the scale of the system. Also, because of the various corrections which must be applied, it is likely that a sophisticated control structure will be required in any event. In particular, most satellite SAR systems require special range cell migration correction (RCMC) techniques to

correct the quadratic component of RCM (QRCM). In order to perform RCMC efficiently, it is necessary either to isolate a number of targets in the same area or to separate the azimuth signal into distinct sections. The algorithms which allow this to happen are pointed out.

Kirk [20] has presented an assessment of digital algorithms for airborne SAR systems. Bennett et al [6] and Wu [36] have considered the applicability of various pulse compression algorithms to satellite SAR processing. In the following sections, we will consider the following pulse compression techniques and their applicability to SAR azimuth processing:

1) time-domain convolution,
2) fast convolution,
3) basic spectral analysis, and
4) bandpass filter spectral analysis.

Basic spectral analysis is described in greater detail since it provides the basis for the step transform.

2.1 Time-Domain Convolution

The time-domain convolution technique is essentially a straightforward implementation of the convolution concept without any shortcuts. Thus it is the most accurate technique and exhibits a relatively simple control structure. However, the computation rate increases as $(R/\Delta)\cdot M$ where

M = the number of azimuth samples for a single point target and R/Δ = length of the input data vector.

It becomes prohibitive for large M. The algorithm also requires that RCMC be performed for each target individually. If quadratic RCMC is required, the technique becomes extremely inefficient. Computationally, time domain convolution is the most efficient algorithm for $M \leq 32$. However, the simple control structure makes it applicable for situations where $M \leq 50$.

Because of the large number of repetitive operations and inherent parallelism, time-domain convolution also becomes more attractive if a custom VLSI implementation is considered feasible. This approach was chosen by JPL for the development of satellite SAR systems with on-board processing, as described by Arens [1] and Wu [37]. Kuhler [21] and Tyree [34] assessed VLSI technologies to determine the viability of such an approach, with a major focus on CCD's.

2.2 Fast Convolution

The fast convolution technique performs the convolution operation in the frequency domain. It involves the following steps:

1) translate the input signal to the frequency domain using a Fourier transform,
2) multiply the result by a reference signal (in the frequency domain),
3) translate the result to the time domain using an inverse Fourier transform.

This technique is computationally more efficient than the time-domain method since the number of computations required in step 2 increases as $(R/\Delta)\cdot\log_2\{M\}$. The forward and reverse Fourier transforms can be performed using an FFT algorithm which requires $M\cdot\log_2\{M\}/2$ complex multiplications if M is a power of 2. The computational efficiency is increased dramatically for large M.

Quadratic RCMC can be performed more efficiently than in the time-domain method. When the input signal is translated to the frequency domain, all targets at the same slant range are aligned on top of each other in signal memory. Thus the correction for all targets at the same slant range can be performed simultaneously. It is also possible to separate out portions of the azimuth signal. Implementations of this method are described by Bennett and Cumming [4], van de Lindt [35], and Ellis [14], among others.

If the SAR processor being designed is required to perform both range and azimuth pulse compression, this technique makes it possible to perform the complete operation at once using two dimensional FFT's.

2.3 Spectral Analysis

The fundamental basis for the step transform technique is the concept of spectral analysis [24]. The spectral analysis technique of pulse compression will be considered from both a theoretical and practical viewpoint. Some of the problems and

proposed solutions will be considered.

Consider an input signal

$$s(t) = \exp\{-j\pi Kt^2\} \ , \ -T/2 \le t \le T/2.$$

Sampling at a rate $F = 1/\Delta$, the discrete form of the signal is

$$s(k) = \exp\{-j\pi K\Delta^2 k^2\}, \ k = -T/2\Delta \ . \ . \ . \ -1,0,1 \ . \ . \ . \ T/2\Delta - 1$$

and for a signal with a time delay of k_1 samples

$$s(k) = \exp\{-j\pi K\Delta^2 (k-k_1)^2\},$$

$$k = -T/2\Delta + k_1 \ . \ . \ . \ -1,0,1 \ . \ . \ . \ T/2\Delta + k_1 - 1$$

A matched filter operation is performed on this signal by performing the following computation:

$$m(r) = \sum_{k=-T/2\Delta+k_1}^{T/2\Delta+k_1-1} s(k-k_1)\, s^*(r-k)$$

$$= \sum_k s(k-k_1) \exp\{j\pi K\Delta^2 (r^2 - 2rk + k^2)$$

$$= \exp\{j\pi K\Delta^2 r^2\} \sum_k s(k-k_1) \exp\{j\pi K\Delta^2 k^2\} \exp\{-j2\pi K\Delta^2 rk\}$$

Since the objective is to detect the magnitude of the output, the phase term outside the summation can be discarded.[2] With the restriction that $T = 1/K\Delta$, the summation then represents the discrete Fourier transform of the product of the input signal and a replica with the opposite slope. Computing this product,

$$P(k) = \exp\{-j\pi K\Delta^2 (k-k_1)^2\} \exp\{j\pi K\Delta^2 k^2\}$$

$$= \exp\{-j\pi K\Delta^2 k_1 (k_1 - 2k)\}$$

Thus P(k) is a constant frequency signal and the actual

---

[2] This is not the case for the step transform, where this phase information is used to perform a second stage of processing.

frequency is dependent only on the time delay, k_1, of the input signal. The above analysis suggests an equivalent method of performing the matched filtering operation would be to multiply the target return by a reference function of opposite slope (FM modulation) and then perform a DFT.[3] The major advantage of this concept is that only one FFT is required, as opposed to the fast convolution technique which requires both forward and inverse FFT's. However, spectral analysis is applicable only to linear FM signals, whereas both time-domain convolution and fast convolution can be used for other types of signal coding.

2.3.1 Reference Function Bandwidth Limitations

It is necessary to consider the effect of a finite time aperture and sampling in the time domain. A time-frequency plot of the sampled reference function is shown in Figure 1a. Due to sampling of the waveform at the pulse repetition frequency (PRF) the plot forms a sawtooth pattern with a period of F/K seconds. This leads to the question of what happens to a point target return which straddles the discontinuity as in Figure 1b. After the mixing operation, the signal to the left of the "discontinuity" has a frequency $K\Delta^2 k_1$. To the right of the discontinuity, the reference function has been shifted in time F/K seconds. Therefore

$$P(k) = s(k-k_1)\, s^*(k - 1/K\Delta)$$

---

[3] This concept is also used in the design of frequency synthesizers, as described by Darby and Hannah [12].

Figure 1 - Reference and Target Return Signal in Spectral Analysis

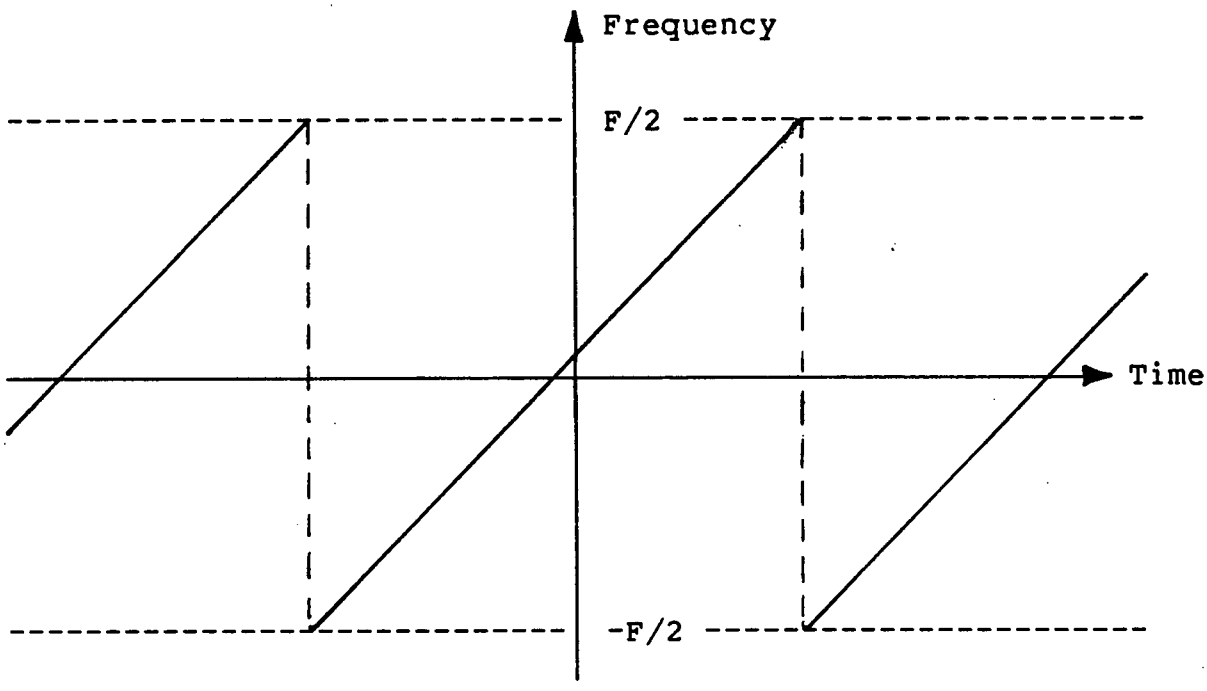

a. The Sampled Reference Function

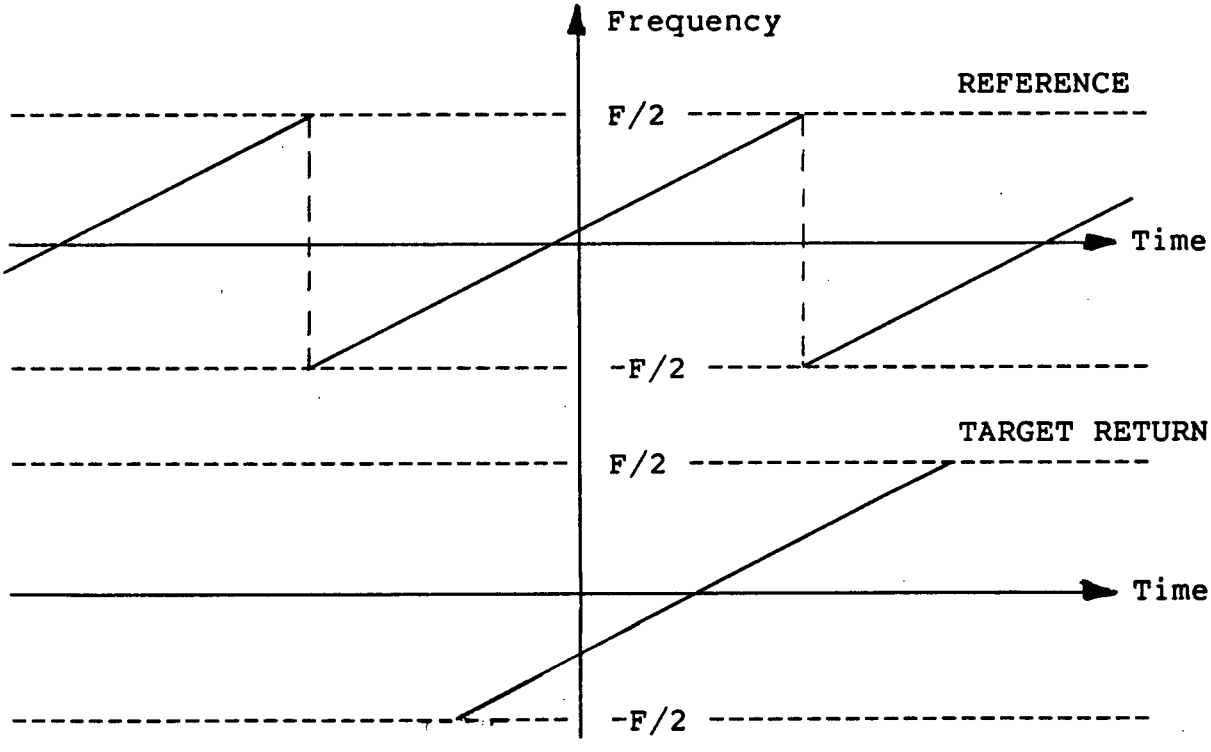

b. Target Return in Relation to Reference

$$= \exp\{-j\pi K\Delta^2(k-k_1)^2\} \exp\{j\pi K\Delta^2(k - 1/K\Delta)^2\}$$

$$= \exp\{-j\pi K\Delta^2(k_1^2 - 2kk_1 + 2k/K\Delta - 1/K^2\Delta^2)\}$$

Thus the frequency on both the left and right hand sides of the discontinuity are the same. The discontinuity is at $k = 1/2K\Delta$. The phase on the right side of the discontinuity is

$$-\pi K\Delta^2(k_1^2 + 2k/K\Delta - 1/K^2\Delta^2) = -\pi K\Delta^2 k_1^2.$$

This is exactly the phase on the left side of the discontinuity. Thus, the reference function discontinuity does not have any effect on the DFT processing, since there is no apparent discontinuity after the mixing operation.

This result can be explained by considering the addition of frequencies in the mixing operation to be done with modular arithmetic because of the sampling of the waveforms. Alternatively, one can consider the reference function to continue upward in frequency instead of taking the sawtooth pattern shown, bounded by the sampling frequency F.

In some papers on the step transform [28][29], a rudimentary description of the spectral analysis technique is given. The implication is made that the reference function must be of a finite duration of F/K seconds and, because the target return does not usually overlap exactly with the reference, there is an energy loss during the mixing operation. In fact, the above results show that the reference function does not have to be of finite duration, contradicting the assertions made in the above cited papers. There are problems, however, because of the finite length of the FFT aperture.

2.3.2 Application To SAR Azimuth Processing

The fact that the target return signal occurs only over a finite aperture imposes a more significant limitation on the basic spectral analysis approach. Adjacent targets do not occupy exactly the same aperture after the mixing operation, as shown in Figure 2. (In fact, a parallelogram-shaped processing region is formed.) As a result, using a single FFT to compress both targets results in a loss of information (if the FFT is too short) or aliasing of adjacent targets F/K seconds away (if the FFT is too long).

There are several ways of dealing with this problem. The most obvious is to simply overlap the FFT's so each target is covered significantly by at least one FFT aperture. FFT output points which contain a significant amount of energy from two different targets are rejected. Thus, a crude filtering operation is performed to prevent a significant degree of aliased energy from adjacent point targets being resolved. For the production of lower resolution images, this method works very well.

By performing this filtering operation in a more sophisticated manner, the computation rate can be reduced significantly for high resolution systems. For many SAR systems, it is also necessary to isolate small groups of targets in the same area to perform efficient range cell migration correction, as discussed in Chapter VI. For these reasons, alternatives to the basic spectral analysis approach are sought.

Figure 2 - Time-Frequency Plot After Mixing

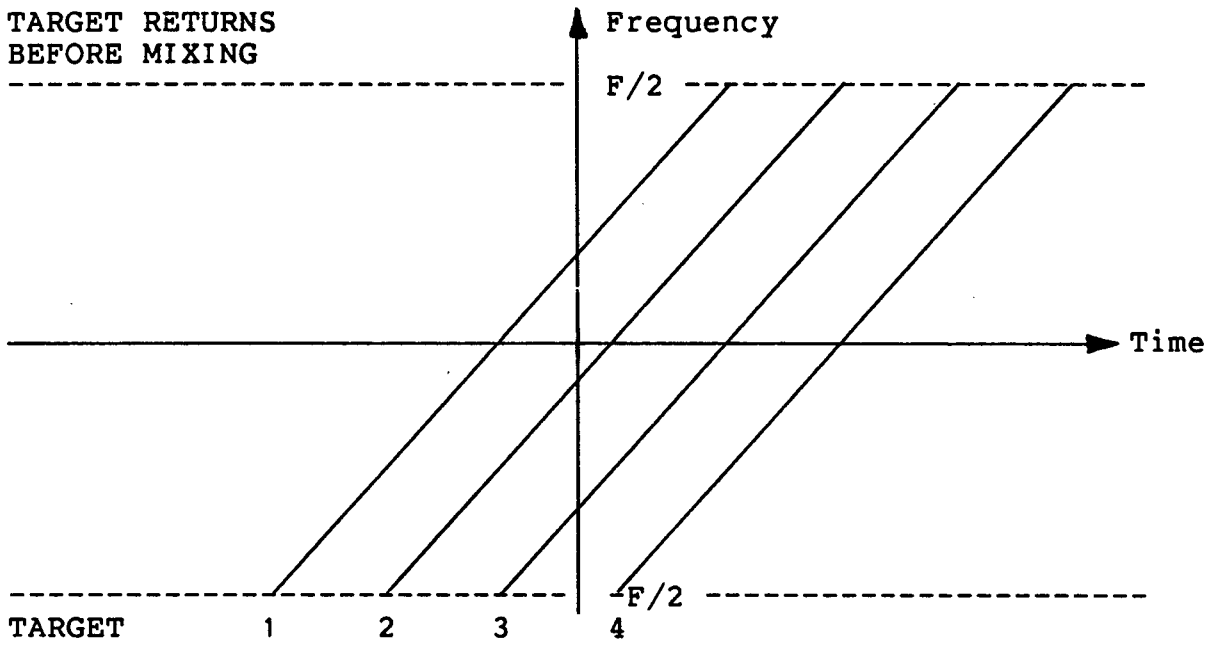

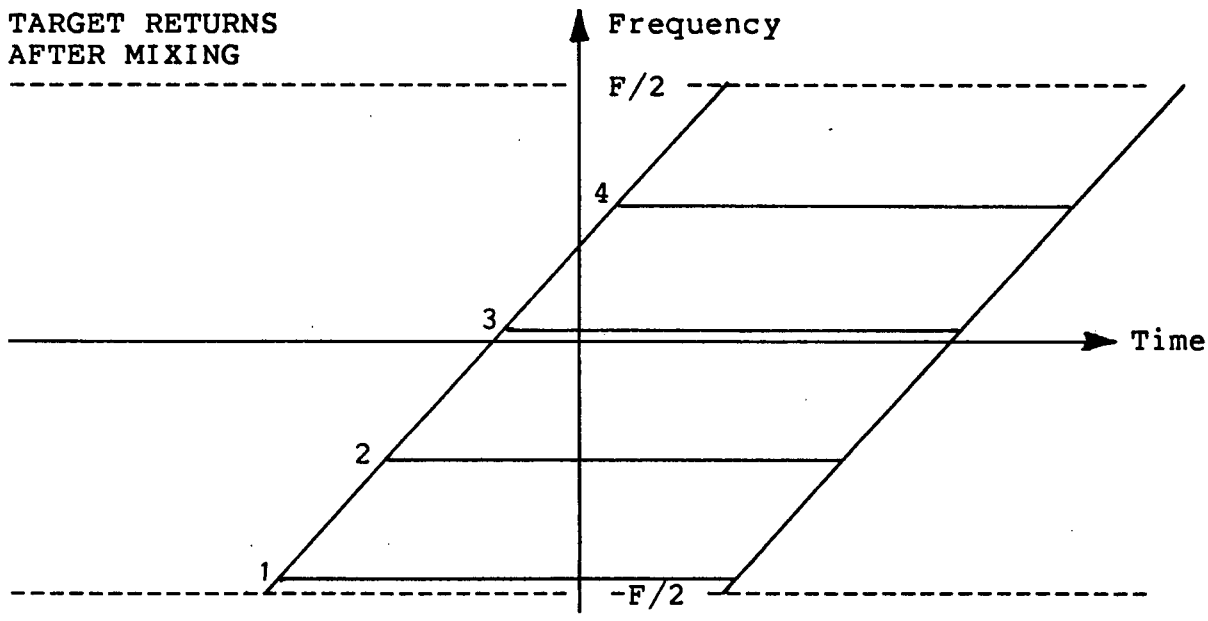

2.4 Bandpass Filter Spectral Analysis

One such alternative is to directly filter the output of the mixer into several distinct passbands, as shown in Figure 3 and described in [24]. Thus the processing region is divided up into several subregions, in each of which the energy loss or aliasing is minimized. An FFT is performed on each subregion to resolve the point targets. Since each passband is down-converted to baseband and subsampled, the number of FFT points to be processed is approximately the same as if there was no overlapping of the FFT's. The decrease in the number of FFT points largely compensates for the additional computations required to perform the bandpass filtering operation. Since each filter separates out targets in azimuth proximity to each other, it is possible to perform a single quadratic RCMC operation on a group of targets, allowing this correction to be performed efficiently. This method is called bandpass filter spectral analysis (BPF SPECAN). In succeeding chapters, some analogies will be drawn between the BPF SPECAN and step transform approaches.

Figure 3 - Bandpass Filter Spectral Analysis

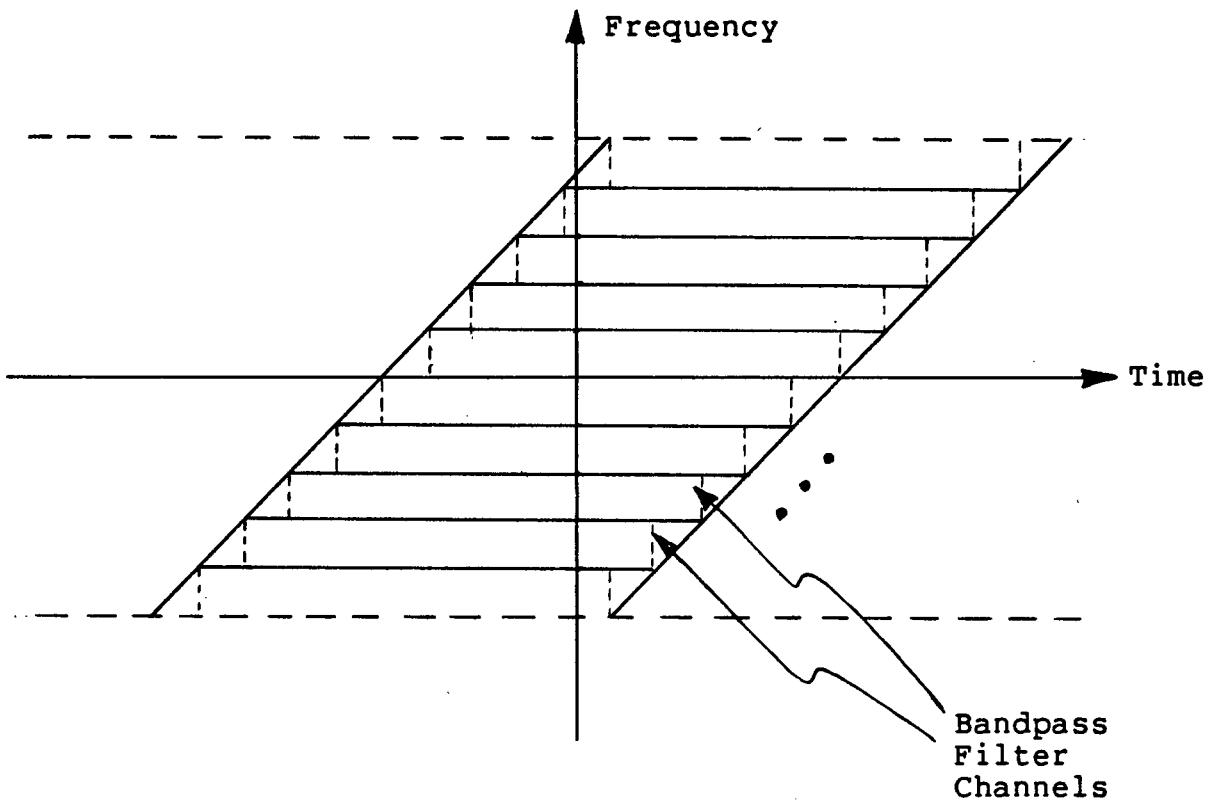

III. THE STEP TRANSFORM

In this chapter, a rigorous theoretical analysis of the step transform is presented in order to gain some insight into the fundamental limitations of the technique. This analysis is useful for any linear FM pulse compression application, not just SAR azimuth processing.

Step transform pulse compression is performed in several stages of computation and data manipulation. Initially, the target return signal is mixed with a series of short overlapping reference signals. The reference signals have the same FM rate but opposite slope to that of the target return. The time extent of each short reference signal is a coarse resolution aperture. An appropriate window function is also applied to each coarse resolution aperture to reduce the sidelobes on the FFT output. The amount of overlapping of the coarse resolution apertures is determined by the width of the mainlobe of the window function chosen. For a single point target, the data in each aperture represents a constant frequency signal. The exact frequency is dependent on the position of the point target (see Sec. 2.3) and the frequency from one aperture to the next is incremented by a constant value.

An FFT is applied to each coarse resolution aperture to compress the information from a single point target into a small number of FFT output bins. Thus, the relevant data from a single point target lies in different output bins in each successive coarse resolution FFT. The data is related by a linear phase term dependent on the target return and a quadratic

phase term dependent on the position of the short reference ramp. The quadratic phase term is removed and the data is aligned sequentially in a fine resolution aperture. This aperture now contains a constant frequency signal, the frequency of which is dependent only on the point target position. A suitable data window (to reduce sidelobes in the final output image) and FFT are applied to each fine resolution aperture. Due to overlapping of the coarse resolution apertures and possible aliasing between coarse resolution output pulses, not all of the fine resolution FFT output data is valid and, therefore, a data selection process must be included. Since the coarse resolution FFT output function is sampled at a different position for each target, it may be necessary to perform a scaling operation to produce a high quality output image.

3.1 Mathematical Analysis

Initially, the step transform will be considered strictly on a theoretical level to gain a better understanding of the mechanisms involved.[4] The target return signal is represented by the function

$$s(t) = \exp\{j(\pi B/T)t^2\}$$

and is valid over the region $-T/2 \leq t \leq T/2$. The reference signal is represented by a series of ramps of the following form:

---

[4] Preliminary portions of this derivation essentially parallel the analysis presented by Perry and Martinson [29].

$$s^*(t) = \exp\{-j(\pi B/T)t^2\} \ , \ -T'/2 \le t \le T'/2$$

The initial analysis uses only one reference ramp at position $t = n\Delta$ multiplied by a target return signal at position $t = -m\Delta$, as shown in Figure 4a.[5] The resulting expression is as follows:

$$s(t+m\Delta)\ s^*(t-n\Delta) = \exp\{j(\pi B/T)(t+m\Delta)^2\}\ \exp\{-j(\pi B/T)(t-n\Delta)^2\}$$

Let the sample interval be Δ and k be an integer sample number over the time aperture of the reference ramp, $0 \le k \le T'/\Delta - 1$. Therefore $t = k\Delta + n\Delta - T'/2$ and

$$\begin{aligned} s(t+m\Delta)\ s^*(t-n\Delta) &= s(k,m)\ s^*(k,n) \\ &= \exp\{j(\pi B/T)(k\Delta + n\Delta - T'/2 + m\Delta)^2\} \\ &\quad \cdot \exp\{-j(\pi B/T)(k\Delta + n\Delta - T'/2 - n\Delta)^2\} \\ &= \exp\{j(\pi B/T)(2k\Delta^2(m+n))\} \\ &\quad \cdot \exp\{j(\pi B/T)(m^2\Delta^2 - T'\Delta m)\} \\ &\quad \cdot \exp\{j(\pi B/T)(n^2\Delta^2 - T'\Delta n)\} \\ &\quad \cdot \exp\{j(\pi B/T)(2mn\Delta^2)\} \end{aligned}$$

The first factor, which includes the variable k, is resolved by the coarse resolution FFT applied over the time aperture of the reference ramp. This phase factor determines the frequency of the signal to be resolved by the FFT. The other phase factors are constant within the time aperture of the ramp and are dealt with at later stages of the step transform process. Therefore let

$$\phi = (\pi B/T)((m^2\Delta^2 - T'\Delta m) + (n^2\Delta^2 - T'\Delta n) + (2mn\Delta^2)) \quad (1)$$

---

[5] Figure 4 shows the target and reference signals as being parallel. In reality, the slopes are exactly opposite. The drawing is meant to illustrate that the two signals have the same FM rate.

Figure 4 - Positions of Target Return and Reference Signals

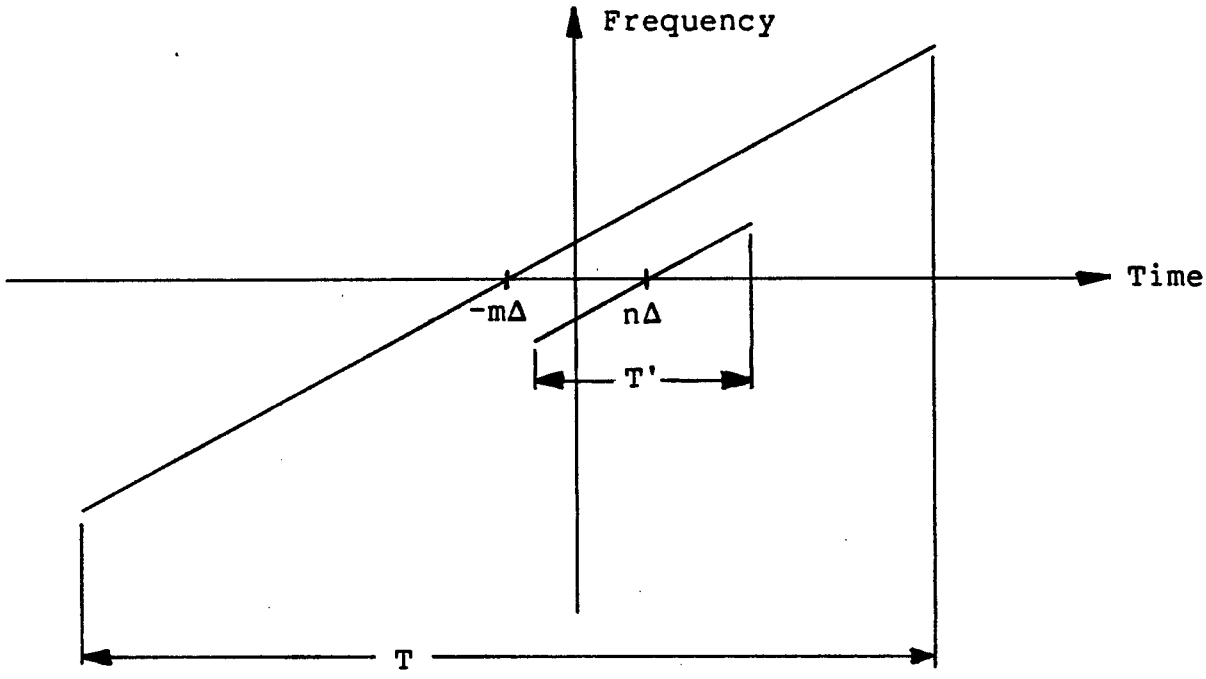

a. Target Return Signal and Reference Ramp

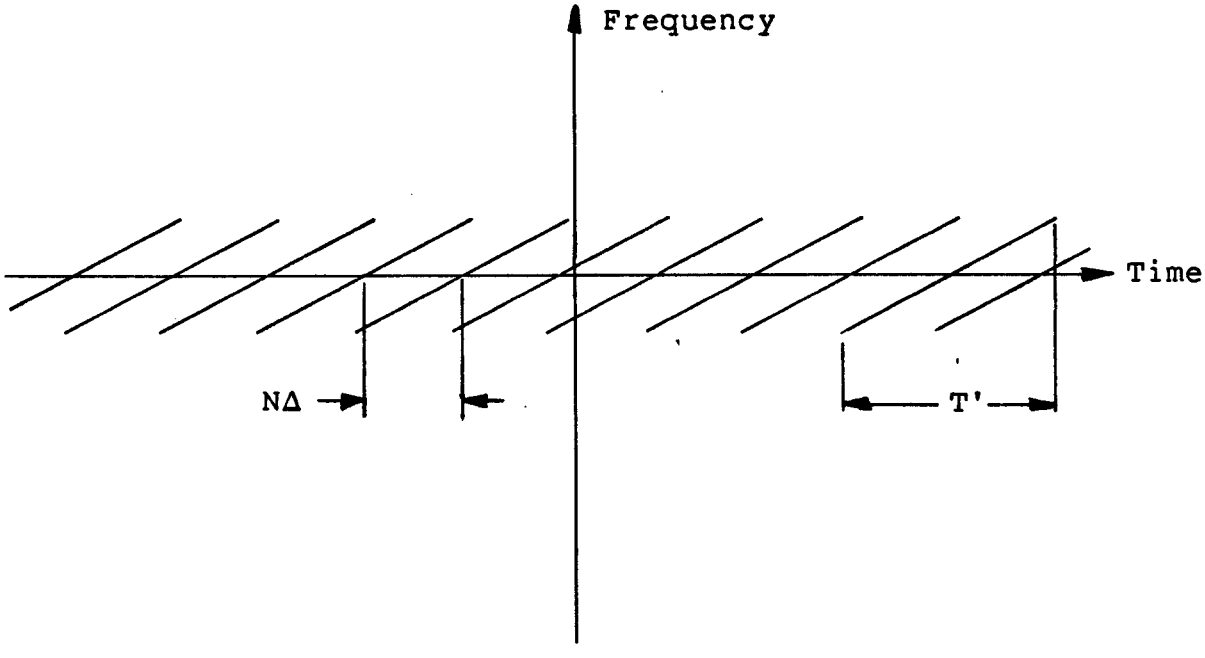

b. Multiple References Spaced at Regular Intervals

so that

$$s(k,m)\ s^*(k,n) = \exp\{j\phi\}\ \exp\{j(\pi B/T)(2k\Delta^2(m+n))\}$$

The next stage requires that an FFT of length T'/Δ be applied to the product calculated above. A data window (represented by $W_1(k)$) may also be applied to the signal to reduce sidelobes. The resulting output is a sequence of values determined as follows:

$$s(r) = \sum_{k=0}^{T'/\Delta - 1} W_1(k)\ s(k,m)\ s^*(k,n)\ \exp\{-j(2\pi\Delta/T')kr\}\ ,$$

$$r = 0\ .\ .\ .\ T'/\Delta - 1$$

In order to simplify the mathematics initially, a boxcar window will be used so that $W_1(k)=1$ for all k. Thus

$$s(r) = \exp\{j\phi\} \sum_{k=0}^{T'/\Delta - 1} \exp\{j(\pi B/T)(2k\Delta^2(m+n))\}\ \exp\{-j(2\pi\Delta/T')kr\}$$

$$= \exp\{j\phi\} \sum_{k=0}^{T'/\Delta - 1} \exp\{j2\pi k\Delta(B\Delta(m+n)/T - r/T')\}$$

Evaluating the summation using the series

$$\sum_{k=0}^{X} \exp\{jk\Theta\} = \exp\{jX\Theta/2\}\ \frac{\sin\{(X+1)\Theta/2\}}{\sin\{\Theta/2\}}\ ,\ \Theta \neq 0$$

$$= X + 1\ ,\ \Theta = 0$$

such that $X = T'/\Delta - 1$ and $\Theta = 2\pi\Delta(B\Delta(m+n)/T - r/T')$, the output of the coarse resolution FFT may be expressed as

$$s(r) = \exp\{j\phi\}\exp\{j(T'/\Delta - 1)(\pi\Delta(B\Delta(m+n)/T - r/T'))\}$$
$$\cdot \frac{\sin\{\pi T'(B\Delta(m+n)/T - r/T')\}}{\sin\{\pi\Delta(B\Delta(m+n)/T - r/T')\}}, \quad r \neq T'B\Delta(m+n)/T$$
$$= T'/\Delta, \quad r = T'B\Delta(m+n)/T$$

Thus s(r) is a pulse centred at $r = T'B\Delta(m+n)/T$. Note that for most point targets, this will not evaluate to an integer value of r.

It is now necessary to consider the processing of data from many reference ramps. The ramps are spaced $N\Delta$ time units apart at $n = N(i+a)$, $i+a = \ldots -2,-1,0,1,2, \ldots$ (Figure 4b). The variable i is used to index data within each fine resolution aperture while a denotes the coarse resolution aperture from which the first data point is picked. Substituting this formula for n, the centre position of the coarse resolution FFT output pulses may be expressed as $r = T'B\Delta(m+N(i+a))/T$. Thus the number of coefficients separating pulses in successive coarse resolution apertures is $H = BT'\Delta N/T$. This value is used to increment r when data is reordered for input to the fine resolution FFT. Since r is an integer, the increment H must also be a positive integer value or close to it to minimize undesired amplitude modulations. (Alternatively, H may be the inverse of an integer value. In that case, fine resolution aperture data would be picked from every 1/H coarse resolution apertures. The derivation for this case is presented in the next section.) Since the range of values for r is $0 \ldots T'/\Delta - 1$, the number of samples in each fine resolution

aperture is $\frac{T'/\Delta}{H} = T/B\Delta^2N$.[6] A mathematical expression for the input data to the fine resolution FFT is derived by substituting $n = N(i+a)$ and $r = iBT'\Delta N/T$ into the expression for s(r). Thus

$$B\Delta(m+n)/T - r/T' = B\Delta(m+N(i+a))/T - iBT'\Delta N/(TT')$$
$$= B\Delta(m+Na)/T$$

Leaving the ϕ phase factor alone for the moment, we see that the expression for s(r) becomes

$$s(i,a) = \exp\{j\phi\} \exp\{j(T'/\Delta - 1)(\pi\Delta^2B(m+Na)/T)\} \cdot \frac{\sin\{\pi T'B\Delta(m+Na)/T\}}{\sin\{\pi\Delta^2B(m+Na)/T\}}, \quad i = 0 \ldots (T/B\Delta^2N) - 1$$

Since the variable a is a constant over the complete fine resolution aperture, the function s(i,a) has a constant amplitude for each value of i. The phase is modified only by the factor $\exp\{j\phi\}$.

The reordering process is better understood with the help of Figure 5. In this illustration, each column represents the data output of one coarse resolution FFT. Some of the pulses for a single point target are drawn in their relative positions. The objective of the reordering process is to assemble all of the samples from the same target and with the same magnitude, as shown by the diagonal lines, in sequence. This is possible

---

[6] Perry and Martinson [29] cite an example in which the coarse resolution FFT contains 32 samples while the fine resolution FFT contains 64 samples (corresponding to 2 coarse resolution apertures). The analysis presented here suggests that such an implementation would not work very well, since there would be a distinct phase and magnitude discontinuity in the middle of the fine resolution FFT data. Further comments will be made in Sec. 4.4, where multilooking is discussed.

Figure 5 - Reordering the Data for Input to the Fine Resolution FFT

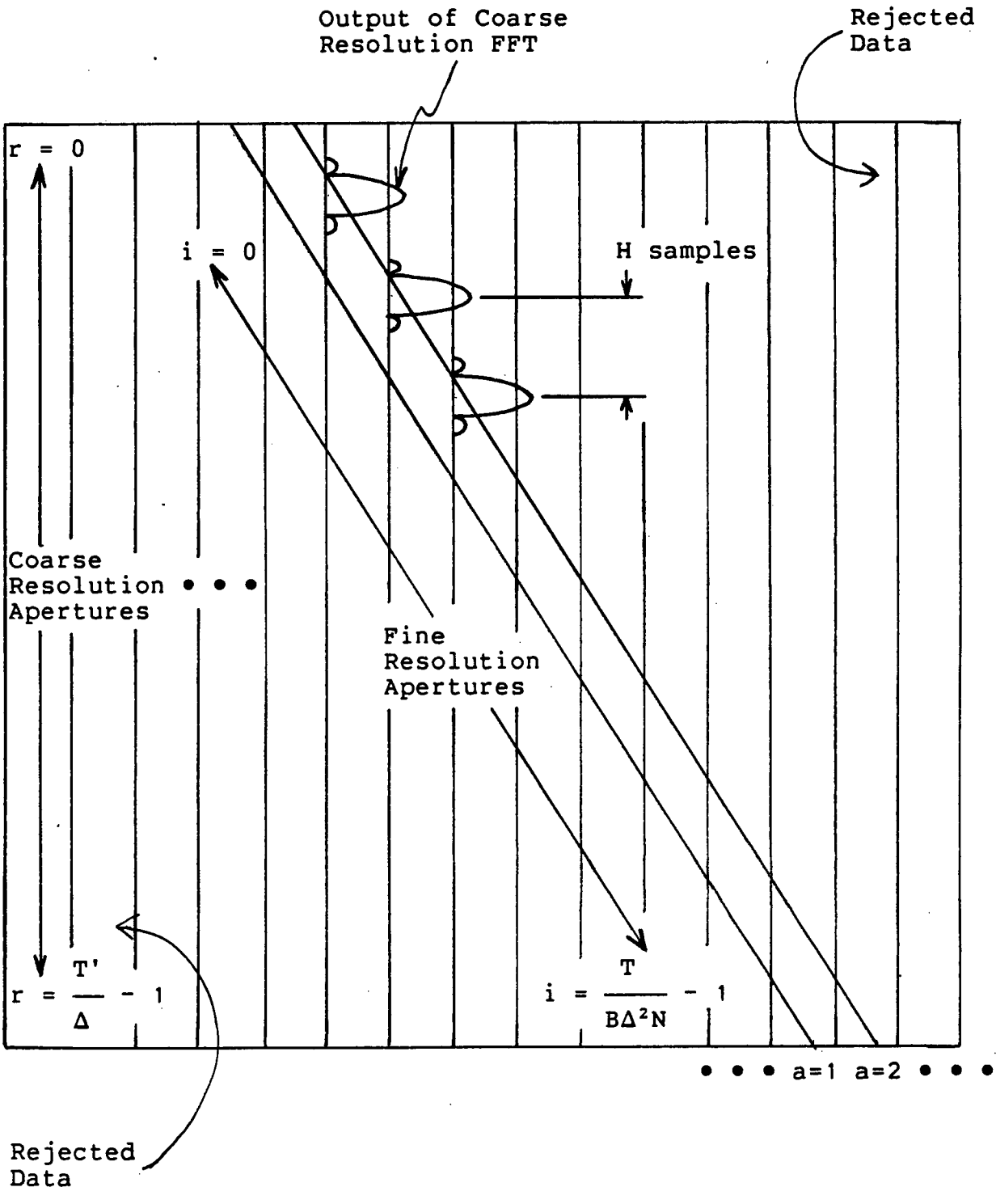

because the output of each coarse resolution FFT is exactly the same, except for an appropriate shift in frequency and phase. Note also the triangular regions of unused data at each end.

The situation where H = 1 is quite easy to visualize in terms of the processing algorithm and mathematical analysis being described. However, the situation where H > 1 is not quite so simple. In this case, the reordering process is modified so that data for H fine resolution apertures is picked from the same set of coarse resolution apertures. The range of values for i for each of the fine resolution apertures would be as follows:

1st - 0 . . . $T/B\Delta^2N - 1$

2nd - 1 . . . $T/B\Delta^2N$

. . .

. . .

. . .

Hth - H-1 . . . $T/B\Delta^2N - 2 + H$

The variable a is incremented by 1 after every Hth fine resolution aperture.

The limitation on the value of H is explained in another way by following the reasoning of Elachi et al [13] in their treatment of the step transform. A condition is imposed that the number of coarse resolution apertures over the return signal be equal to the number of frequency resolution elements in the output of the coarse resolution FFT, which cover the bandwidth of the return signal. This statement may be expressed in the following equation

$$\frac{T}{N\Delta} = \frac{T'}{\Delta} \cdot B\Delta \quad \text{or} \quad \frac{BT'\Delta N}{T} = 1$$

Note that the left-hand side of the second equation is simply H, the value used to increment r. Elachi uses the simplified case of no overlap, i.e. T' = NΔ, to conclude that T' = SQRT{T·B}. Clearly, this is in error and should read T' = SQRT{T/B}. This statement by Elachi may have been inspired by Martinson's assertion [25] that the time-bandwidth product of a single reference ramp should be approximately equal to the square root of the time-bandwidth product of the return signal, which is likely also in error.

The variable ϕ, as defined in equation (1), has three main components. The term $(\pi B/T)(2mn\Delta^2) = (\pi B/T)(2mN(i+a)\Delta^2)$ increments the phase of s(i,a) by a constant value for each succeeding term. This represents a CW signal whose frequency is dependent on m, the position of the target return signal. The fine resolution FFT resolves the information presented in this phase factor. The term $(\pi B/T)(n^2\Delta^2 - T'\Delta n)$ represents a quadratic phase factor which is dependent on n, the position of the coarse resolution aperture and is independent of point target position. It must be removed prior to processing the fine resolution FFT, to make the input to this FFT a CW signal. Note that removal of this factor can be done at any time prior to processing of the fine resolution FFT, including during the multiplication of the reference and target return signals. The term $(\pi B/T)(m^2\Delta^2 - T'\Delta m)$ represents a quadratic phase factor which is constant across all of the target return data and

therefore does not affect processing of the data. Thus the input data to the fine resolution FFT takes the following form:

$$s(i,a) = \exp\{j(\pi B/T)(2mNi\Delta^2)\} \cdot \exp\{j(\pi B/T)(\Delta^2 m)(m-1)\} \exp\{j(\pi B/T)(\Delta Na)(2m\Delta-\Delta+T')\} \cdot \frac{\sin\{(\pi B/T)(T'\Delta)(m+Na)\}}{\sin\{(\pi B/T)(\Delta^2)(m+Na)\}} \cdot \quad (2)$$

The output of the FFT is obtained by evaluating the following expression:

$$s(c,a) = \sum_{i=0}^{T/B\Delta^2N-1} W_2(i)\, s(i,a) \exp\{-j2\pi(B\Delta^2N/T)ic\}\ ,$$

$$c = 0 \ . \ . \ . \ T/B\Delta^2N - 1$$

$W_2(i)$ is a data window chosen to minimize sidelobes in the final output. For the purposes of this analysis, it is assumed that $W_2(i)=1$, i.e. a boxcar window is used. Thus,

$$s(c,a) = \exp\{j(\pi B/T)(\Delta^2 m)(m-1)\} \cdot \exp\{j(\pi B/T)(\Delta Na)(2m\Delta + T' - \Delta)\} \cdot \frac{\sin\{(\pi B/T)(T'\Delta)(m+Na)\}}{\sin\{(\pi B/T)(\Delta^2)(m+Na)\}} \cdot \sum_{i=0}^{T/B\Delta^2N-1} \exp\{j(\pi B/T)(2mNi\Delta^2)\} \exp\{-j(\pi B/T)(2Nic\Delta^2)\}$$

The summation evaluates to the following expression:

$$s(c,a) = \exp\{j\pi m\} \exp\{j(\pi B/T)(\Delta^2 m)(m-N-1)\} \cdot \exp\{j(\pi B/T)(\Delta Na)(2m\Delta + T' - \Delta)\} \cdot \frac{\sin\{(\pi B/T)(T'\Delta)(m+Na)\}}{\sin\{(\pi B/T)(\Delta^2)(m+Na)\}} \cdot \exp\{-j\pi c\}\exp\{j(\pi B/T)(cN\Delta^2)\}$$

$$\cdot \frac{\sin\{\pi(m-c)\}}{\sin\{(\pi B/T)(N\Delta^2)(m-c)\}}$$

and

$$|s(c,a)| = \frac{\sin\{(\pi B/T)(T'\Delta)(m+Na)\}}{\sin\{(\pi B/T)(\Delta^2)(m+Na)\}} \cdot \frac{\sin\{\pi(m-c)\}}{\sin\{(\pi B/T)(N\Delta^2)(m-c)\}} \qquad (3)$$

The magnitude of s(c,a) is the data from which the final output image is obtained. In order to prevent multiple images it may be necessary to reject some data. An explanation of the data selection procedure is provided in Sec. 3.4, after the need to produce this data in the first place has been justified.

Suitable data windows on the coarse and fine resolution apertures are required to produce images with sidelobes levels acceptable for most SAR applications. The first line of equation (3) would be modified according to the window chosen for the coarse resolution aperture, W_1, while the window chosen for the fine resolution aperture, W_2, would result in appropriate modifications to the second line.

3.2 Alternative Case

For the case where $H < 1$, the number of fine resolution aperture samples is T'/Δ. Substituting $n = N(i+a)/H$ and $r = i$ into the equation for s(r) and noting that $H = BT'\Delta N/T$ results in the following expression:

$$B\Delta(m+n)/T - r/T' = B\Delta(m+N(i+a)/H)/T - i/T'$$

$$= B\Delta m/T + a/T'$$

Therefore the fine resolution aperture data may be expressed as follows after removing the quadratic phase factor:

$$s(i,a) = \exp\{j(\pi B/T)(m^2\Delta^2 - T'\Delta m)\} \cdot \exp\{j(\pi B/T)(2mN(i+a)\Delta^2/H)\} \cdot \exp\{j(T'/\Delta - 1)(\pi\Delta(B\Delta m/T + a/T'))\} \cdot \frac{\sin\{\pi T'(B\Delta m/T + a/T')\}}{\sin\{\pi\Delta(B\Delta m/T + a/T')\}}$$

Applying an FFT to this data as before,

$$s(c,a) = \sum_{i=0}^{T'/\Delta - 1} W_2(i)\, s(i,a) \exp\{-j2\pi ic(\Delta/T')\}$$

Assuming $W_2(i) = 1$ for all i,

$$s(c,a) = \exp\{j(\pi B/T)(\Delta^2 m(m - 1 + 2Na/H))\} \cdot \exp\{j\pi a(1 - \Delta/T')\} \cdot \frac{\sin\{\pi T'(B\Delta m/T + a/T')\}}{\sin\{\pi\Delta(B\Delta m/T + a/T')\}} \cdot \exp\{j\pi(m - c)(1 - \Delta/T')\} \cdot \frac{\sin\{\pi(m-c)\}}{\sin\{\pi(m-c)\Delta/T'\}}$$

and

$$|s(c,a)| = \frac{\sin\{\pi T'(B\Delta m/T + a/T')\}}{\sin\{\pi\Delta(B\Delta m/T + a/T')\}} \cdot \frac{\sin\{\pi(m-c)\}}{\sin\{\pi(m-c)\Delta/T'\}}$$

This, of course, is very similar to the expression derived in the preceding section and the same comments apply. In fact, for

$H = 1$, they turn out to be identical.

The reordering process has basically been described in the previous section. The variable a is incremented by 1 for each fine resolution aperture but successive fine resolution data points are taken from every $1/H$ apertures.

3.3 The Aliasing Problem

With the above background information, it is possible to consider some of the parameter limitations in order to be able to resolve individual point targets. Again, the situations for $H < 1$ and $H \geq 1$ must be dealt with separately.

Considering the situation where $H \geq 1$ first, the magnitude of the input data to the fine resolution FFT as a function of a is determined by the data window for the coarse resolution aperture, W_1. From equation (2)

$$|s(i,a)| = \frac{\sin\{(\pi B/T)(T'\Delta)(m+Na)\}}{\sin\{(\pi B/T)(\Delta^2)(m+Na)\}}$$

for a boxcar window. The set of input data for each fine resolution FFT has a frequency determined by the phase factor $\exp\{j(\pi B/T)(2mNi\Delta^2)\}$. Consider the situation where both point targets of Figure 6 have the same frequency as seen by the fine resolution FFT, i.e.

$$(\pi B/T)(2m_1N\Delta^2) = (\pi B/T)(2m_2N\Delta^2) + 2\pi l \ , \ l = \text{any integer}$$

Since the target return information is spread over many coarse resolution apertures and the FFT does not concentrate the energy from a target into a single output coefficient, there is a

Figure 6 - Input Data to the Fine Resolution FFT for 2 Point Targets

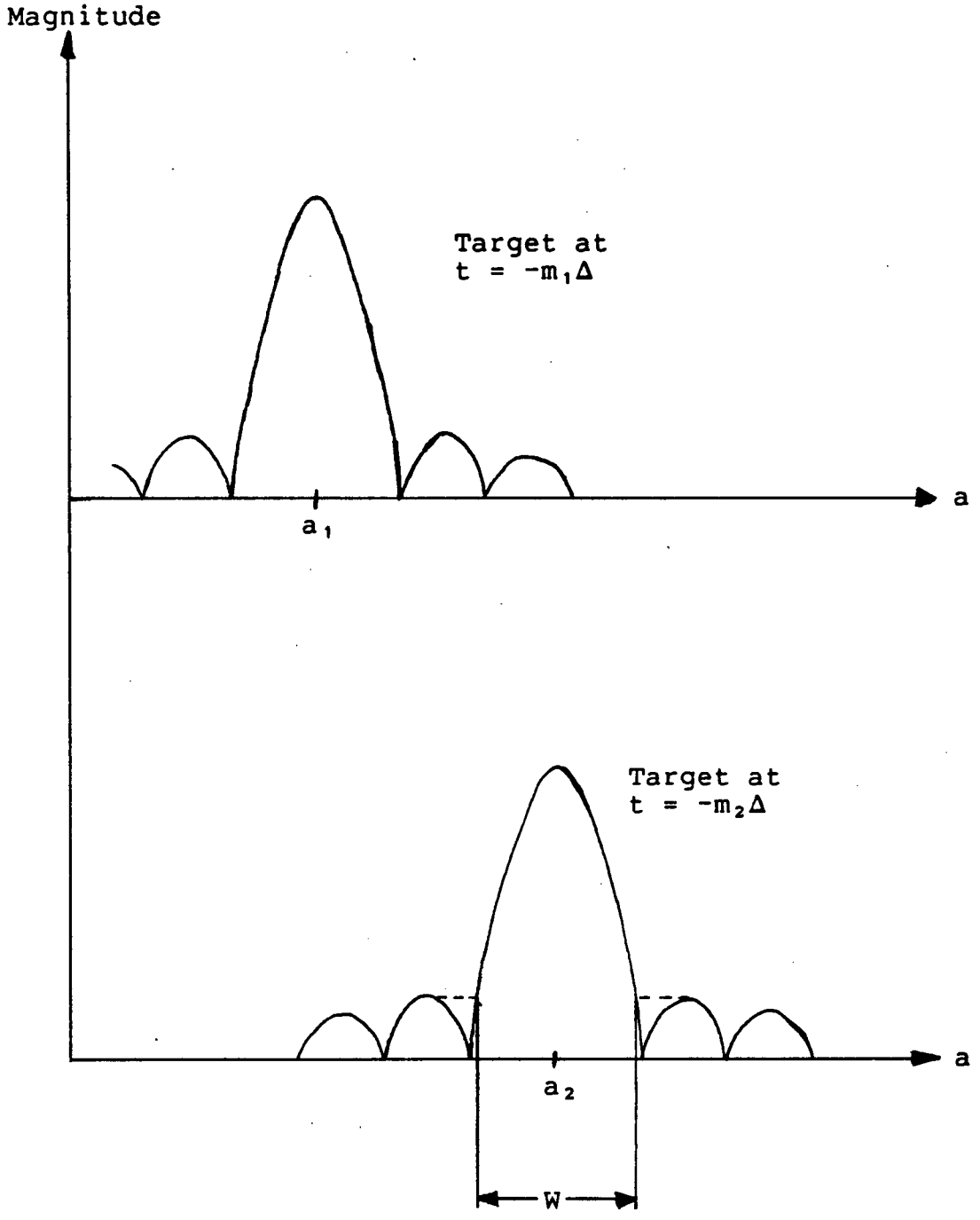

potential aliasing problem between the two targets. For the two closest such point targets l=1 and $m_1-m_2 = T/BN\Delta^2$. The number of coarse resolution apertures separating the two targets is given by

$$\begin{aligned} a_2 - a_1 &= (m_2-m_1)/N \\ &= T/BN^2\Delta^2 \\ &= (T'/N\Delta) \cdot (T/BT'\Delta N) \\ &= (T'/N\Delta) \; / \; H \\ T'/N\Delta &= (a_2 - a_1) \cdot H \end{aligned}$$

Thus the overlap ratio, $T'/N\Delta$, exactly defines the number of samples separating the coarse resolution FFT output pulses for the two targets and the number of fine resolution apertures between them.

In order to minimize this aliasing effect in processing the fine resolution aperture, processing parameters must be chosen to ensure that such interference occurs only at the sidelobe levels of the windows chosen for the coarse resolution aperture. The spacing between main lobes of potentially interfering targets can be expressed as the product $H(a_1-a_2)$ and must be kept above a certain minimum. Since $T'/\Delta N$ is directly proportional to the amount of computation required in processing the coarse resolution apertures, it is desirable to minimize this value. A critical parameter in determining the minimum permissible value of $T'/\Delta N$ is the width, W, of the main lobe of the window chosen for the coarse resolution aperture. Consider the three situations depicted in Figure 7. The image quality which can be gained by using a main lobe separation as shown in

Figure 7 - Spacing of Data Input to Fine Resolution FFT

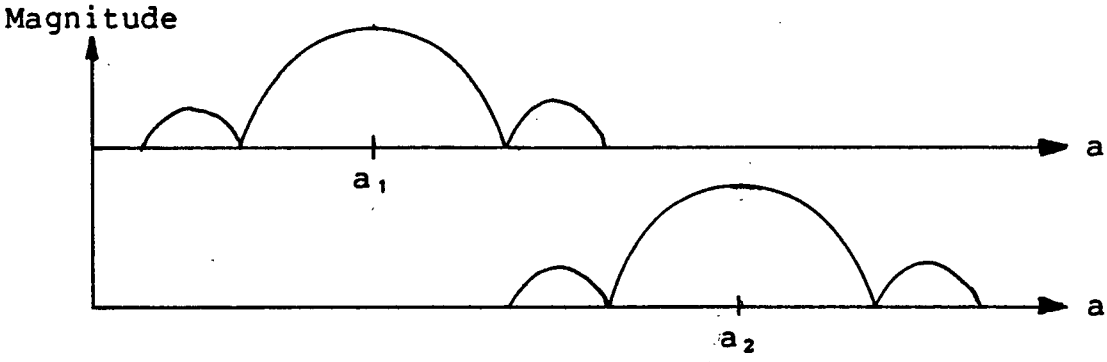

a. Interference at Sidelobe Levels Only

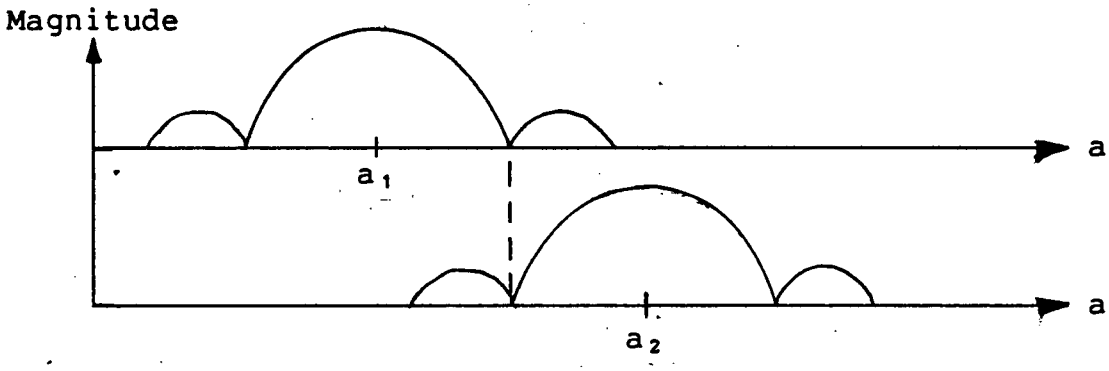

b. Borderline Interference in Main Lobe

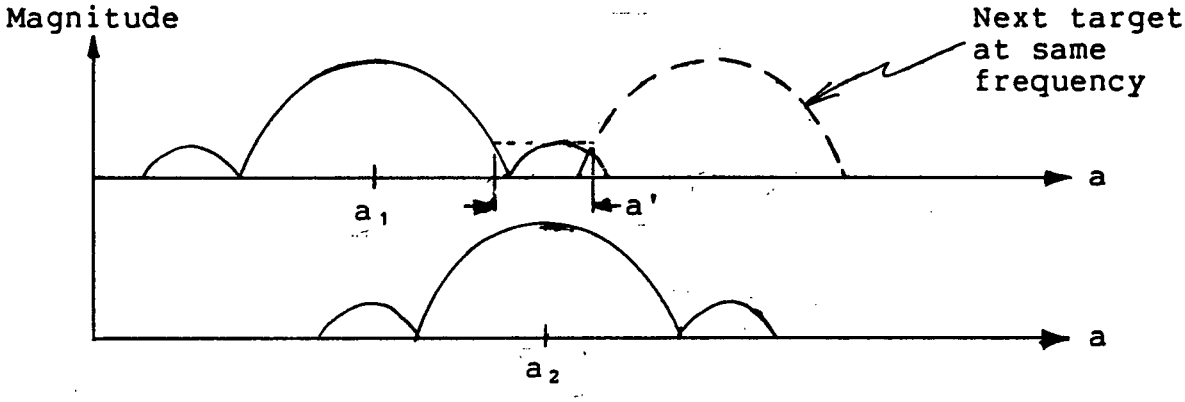

c. Definite Interference in Main Lobe

Figure 7a is minimal. This is especially true for windows with constant sidelobe levels, eg. Dolph-Chebyshev. It is actually permissible to allow some interference of the main lobes as long as the dimension $a' \geq 1$ (Figure 7c). This ensures that there is at least one fine resolution aperture for each point target which does not experience interference from other targets at the same frequency (other than at sidelobe levels). For this condition, $T'/N\Delta \geq (W+1)/2$.

For the situation where $H < 1$, the frequency of the fine resolution aperture is determined by the factor $\exp\{j(\pi B/T)(2mNi\Delta^2/H)\}$. For two point targets with the same frequency

$$(\pi B/T)(2m_1N\Delta^2/H) = (\pi B/T)(2m_2n\Delta^2/H) + 2\pi l.$$

For the two closest targets $m_1 - m_2 = TH/BN\Delta^2$

The number of coarse resolution apertures separating the two targets is given by $a_1 - a_2 = T'/N\Delta$

In choosing processing parameters for this situation, it must be considered that the coarse resolution FFT output function is actually sampled at a rate $1/H$ times that of the situation where $H \geq 1$. Therefore, the mainlobe target data is contained in $1/H$ times as many fine resolution apertures and the processing parameters are restricted by the relationship

$$(T'/N\Delta)\cdot H \geq (W+H)/2$$

Substituting $H = BT'\Delta N/T$, the relationship becomes

$$BT'^2/T \geq (W+H)/2.$$

By substituting in some actual values, it can be demonstrated that, if T' is large enough to satisfy the above relationship,

then $H \geq 1$. Values for some typical SAR systems are specified in Appendix C and the methodology used to choose the processing parameters is discussed in Chapter VII. The mainlobe width, W, along with other figures of merit for some typical windows, is discussed in the next chapter.

3.4 Data Selection

It is now appropriate to discuss the process by which redundant or aliased data is removed to produce the final output image. From the derivations of Sec. 3.1 and 3.2, it is observed that there is a direct correspondence between the target return position in the input and output data of the step transform. Thus, the output pulse position is displaced one sample for each unit time sample displacement of the input target return sample. (In the following discussion, it will be assumed that targets may only be positioned at unit sample spacings to simplify the explanation.) This means that each FFT output bin corresponds to a single target. The overlap ratio $T'/N\Delta$ also specifies the ratio of the total data produced to the number of point targets. Therefore, the number of data points retained from each FFT must be $\frac{T'/\Delta H}{T'/N\Delta} = N/H$, which is the ratio of the length of the fine resolution FFT to the overlap ratio. This ensures that only one data point is retained for each target.

The actual data selection process is set up by choosing a single target as a reference. The most appropriate choice for a

reference target is one which results in sampling of the coarse resolution FFT output exactly at the peak of the pulse. By calculating the frequency of the fine resolution aperture data for that target, the position of the output pulse in the fine resolution FFT output data stream can be predicted. The FFT from which the data is picked is the one which used the data sampled from the peak of the coarse resolution FFT output pulse as input. The best available data (i.e. minimum aliasing) for the adjacent N/H - 1 targets is found in the adjacent N/H - 1 samples in the same FFT. (If the overlap ratio is not large enough for the coarse resolution aperture window, there may be no unaliased data for some targets. The above procedure will ensure that the data with the least amount of aliasing is retained.) For the next N/H targets, N/H output samples are picked from the next fine resolution FFT, starting at the bin after the one left off at in the previous FFT. The data is scaled by calculating the Fourier transform of the coarse resolution window in the bin around the peak of the function and using that data to scale the N/H samples picked from each fine resolution FFT.

The above procedure can also be illustrated by the use of an example, as follows. The length of the coarse resolution FFT is 128 and H = 1. The spacing of the coarse resolution apertures is 42 samples. Therefore, the length of the fine resolution FFT is 128 and 42 data points must be picked from each. If the reference target chosen produces "good" data in fine resolution FFT #3 at bin 78, data must be picked as

follows:

1) from FFT #1, bins 102-127 and 0-15,

2) from FFT #2, bins 16-57,

3) from FFT #3, bins 58-99,

4) from FFT #4, bins 100-127 and 0-13,

5) from FFT #5, bins 14-55, etc.

It should be noted that an average of N/H points must be picked from each FFT. If N/H = 40.5, for example, the procedure must be set up so that 40 points are picked from the first FFT and 41 from the next.

In situations where the fine resolution aperture is padded with extra zeros, there are two effects. Firstly, the frequency resolution of the fine resolution FFT is increased so that each output bin does not correspond to a single point target. In effect, the filter output is oversampled. Secondly, the formula N/H can no longer be used to determine the number of points retained from each FFT. It is necessary to use the actual length of the fine resolution FFT in calculating this value.

IV. CHOOSING STEP TRANSFORM PROCESSING PARAMETERS

The last chapter outlined the basic operations of the step transform process. In this chapter, some information will be presented which is useful in determining the processing parameters used in an actual design. The quality of the output image is determined in part by the data windows used. The data window used for the coarse resolution aperture also plays a significant role in determining the computation rate required. The properties of windows which are critical to the step transform process will be examined and figures of merit will be presented for several common windows.

The step transform will then be examined to determine the amount of computation required at each stage. Formulae are derived which specify the total computation rate per output pixel. A significant factor in determining computation rates in SAR processing is the requirement for multilooking. A method for performing this operation is presented and its effect on the computation rate is determined. Basic memory requirements for the step transform process are also determined.

Finally, having stepped back to take a global view of the step transform technique, it will be appropriate to compare it with a very similar technique, bandpass filter spectral analysis. Because of the similarities between the two, it is possible to compare individual steps in each that have similar functions.

4.1 Windows

Data windows serve the very important function, in most pulse compression algorithms, of reducing the amount of energy contained in the sidelobes to acceptable levels. In the step transform process, both the coarse and fine resolution apertures must be windowed to obtain images of acceptable quality, i.e. sidelobes lower than the nominal 13 dB for the boxcar window. The window chosen for the fine resolution aperture only has an effect on the output image in close proximity to the final compressed pulse, i.e. within the same fine resolution aperture. Therefore, its effect on the final output can be directly observed from the properties of the window. For example, the 3 dB width of the output pulse will be approximately the same as the 3 dB width of the window chosen. The usual figures of merit, such as integrated side lobe ratio and 3 dB width, can be used in choosing an appropriate window.

The window chosen for the coarse resolution aperture, however, affects the image over many fine resolution apertures. As shown in Figure 8, the magnitude of the input data to each fine resolution aperture corresponds to some point on the Fourier transform of the window function chosen for the coarse resolution aperture. Since this data has itself been windowed and Fourier transformed, one spurious peak will appear at the same position in each fine resolution aperture. Since the output function of the coarse resolution aperture is actually sampled to obtain input data for the fine resolution aperture, the peak sidelobe levels will not actually be observed for all

Figure 8 - Data Input and Output for the Fine Resolution FFT

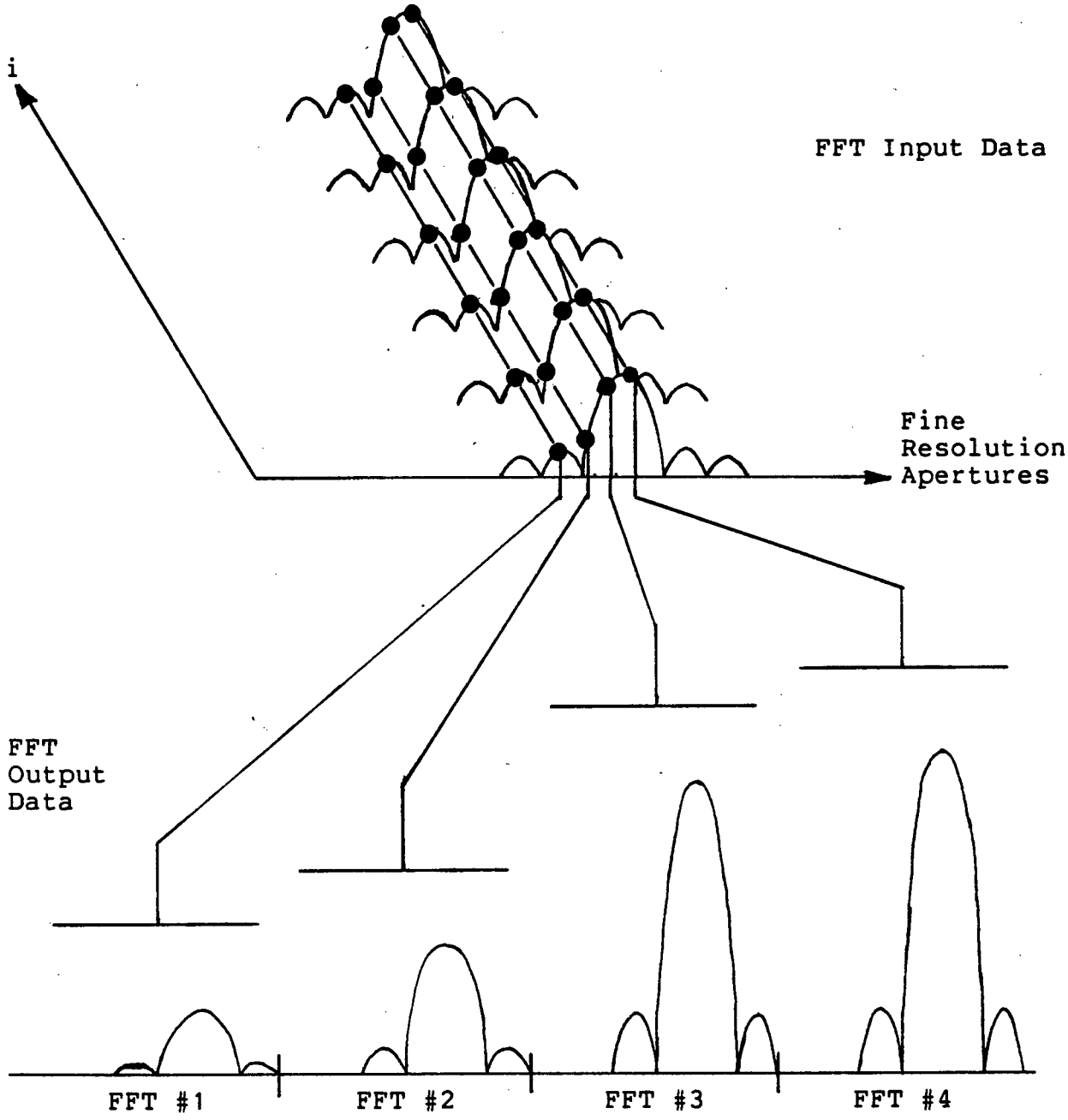

point target positions.

In addition to sidelobe level, the width of the mainlobe must also be considered in choosing a window function for the coarse resolution aperture. As was noted in Sec. 3.3, where the aliasing problem was discussed, the width of the mainlobe is directly related to how much the coarse resolution apertures must be overlapped to prevent aliasing. For the best image quality, it is desired to reduce the sidelobe levels as much as possible. However, in general, windows with lower sidelobes have wider mainlobes. Thus, for a particular application where the step transform is to be used, the highest acceptable sidelobe levels should be specified. A coarse resolution window which meets that specification and minimizes the mainlobe width is then chosen. Following this procedure ensures that acceptable image quality will be maintained, while at the same time minimizing the amount of processing required.

Relevant figures of merit were measured for several types of window, as specified in Appendix A. The data was obtained by evaluating the Fourier transform of each window at 0.01 bin intervals in the region of the main lobe. The only windows which gave questionable results were the Dolph-Chebyshev and Barcilon-Temes windows. In particular, the sidelobe levels obtained for these windows do not match those specified by Harris [16]. (For the Dolph-Chebyshev window, the sidelobe level should be -20α.) Also, the mainlobe width follows some slightly eccentric variations as a function of the aperture length. This might be due to the fact that the procedure to

Table I - Mainlobe Width at Highest Sidelobe Level for Various Windows

Window	a	Length of Window						
		8	16	32	64	128	256	512
Hamming		3.70	3.80	3.84	3.84	3.84	3.84	3.84
Minimum 3-term Blackman-Harris		5.72	5.80	5.86	5.90	5.90	5.90	5.90
3-term Blackman-Harris		5.26	5.28	5.34	5.38	5.38	5.38	5.38
Minimum 4-term Blackman-Harris			7.86	7.88	7.88	7.88	7.88	7.88
4-term Blackman-Harris		6.44	6.32	6.30	6.30	6.30	6.30	6.30
Rectangle		1.62	1.62	1.62	1.62	1.62	1.62	1.62
4-sample Kaiser-Bessel	3.0	6.10	6.16	6.16	6.16	6.16	6.16	6.16
Exact Blackman		6.20	5.98	5.90	5.88	5.88	5.88	5.88
Blackman		5.92	5.66	5.64	5.66	5.64	5.64	5.64
Gaussian	2.0	3.20	3.12	3.10	3.10	3.10	3.10	3.10
Gaussian	2.5		5.86	5.88	5.90	5.90	5.90	5.90
Gaussian	3.0		6.80	6.72	6.70	6.70	6.70	6.70
Gaussian	3.5		9.90	9.90	9.90	9.90	9.90	9.90
Gaussian	4.0		11.2	11.2	11.1	11.1	11.1	11.1
Kaiser-Bessel	2.0	4.22	4.28	4.30	4.30	4.32	4.32	4.32
Kaiser-Bessel	2.5	5.38	5.28	5.26	5.26	5.26	5.26	5.26
Kaiser-Bessel	3.0	6.22	6.24	6.22	6.20	6.22	6.22	6.22
Kaiser-Bessel	3.5	7.16	7.18	7.18	7.18	7.18	7.18	7.20
Kaiser-Bessel	4.0		8.12	8.14	8.16	8.16	8.16	8.16

a is a parameter used in some windows to govern the tradeoff between sidelobe level and mainlobe width. See Appendix A for complete definition of windows.

Table I - continued

Window	α	Length of Window						
		8	16	32	64	128	256	512
Dolph-Chebyshev	2.0		3.24	3.22	3.22	3.22	3.22	3.20
Dolph-Chebyshev	2.5		3.82	3.94	3.94	3.94	3.94	3.94
Dolph-Chebyshev	3.0		4.48	4.78	4.74	4.74	4.74	4.80
Dolph-Chebyshev	3.5		5.20	5.42	5.54	5.56	5.54	5.62
Dolph-Chebyshev	4.0		5.58	6.04	6.26	6.30	6.24	6.04
Barcilon-Temes	2.0	3.26	3.46	3.54	3.56	3.54	3.56	3.52
Barcilon-Temes	2.5	3.56	3.82	3.94	3.98	3.98	3.96	3.98
Barcilon-Temes	3.0	3.82	4.44	4.60	4.64	4.64	4.64	4.72
Barcilon-Temes	3.5	4.10	5.10	5.32	5.38	5.42	5.40	5.62
Barcilon-Temes	4.0	4.40	5.68	6.06	6.16	6.16	6.18	6.06

calculate the window function essentially involves specifying the Fourier transform (for the Dolph-Chebyshev window). The Fourier transform function is sampled and an inverse FFT is performed to obtain the time domain data coefficients. Possibly, the Fourier transform function sampling interval must be decreased in order to obtain agreement with Harris' results. Also, there are certain errors in the window specifications presented by Harris, as noted in Appendix A.

In Table I, the mainlobe width (W as depicted in Figure 6), is presented. In Table II, the mainlobe width is converted to the amount of overlapping of the coarse resolution apertures required for $H \geq 1$ by utilizing the restriction on the value of the overlap ratio derived in Sec. 3.3. This figure is presented

Table II - Overlap Required and Sidelobe Levels for Various Windows

Window	α	Sidelobe Falloff (dB/oct)	Length of Window						
			8	16	32	64	128	256	512
Rectangle		-6	1.31 -13	1.31 -13	1.31 -13	1.31 -13	1.31 -13	1.31 -13	1.31 -13
Gaussian	2.0	-6	2.10 -30	2.06 -31	2.05 -32	2.05 -32	2.05 -32	2.05 -32	2.05 -32
Dolph-Chebyshev	2.0	0		2.12 -34	2.11 -34	2.11 -33	2.11 -34	2.11 -33	2.10 -34
Barcilon-Temes	2.0	-6	2.13 -28	2.23 -34	2.27 -38	2.28 -38	2.27 -38	2.28 -39	2.26 -38
Barcilon-Temes	2.5	-6	2.28 -32	2.41 -38	2.47 -40	2.49 -39	2.49 -41	2.48 -40	2.49 -41
Hamming		-6	2.35 -34	2.40 -40	2.42 -42	2.42 -42	2.42 -43	2.42 -43	2.42 -43
Gaussian	2.5	-6		3.43 -42	3.44 -43	3.45 -43	3.45 -43	3.45 -43	3.45 -43
Dolph-Chebyshev	2.5	0		2.41 -39	2.47 -45	2.47 -44	2.47 -44	2.47 -44	2.47 -44
Kaiser-Bessel	2.0	-6	2.61 -43	2.64 -44	2.65 -45	2.65 -45	2.66 -46	2.66 -46	2.66 -46
Barcilon-Temes	3.0	-6	2.41 -35	2.72 -45	2.80 -48	2.82 -49	2.82 -48	2.82 -48	2.86 -51
Dolph-Chebyshev	3.0	0		2.74 -45	2.89 -55	2.87 -54	2.87 -54	2.87 -54	2.90 -52
Gaussian	3.0	-6		3.90 -54	3.86 -56	3.85 -56	3.85 -56	3.85 -57	3.85 -57
Barcilon-Temes	3.5	-6	2.55 -37	3.05 -53	3.16 -56	3.19 -58	3.21 -57	3.20 -56	3.31 -63
4-term Blackman-Harris		-6		3.72 -60	3.66 -57	3.65 -57	3.65 -57	3.65 -57	3.65 -57

Table II - continued

Window	a	Sidelobe Falloff (dB/oct)	Length of Window						
			8	16	32	64	128	256	512
Kaiser-Bessel	2.5	-6	3.19 -60	3.14 -59	3.13 -58	3.13 -58	3.13 -58	3.13 -58	3.13 -58
Blackman		-18	3.46 -74	3.33 -58	3.32 -58	3.33 -58	3.32 -58	3.32 -58	3.32 -58
Dolph-Chebyshev	3.5	0		3.10 -50	3.21 -59	3.27 -64	3.28 -63	3.27 -63	3.31 -60
3-term Blackman-Harris		-6	3.13 -49	3.14 -54	3.17 -58	3.19 -61	3.19 -62	3.19 -62	3.19 -62
Exact Blackman		-6	3.33 -54	3.38 -60	3.42 -65	3.43 -67	3.44 -68	3.44 -68	3.44 -68
4-sample Kaiser-Bessel	3.0	-6	3.55 -62	3.58 -66	3.58 -66	3.58 -66	3.58 -66	3.58 -66	3.58 -66
Barcilon-Temes	4.0	-6	2.70 -39	3.34 -59	3.53 -66	3.58 -68	3.58 -67	3.59 -69	3.53 -62
Minimum 3-term Blackman-Harris		-6	3.36 -57	3.40 -62	3.43 -67	3.45 -70	3.45 -71	3.45 -71	3.45 -71
Kaiser-Bessel	3.0	-6	3.61 -67	3.62 -70	3.61 -69	3.60 -68	3.61 -70	3.61 -70	3.61 -70
Dolph-Chebyshev	4.0	0		3.29 -55	3.52 -66	3.63 -74	3.65 -74	3.62 -73	3.52 -71
Gaussian	3.5	-6		5.45 -68	5.45 -70	5.45 -71	5.45 -71	5.45 -71	5.45 -71
Kaiser-Bessel	3.5	-6	4.08 -77	4.09 -82	4.09 -81	4.09 -81	4.09 -81	4.09 -81	4.10 -83
Gaussian	4.0	-6		6.11 -83	6.08 -87	6.05 -87	6.04 -87	6.04 -88	6.04 -88
Minimum 4-term Blackman-Harris		-6		4.43 -90	4.44 -92	4.44 -92	4.44 -92	4.44 -92	4.44 -92
Kaiser-Bessel	4.0	-6		4.56 -92	4.57 -93	4.58 -94	4.58 -94	4.58 -94	4.58 -94

Table III - Attenuation of Main Lobe at 0.5 bins from Centre

Window	a	Length of Window						
		8	16	32	64	128	256	512
Hamming		1.8	1.8	1.8	1.8	1.8	1.8	1.8
Minimum 3-term Blackman-Harris		1.1	1.1	1.1	1.1	1.1	1.1	1.1
3-term Blackman-Harris		1.3	1.3	1.3	1.3	1.3	1.3	1.3
Minimum 4-term Blackman-Harris			0.8	0.8	0.8	0.8	0.8	0.8
4-term Blackman-Harris			0.9	1.0	1.0	1.0	1.0	1.0
Rectangle		3.9	3.9	3.9	3.9	3.9	3.9	3.9
4-sample Kaiser-Bessel	3.0	0.8	0.9	1.0	1.0	1.0	1.0	1.0
Exact Blackman		0.9	1.0	1.1	1.1	1.1	1.1	1.2
Blackman		0.8	1.0	1.0	1.1	1.1	1.1	1.1
Gaussian	2.0	2.1	2.1	2.1	2.1	2.1	2.1	2.1
Gaussian	2.5		1.6	1.6	1.6	1.6	1.6	1.6
Gaussian	3.0		1.2	1.2	1.2	1.2	1.2	1.2
Gaussian	3.5		0.9	0.9	0.9	0.9	0.9	0.9
Gaussian	4.0		0.7	0.7	0.7	0.7	0.7	0.7
Kaiser-Bessel	2.0	1.4	1.5	1.5	1.5	1.5	1.5	1.5
Kaiser-Bessel	2.5	1.2	1.2	1.2	1.2	1.2	1.2	1.2
Kaiser-Bessel	3.0	1.0	1.0	1.0	1.0	1.0	1.0	1.0
Kaiser-Bessel	3.5	0.9	0.9	0.9	0.9	0.9	0.9	0.9
Kaiser-Bessel	4.0		0.8	0.8	0.8	0.8	0.8	0.8

Table III - continued

Window	a	Length of Window						
		8	16	32	64	128	256	512
Dolph-Chebyshev	2.0		2.1	2.0	2.0	2.0	2.0	2.0
Dolph-Chebyshev	2.5		1.8	1.7	1.7	1.7	1.7	1.7
Dolph-Chebyshev	3.0		1.5	1.5	1.4	1.4	1.4	1.4
Dolph-Chebyshev	3.5		1.4	1.3	1.2	1.2	1.2	1.3
Dolph-Chebyshev	4.0		1.2	1.1	1.1	1.1	1.1	1.1
Barcilon-Temes	2.0	2.2	2.0	1.9	1.9	1.9	1.9	1.9
Barcilon-Temes	2.5	1.9	1.7	1.6	1.6	1.6	1.6	1.6
Barcilon-Temes	3.0	1.7	1.4	1.4	1.3	1.3	1.3	1.4
Barcilon-Temes	3.5	1.6	1.3	1.2	1.2	1.2	1.2	1.2
Barcilon-Temes	4.0	1.5	1.2	1.1	1.0	1.0	1.0	1.1

along with the highest sidelobe level measured for each window so that the appropriate tradeoffs can be made.

A secondary consideration in the choice of a window is the rate of sidelobe falloff, also presented in Table II. This also affects the amount of energy in the sidelobes and therefore the image quality.

As was mentioned previously, the Fourier transform of the coarse resolution window is actually sampled to obtain input data for the fine resolution apertures. The fine resolution aperture containing the final output pulse for a particular point target may obtain its input data up to 0.5 resolution bins from the peak of the coarse resolution FFT output pulses. This will result in attenuation of the output image for certain point

targets. The severity of this attenuation can be measured by determining the level of the coarse resolution window at 0.5 resolution bins from the centre of the pulse. This data is presented in Table III. If the attenuation is severe enough, it may be necessary to perform a scaling operation on the output data from the fine resolution FFT.

4.2 Computation Rates

The processing parameters chosen to perform the step transform process play a major role in determining the computation rate required. The effect of certain parameters, such as the coarse resolution aperture overlap ratio $T'/N\Delta$, is obvious. However, there are other contributing factors whose role is not quite so obvious. The approach taken here will be to break the step transform down into the major computational steps and initially examine the computational requirements of each stage. The overall process will then be examined so that an indication of the optimal values for the processing parameters can be obtained. In succeeding chapters, when the step transform technique is applied to SAR azimuth processing, additional constraints will be imposed on the processing parameters.

No attempt will be made here or in later chapters to account for every single computation which must be performed. Instead, a measure of the computation rate will be obtained by calculating the number of complex multiplications required.

Some stages do not involve complex computations, but require a significant number of real multiplications to be performed. These are included by assuming that 1 complex multiplication is equivalent to 4 real multiplications and making the appropriate conversion.

The step transform process can be broken down into the following major steps:

1) multiplication of reference and target return signals,
2) coarse resolution FFT (windowing of the aperture can be done as part of the multiplication - step 1),
3) quadratic phase correction,
4) re-ordering of the data for the fine resolution FFT,
5) windowing of the fine resolution aperture,
6) fine resolution FFT,
7) data selection, magnitude evaluation and scaling.

The factors which directly affect the computation rate and the stages they impact are as follows:

1) length of the coarse resolution FFT, T', step 2,
2) amount of overlapping of the coarse resolution apertures, expressed as the ratio $T'/N\Delta$, steps 1-3,
3) the length of the fine resolution FFT, $T/B\Delta^2N$, steps 5 and 6.[7]

Note that the above factors are closely interrelated and, in general, affect the image quality as well.

---

[7] It is assumed that the window coefficients are predefined and, therefore, the type of windows used will not affect the computation rate.

As mentioned in the previous chapter, it is only necessary to consider the situation where $H \geq 1$. For efficient FFT processing, the length of the coarse resolution FFT, T'/Δ, is restricted to be a power of 2. For similar reasons, the fine resolution FFT length, $T'/\Delta H$, should also be a power of 2. Thus there is a further restriction on H, that it be a power of 2 as well. For situations where H is not a power of 2, the fine resolution FFT would be somewhat longer. Consider a processing region of length R time units and R/Δ samples. The number of complex multiplications which must be performed at each stage of the step transform process is as follows:

1) Multiplication - $(R/\Delta)(T'/\Delta N)$ complex multiplications

2) Coarse Resolution FFT - there are $R/\Delta N$ FFT's each requiring $T' \cdot \log_2\{T'/\Delta\}/2\Delta$ complex multiplications

   Total = $RT' \cdot \log_2\{T'/\Delta\}/2\Delta^2 N$

3) Quadratic Phase Correction - $(R/\Delta)(T'/\Delta N)$ complex multiplications

4) Windowing the Fine Resolution Aperture - $2T'(R-T)/(\Delta^2 N)$ real multiplications or $T'(R-T)/(2\Delta^2 N)$ complex multiplications

5) Fine Resolution FFT - there are $(R/\Delta - T/\Delta)(T'/\Delta N)$ points to be processed using FFT's of length $T/B\Delta^2 N$ which requires $(R-T)T'B/T$ FFT's. Each FFT requires $T \cdot \log_2\{T/B\Delta^2 N\}/2B\Delta^2 N$ complex multiplications.

   Total = $(R-T)T' \cdot \log_2\{T/B\Delta^2 N\}/2\Delta^2 N$

6) Output scaling - $(R-T)/\Delta$ real multiplications or $(R-T)/4\Delta$ complex multiplications.

$$\text{Total computations} = (T'/\Delta^2N)(2R)$$
$$+ (T'/2\Delta^2N)(R\cdot\log_2\{(T'/\Delta N)(T/B\Delta^2)\})$$
$$- (T'/2\Delta^2N)(T\cdot\log_2\{T/B\Delta^2N\})$$
$$+ (T'/2\Delta N + 1/4)(R-T)/\Delta$$

To find the amount of computation per input data point, CP, divide by R/Δ.

$$CP = 2T'/\Delta N$$
$$+ (T'/2\Delta N)\cdot\log_2\{T'/\Delta\}$$
$$+ (T'/2\Delta N)(1 - T/R)\cdot\log_2\{T/B\Delta^2N\}$$
$$+ (T'/2\Delta N + 1/4)(1 - T/R) \qquad (4)$$

Assuming $T << R$

$$CP = (T'/\Delta N)(2.5 + \log_2\{(T'/\Delta)(T/B\Delta^2N\}/2) + 1/4$$
$$= (T'/\Delta N)(2.5 + \log_2\{(T'/\Delta N)(T/B\Delta^2)\}/2) + 1/4$$

Thus, for $H \geq 1$, the only means of varying the computation rate is by changing the overlap ratio $T'/N\Delta$.

For the situation where T is close to the same length as R, the amount of data rejected during the reordering process (see Figure 5) plays a significant role in determining the computation rate. The most significant computation done on this data is the coarse resolution FFT. The actual amount of data rejected is dependent only on the overlap ratio, $T'/N\Delta$. Thus, in this situation, it becomes desirable to minimize the length of the coarse resolution aperture. Overall, it would appear that the situation where H = 1 seems to minimize the computation requirements.

4.3 Memory Requirements

Before attempting to assess the memory requirements of the step transform process, it is necessary to do some basic analysis of the architecture which might be used to implement the technique. Martinson, in his description of a step transform processor implementation [25], considers this issue in some detail. The analysis presented here will basically follow the same lines of reasoning, but will incorporate the additional results presented in previous sections. Note that some of the basic issues related to SAR azimuth processing, such as RCMC, which requires that data across several range cells be accessible at the same time, will not be considered at this point.

The step transform processor described by Martinson uses a pipeline architecture, and is designed to perform the pulse compression operation in real-time as the data is received. Two memory banks are used so that data can be written into one module from the coarse resolution FFT output while data is read to the fine resolution FFT input from the other memory module. When unit slope diagonalization ($H = 1$) is required, this method allows both memory modules to be in use at all times. For the situation where $H > 1$, the only solution which was found to the problem of reading and writing at the same time, is to provide a separate bank for each FFT output bin.

The actual amount of memory storage required is determined by the number of coarse resolution apertures which must be used to obtain data for one complete fine resolution aperture. Since

each coarse resolution aperture contains T'/Δ samples, the dimensions of the matrix are T'/Δ by $T'/\Delta H$. The total number of data elements is therefore $T'^2/\Delta^2 H$. Since $H = BT'\Delta N/T$,

$$\text{Total memory words } TM = T'T/B\Delta^2 N$$

$$= (T'/\Delta N) \cdot (T/B\Delta^2)$$

Thus, the amount of memory is independent of all processing parameters except the overlap ratio $T'/N\Delta$. For the situation where $H = 1$, it can be demonstrated that only $(T'/2\Delta)(T'/\Delta - 1) + 1$ memory locations in the reorder memory contain valid data at any one time. It may be possible to develop an address sequencing algorithm such that the actual size of the reorder memory can be reduced to this amount, as described by Martinson. No attempt will be made to develop such an algorithm here. Therefore memory requirements will be specified approximately as being in the range TM/2 to TM.

4.4 Multilooking

An additional consideration which affects the computation rate is the requirement to reduce speckle noise in the output image. The phenomenon of speckle occurs in all imaging systems which use phase information to reconstruct the image and was first observed in holographic experiments. The statistical properties of speckle have been described in detail by Dainty [11].

There are two basic methods of speckle noise reduction. In the first category, speckle noise is reduced by smoothing the

final image data [22]. In the second category, the azimuth signal is divided up into several sections or looks. Each section is processed separately and the results are added incoherently by throwing away the phase information [30].

The second method must be integrated into the pulse compression operation and only the impact on step transform processing will be considered here. A somewhat subjective judgment must be made to determine the number of looks required, usually on the basis of the type of terrain and the application for which the final image is to be used. Ford has done a survey of user preferences [15] which suggests that the optimum number of looks may vary from 2 to 32 for geological applications.

In the step transform technique, multilook processing can be performed as follows. The output data of the coarse resolution FFT's is partitioned according to the number of looks required. A fine resolution FFT is performed on each look and the data from these FFT's is added incoherently. The data selection process described in Sec. 3.4 is modified so that N/HL points are selected from each FFT, where L is the number of looks. Since the length of the fine resolution FFT's is changed, the computation rates will change as well.

Ideally, each look should contain completely independent data. However, a small amount of overlapping will not seriously affect the speckle noise reduction properties of this process [8]. Therefore, it is possible to vary the length of the fine resolution FFT's to a certain extent and the restriction that H be a power of 2 may be removed. Note that the length of the

fine resolution FFT's cannot be allowed to become too short or else there will be aliasing effects due to the wraparound properties of the FFT. In general, the FFT length should not be shorter than 16 samples. Also, look overlap should not be greater than 50%. Normally, it is expected that the output resolution is reduced by the number of looks.

The effect on the computation rates is dependent, to a large extent, on the number of looks required. If the fine resolution aperture can be greater than approximately 16L samples, there is not likely to be a radical change in the computation requirements. The single fine resolution FFT considered in Sec. 4.2 is replaced by L FFT's of length $T'/\Delta HL$ samples. The total number of complex multiplications is reduced to

$$L \cdot T \cdot \log_2\{T/B\Delta^2 NL\}/2B\Delta^2 N$$

for the fine resolution FFT stage. However, the looks must then be combined incoherently in a look summation stage.

The length of the fine resolution aperture can be increased to accommodate a greater number of looks by increasing the size of the coarse resolution aperture while maintaining H constant.[8] This results in an increase in the overlap ratio $T'/N\Delta$ and a corresponding increase in the computation rate. In general

---

[8] Perry and Martinson [29] lengthen the fine resolution FFT by concatenating two apertures together. As discussed in Sec. 3.1, this would not seem to work very well. One might speculate that this is done to provide greater flexibility in the number of looks. However, since the data in the apertures comes from exactly overlapping portions of the target return, the speckle noise would not be reduced by this additional processing.

terms, it means that there is a certain number of looks which can be handled without a significant change in computation rates. Above that value of L, some significant increase in the overlap ratio is required with a corresponding increase in the computation rate.

4.5 Comparison With Bandpass Filter Spectral Analysis

BPF SPECAN pulse compression is similar in many ways to the step transform. Both employ essentially the same stages of processing conceptually, although the implementation of the concepts is quite different. After performing the initial mixing operation, the BPF SPECAN method uses filters to separate groups of adjacent targets. In the step transform, this stage is implemented using the coarse resolution FFT's which separate groups of adjacent targets into separate FFT output bins. Both techniques then employ an FFT to perform the final output resolution.

The major difference between the two techniques is in the degree of flexibility afforded. The step transform employs a very specific coarse resolution filter, the FFT. The number of targets included in a specific FFT output bin is determined largely by the requirements of the step transform process, as outlined in Chapter III. There is not a great deal of flexibility to adapt to the requirements of the individual SAR system. BPF SPECAN, on the other hand, allows a great deal of flexibility in the choice of processing parameters. The number

of filters required and the type of filter may be adapted to the particular application. As will be seen in later chapters, this proves to be a distinct advantage in the SAR azimuth processing application.

V. DETAILS OF SAR AZIMUTH PROCESSING

In this chapter, the process of fitting the step transform into the SAR azimuth signal processing problem is begun. In order to do this, the coding of azimuth signal will be briefly described and some of the problems which occur when one attempts to process this signal using a digital processor will be pointed out. It will be shown that the linear FM rate of the azimuth signal is not constant, but varies as a function of target range. The azimuth signal for a single point target may also migrate between range cells and does not maintain a constant amplitude. The signal is actually attenuated as a function of the antenna profile. The performance of the step transform with regard to many of these effects cannot be predicted mathematically, since it is not possible to obtain a closed form mathematical solution as was done in previous chapters. A simulation program, which was used to observe the performance of the step transform in a quantifiable manner, is described.

5.1 The SAR Azimuth Signal

The basic principles of synthetic aperture radar have been thoroughly investigated in the literature [9][10][33]. Bennett et al [5] have provided a description of the encoding of the azimuth signal which is particularly useful for the topics under discussion in this chapter. Consider a radar platform moving above the earth's surface as depicted in Figure 9. With reference to the geometry of Figure 9, the instantaneous slant

Figure 9 - SAR Geometry

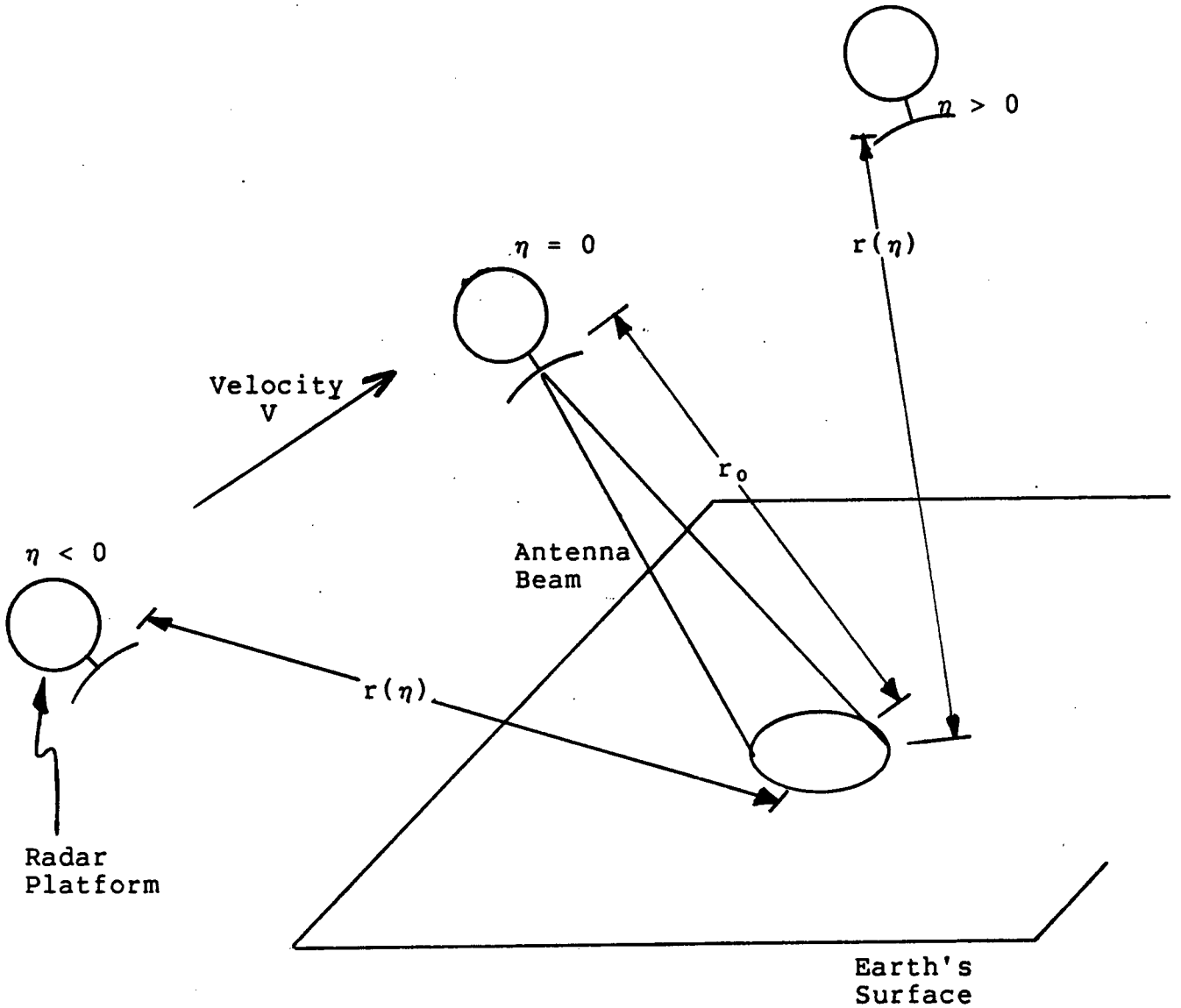

range to a point target can be approximated by the function

$$r(\eta) = r_o + \frac{(V\eta)^2}{2r_o} \qquad (5)$$

where r_o = slant range of closest approach

η = elapsed time since $r(\eta) = r_o$

V = velocity of platform.[9]

The demodulated phase of the radar return signal is

$$\phi(\eta) = \frac{-2}{\lambda} r(\eta) = \frac{-2}{\lambda} (r_o + \frac{V^2\eta^2}{2r_o})$$

where λ is the radar wavelength. The Doppler frequency is

$$f(\eta) = \frac{d\phi}{d\eta} = - \frac{2V^2\eta}{\lambda r_o} \text{ Hz.}$$

The received azimuth signal is

$$s(r_o,\eta) = A(\eta-\eta_o) \exp\{\frac{4\pi j}{\lambda} r(\eta)\}$$

where $A(\eta)$ = the antenna profile function

η_o = the azimuth time offset of the beam centre from from zero Doppler.

This is a linear FM signal with a frequency sweep rate[10]

$$K = \frac{-2V^2}{\lambda r_o} \qquad (6)$$

---

[9] For airborne SAR systems, V is the actual velocity of the plane. For satellite-borne SAR's, the earth's curvature and rotation must be taken into account and V is a derived parameter called the radar velocity.

[10] In the theoretical analysis of Chapter III, the FM rate is defined as the ratio B/T. If B is defined to be the PRF for the SAR azimuth processing situation, then T is the time the target return signal takes to sweep between the frequencies -PRF/2 and PRF/2.

Thus, the FM rate varies as a function of range. To achieve acceptable image quality, and unless processing is done only over a very narrow range, the reference function of the pulse compression algorithm must be changed periodically to take into account this varying FM rate.

From the function $r(\eta)$, it is clear that it is possible for the azimuth signal to migrate between range cells, depending on the parameters of the particular radar involved. In the case of most satellite radars, the azimuth signal lies on a parabolic curve in signal memory which may cross several range cells. In such situations, some form of range cell migration correction (RCMC) is clearly required, since the azimuth signal must lie in a single line in signal memory in order to be processed.

The variable attitude of satellites also presents some problems in processing SAR azimuth signals. Essentially, it means that the antenna may not be pointing broadside to the direction of platform motion. This phenomenon not only intensifies the range cell migration problem, as will be seen in Chapter VI, but also causes the antenna beam centre to be shifted significantly away from the zero Doppler line. This is significant since the processing region is positioned around the beam centre and will change the frequency region occupied by the processed portion of the azimuth signal. Alluding to the theoretical analysis of Chapter III, this means that the output of the coarse resolution FFT's will be rotated in direction and amount corresponding to the shift of the beam centre. This error may cause problems during the reordering process. It is

easily corrected by rotating the FFT outputs the appropriate amount.

5.2 The Antenna Profile

For most situations, the antenna profile may be represented by a sinc function so that

$$A(\eta) = \frac{\sin^2\{k\eta\}}{(k\eta)^2}$$

where k is some constant determined by calibrating the antenna. Thus, the actual signal to be processed is somewhat different than that presented in the theoretical development of Sec. 3.1. Not only does the signal not have a constant magnitude but it also does not have a finite time duration. This implies that the Doppler frequency of the azimuth signal also is not bounded. Since the azimuth signal is sampled at a rate determined by the PRF, there will be some aliased energy in the signal. The SAR parameters must be chosen to minimize this aliasing effect and ensure good image quality [19]. One problem which must be handled by the pulse compression algorithm is that the energy towards the edges of the signal returns is decreased significantly from that at the centre. This attenuation, caused by the antenna profile, may be so severe that the signal information is obliterated by noise. In such cases, it is necessary to filter out that portion of the signal return. In the step transform, this may be done by discarding appropriate coarse resolution output bins, since there is a direct

correspondence between the time position of the coarse resolution aperture and the frequency seen by the coarse resolution FFT. The data region rejected is called the guardband and may be expressed as a fraction, β, of the PRF. Since some good signal information is discarded as well, this does have the effect of broadening the final output pulse.

This technique is also used in non-SAR applications, where the input signal is normally sampled at a rate somewhat greater than Nyquist. In that situation, the coarse resolution FFT output bins at frequencies above Nyquist do not contain valid data and are rejected.

5.3 The Simulation Program

The program was written in FORTRAN on the MTS computer system at UBC. The basic modular structure of the program is presented in the flowchart in Figure 10. Appendix D contains a basic functional specification of the program. It follows the stages of the step transform process as outlined in previous chapters. However, there are some additional steps. At the beginning, the processing parameters are chosen either from preset values or information entered by the user. At the end, some analysis of the output is carried out and the result may be plotted, if requested by the user.

The following SAR system and processing parameters may be altered by the user:

1) data windows for coarse and fine resolution apertures,

Figure 10 - Flowchart of Simulation Program

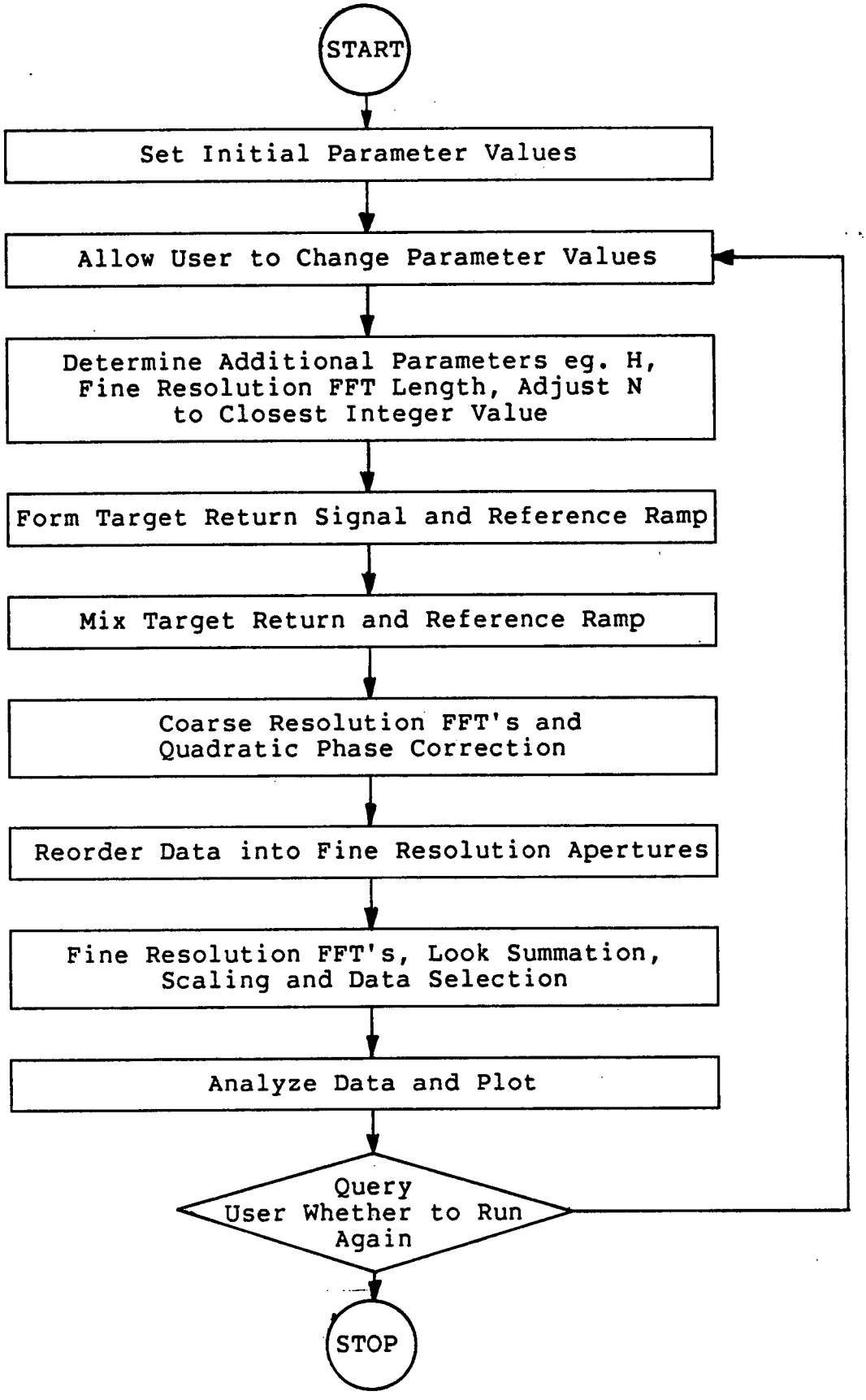

2) coarse resolution time extent and overlapping,

3) number of looks,

4) guardband,

5) antenna attenuation profile,

6) FM rate error and time extent of target return signal,

7) point target position,

8) resolution of the final output image.

All time apertures are specified in terms of the number of samples. The user is able to specify a factor by which the fine resolution FFT's can be lengthened (padded with zeros) to obtain greater resolution in the final output image. The final output data is analyzed using an interpolation routine which uses exponential functions and variable "tension" parameters. The routine is called SMOOTH and is resident on the MTS computer system [27].

The antenna constant, k, was chosen individually for each system. For the SEASAT SAR, the attenuation profile of the antenna used on the satellite was chosen, such that k = 142.37. For the JPL Nominal and COMSS/LASS systems, no such data was available. Therefore, an antenna profile was chosen such that the signal was attenuated by -6 dB at the ends of the aperture.

Although the user has a large degree of freedom in choosing the processing parameters, there are some restrictions. The time extent of the coarse resolution apertures is restricted to values such that the number of samples is a power of 2. This is done for efficient processing of the coarse resolution FFT. Secondly, the amount of overlapping is adjusted to ensure the

frequency steps between coarse resolution apertures are as close as possible to integer values when the FFT outputs are computed. Because of these two restrictions, it is not possible to ensure that different SAR systems have identical processing parameters, such as the amount of overlapping. Since overlapping of the coarse resolution apertures is a large determinant in the computational efficiency of the step transform, it is possible that the computation rates will vary from one system to another. The data window for the coarse resolution apertures was chosen to obtain the minimum sidelobe levels without introducing aliasing problems for that particular SAR system. The processing parameter values used to simulate each particular SAR sytem are specified in Appendix C.

As will be described in the next chapter, in actual SAR systems, there is a necessity to provide for non-integer sample spacing of the reference ramps. No attempt was made to provide this capability in the simulation program, since this would add the complication of requiring the computation of multiple reference ramps. However, this meant that the system parameters had to be adjusted to obtain ideal pulse compression.

From the experience with the simulation program, some observations can be made about the step transform technique. For the software implementation, large amounts of memory space are required because of the overlapping of the coarse resolution apertures. The mixing operation, coarse resolution FFT, and quadratic phase correction cannot be done in place, i.e. in the data space where the target return signal is stored. For this

reason, two large complex number arrays are required. Array SIGNAL contains the initial point target return signal. The output of the mixing operation is stored in array UNORD, where in-place FFT routines and quadratic phase correction are performed. In order to perform the reordering operation to assemble the fine resolution FFT input data, a third large memory space is required. However, since the target return data is not required anymore, array SIGNAL is used for this purpose. The fine resolution FFT and subsequent processing is performed in array SIGNAL.

VI. STEP TRANSFORM PERFORMANCE ON SAR AZIMUTH SIGNALS

SAR azimuth compression is a special case of radar signal processing which, in many cases, requires special compensations to produce high quality images. In particular, satellite radars present special problems due to the variable platform velocity, large distance from the earth's surface, and variable attitude. Two of the major factors which must be dealt with in satellite SAR signal processing are significant variations in the FM rate and migration of the azimuth signal between range cells. In this chapter, the discussion on azimuth coding of the SAR signal is continued by examining how the step transform is able to deal with the above problems. The simulation program described in the previous chapter was used to obtain quantitative results on the performance of the step transform.

6.1 FM Rate Error

The effects of FM rate errors will initially be considered at a theoretical level by returning to the mathematical analysis of Sec. 3.1. Consider a target return signal whose FM rate is mismatched to the reference function by a fraction b. Thus

$$s(t) = \exp\{j(\pi B/T)(1+b)t^2\}$$

After the mixing operation,

$$s(k,m)\, s^*(k,n) = \exp\{j(\pi B/T)(1+b)(2k\Delta^2(m+n))\}$$
$$\cdot \exp\{j(\pi B/T)(1+b)(m^2\Delta^2 - T'\Delta m)\}$$
$$\cdot \exp\{j(\pi B/T)(1+b)(n^2\Delta^2 - T'\Delta n)\}$$
$$\cdot \exp\{j(\pi B/T)(1+b)(2mn\Delta^2)\}$$
$$\cdot \exp\{j(\pi B/T)(b)(k^2\Delta^2 + T'^2/4 - k\Delta T')\} \quad (7)$$

When an FFT is applied to the above data, the series takes the form

$$s(r) = \sum_{k=0}^{T'/\Delta - 1} W_1(k) \exp\{j(c_1 k + c_2 k^2)\}$$

where c_1 and c_2 are constants. Since this is no longer a geometric series, a closed form evaluation cannot be obtained. Therefore it is not possible to predict, using an exact formula, the effects of the frequency mismatch on image quality.

However, it is possible to make some observations based on the previous insights gained into how the step transform works. In the first place, one observes that the coarse resolution aperture after the mixing operation no longer contains a constant frequency signal. It now contains a residual FM rate as specified in the last line of equation (7). This will result in broadening of the coarse resolution FFT output pulses. This could result in increased aliasing problems and may require increased overlapping of the coarse resolution apertures.

Secondly, the frequency increments between successive coarse resolution apertures has been altered. (The frequency of the coarse resolution aperture is specified in the first line of equation (7).) Thus, when data is reordered for input to the

fine resolution FFT's, there will be some amplitude modulation of the signal. This has the effect of broadening the output pulse. The frequency of the input signal to the fine resolution FFT will also be modified, shown in the fourth line of equation (7).

Lastly, from the third line of equation (7), it will be noted that the quadratic phase factor is also modified and during the process will not be removed completely. This will also modify the input signal to the fine resolution FFT so that it sweeps across some range of frequencies. This will result in some misregistration of looks, since the FFT's will resolve different portions of the target signal to different frequencies.

Thus, it can be seen that all stages of the step transform process are affected to some extent by mismatching of the FM rates. In order to quantify these effects, it is necessary to perform some simulations.

6.1.1 Data For Typical Satellite SAR Systems

In order to present simulation results which are meaningful, it is first necessary to determine how quickly the FM rate changes for typical SAR systems. Using equation (6) of Sec. 5.1, we see that

$$\frac{dK}{dr_o} = \frac{2V^2}{\lambda r_o^2} \text{ Hz}^2/\text{m}$$

Converting this formula to more convenient units,

$$\frac{dK}{dr_o} = \frac{\rho}{r_o} \cdot 100 \text{ \% FM rate error / range cell}$$

where ρ = slant range cell width

Typical values were computed using the data in Appendix C and are presented in Table IV. Note that there is a residual error in the autofocus estimation of the FM rate of approximately ±0.06 % for the JPL Nominal case and ±0.1% for the SEASAT case. These figures should be added to the data of Table IV when considering the maximum possible error.

Table IV - FM Rate Errors for Typical SAR Systems

System	Slant Range km	FM Rate Error		
		Hz^2/m	%/range cell	%/100 range cells
SEASAT	860 810	0.00059 0.00067	0.00077 0.0081	0.08 0.08
JPL Nominal	550 500	0.0016 0.0020	0.0019 0.0021	0.19 0.21
COMSS/LASS	636 586	0.0040 0.0047	0.00090 0.00098	0.090 0.10

Simulation runs to determine FM rate error effects were carried out for the SEASAT, JPL Nominal and COMSS/LASS satellite

SAR systems using the processing parameters specified in Appendix C. The step transform filter output was interpolated by expanding the fine resolution FFT by a factor of eight. The resulting data is summarized in Tables V, VI and VII and shows a wide disparity in the results obtained for the three systems.

Table V - FM Rate Error Simulation Results for SEASAT Parameters

% Rate Error	1 Look			4 Looks		
	3 dB Width	% Broadening	Peak Magnitude	3 dB Width	% Broadening	Peak Magnitude
0.0	1.75	0.0	0.0 dB	1.36	0.0	0.0 dB
0.02	1.76	0.6	-0.03 dB	1.37	0.7	-0.01 dB
0.04	1.80	2.9	-0.2 dB	1.38	1.5	-0.06 dB
0.06	1.87	6.9	-0.3 dB	1.39	2.2	-0.1 dB
0.08	1.97	12.6	-0.6 dB	1.40	2.9	-0.3 dB
0.10	2.10	20.0	-0.9 dB	1.42	4.4	-0.4 dB
0.12	2.27	29.7	-1.2 dB	1.45	6.6	-0.6 dB
0.14	2.47	41.1	-1.6 dB	1.48	8.8	-0.8 dB
0.16	2.69	53.7	-2.0 dB	1.51	11.0	-1.0 dB
0.18	2.92	66.9	-2.3 dB	1.56	14.7	-1.3 dB
0.20	3.15	80.0	-2.6 dB	1.61	18.4	-1.6 dB

Note that % Rate Error = 100·b where b is the variable defined in Sec. 5.2.

There are several different factors which influence the results, each of which will be dealt with individually. The Tables

Table VI - FM Rate Error Simulation Results for JPL Nominal Parameters

% Rate Error	1 Look			4 Looks		
	3 dB Width	% Broadening	Peak Magnitude	3 dB Width	% Broadening	Peak Magnitude
0.0	1.64	0.0	0.0 dB	1.36	0.0	0.0 dB
0.02	1.66	1.2	-0.09 dB	1.37	0.7	-0.03 dB
0.04	1.75	6.7	-0.4 dB	1.39	2.2	-0.1 dB
0.06	1.92	17.1	-0.7 dB	1.41	3.7	-0.3 dB
0.08	2.16	31.7	-1.3 dB	1.44	5.9	-0.6 dB
0.10	2.50	52.4	-1.9 dB	1.49	9.6	-0.9 dB
0.12	2.88	75.6	-2.5 dB	1.56	14.7	-1.3 dB
0.14	3.24	97.6	-3.1 dB	1.64	20.6	-1.7 dB
0.16	3.62	120.7	-3.5 dB	1.75	28.7	-2.2 dB
0.18	4.03	145.7	-3.9 dB	1.90	39.7	-2.8 dB
0.20	4.44	170.7	-4.3 dB	2.08	52.9	-3.3 dB

specify the results obtained for certain measurements made on the main lobe of the output data of the processor. The 3 dB width of the main lobe is specified in terms of the number of output samples. The % broadening is calculated using the 3 dB width of the main lobe at 0% rate error as a reference. For the 4-look situation, because of overlapping of the looks, it was possible to use a data window of the same length as the FFT. Since a Hamming window was used on the fine resolution aperture, the minimum 3 dB width is actually 1.33 bins if the effect of the antenna profile is not considered. For the single-look

Table VII - FM Rate Error Simulation Results for COMSS/LASS Parameters

% Rate Error	1 Look			4 Looks		
	3 dB Width	% Broadening	Peak Magnitude	3 dB Width	% Broadening	Peak Magnitude
0.0	1.64	0.0	0.0 dB	1.38	0.0	0.0 dB
0.1	1.66	1.2	-0.05 dB	1.39	0.7	-0.01 dB
0.2	1.70	3.7	-0.2 dB	1.39	0.7	-0.07 dB
0.3	1.76	7.3	-0.4 dB	1.40	1.4	-0.2 dB
0.4	1.87	14.0	-0.7 dB	1.42	2.9	-0.3 dB
0.5	2.01	22.6	-1.0 dB	1.44	4.3	-0.4 dB
0.6	2.21	34.8	-1.4 dB	1.47	6.5	-0.6 dB
0.7	2.44	48.8	-1.9 dB	1.50	8.7	-0.8 dB
0.8	2.71	65.2	-2.3 dB	1.54	11.6	-1.1 dB
0.9	2.97	81.1	-2.7 dB	1.59	15.2	-1.3 dB
1.0	3.23	97.0	-3.1 dB	1.65	19.6	-1.6 dB

case, however, the data window is reduced by a factor of $(1-\beta)$ with respect to the length of the FFT and, therefore, the window function is sampled at a rate of $1/(1-\beta)$. This accounts for the disparity between the single-look and 4-look cases at 0% rate error. The reference used for the peak magnitude of the main lobe is the value at 0% rate error.

Initially, some simulations were done to determine the effect of point target placement on the filter response. Placement was done for 2 cases such that the coarse resolution FFT output was sampled exactly at the peak of the main lobe and

as far off to the side of the main lobe as possible. The antenna profile was turned off. It was observed that as the FM rate error increased, there was far less magnitude variation in the fine resolution FFT input data for the case where the coarse resolution aperture was sampled at the peak of the main lobe. However, there was no observable difference in the 3 dB width or attenuation of the main lobe between the two cases. This suggests that the most important information for the pulse compression algorithm is contained in the phase of the input signal, not the magnitude. The analysis of Chapter III and the fact that the antenna profile itself introduces considerable magnitude variation tends to support this conclusion. For the data presented here, the point targets were positioned so that the coarse resolution FFT output was sampled at the peak of the main lobe.

The single most significant observed effect of the rate error was to change the fine resolution aperture data from a CW signal to a linear FM signal. There was no measureable shift in the centre frequency and, therefore, there was no significant displacement of the output pulse.[11] The only significant effect for the single look case was some attenuation of the peak of the output pulse and broadening of the main lobe, as can be seen from the data in Tables V, VI and VII and shown in Figure 11.

For multi-look processing, the residual FM component in the

[11] This result is only valid for situations where the antenna beam centre is aligned with the zero Doppler line.

Figure 11 - % Broadening vs. FM Rate Error From Simulation Results

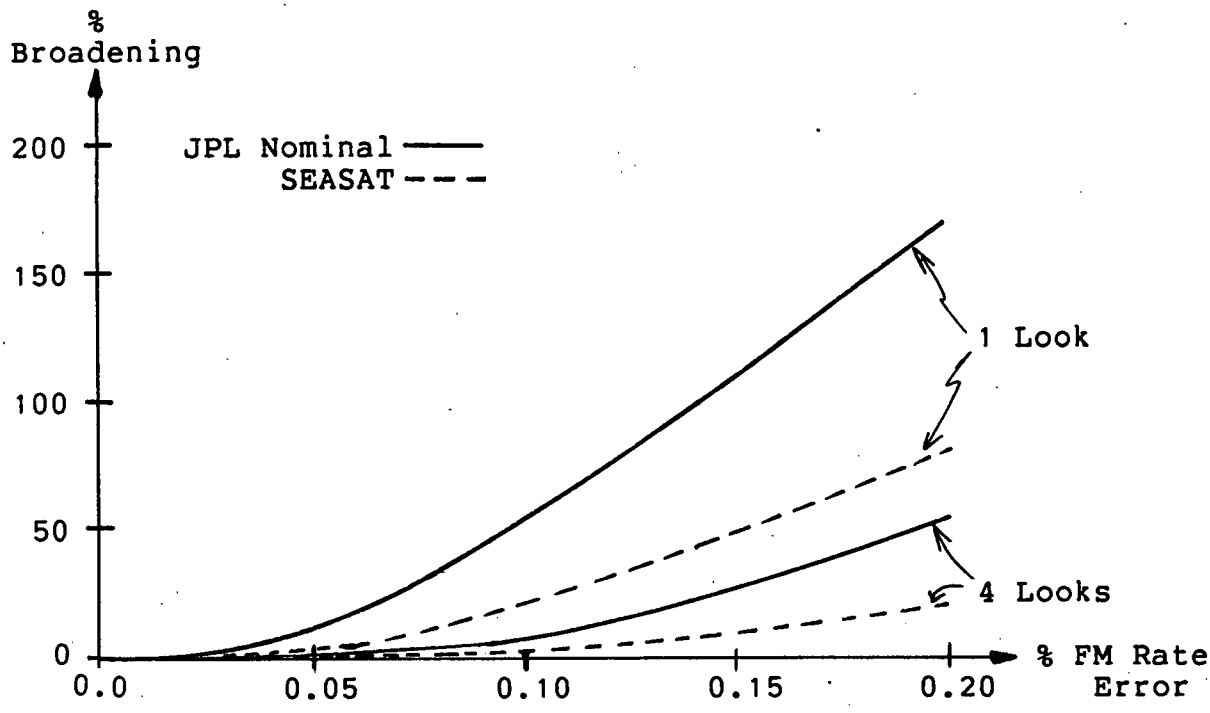

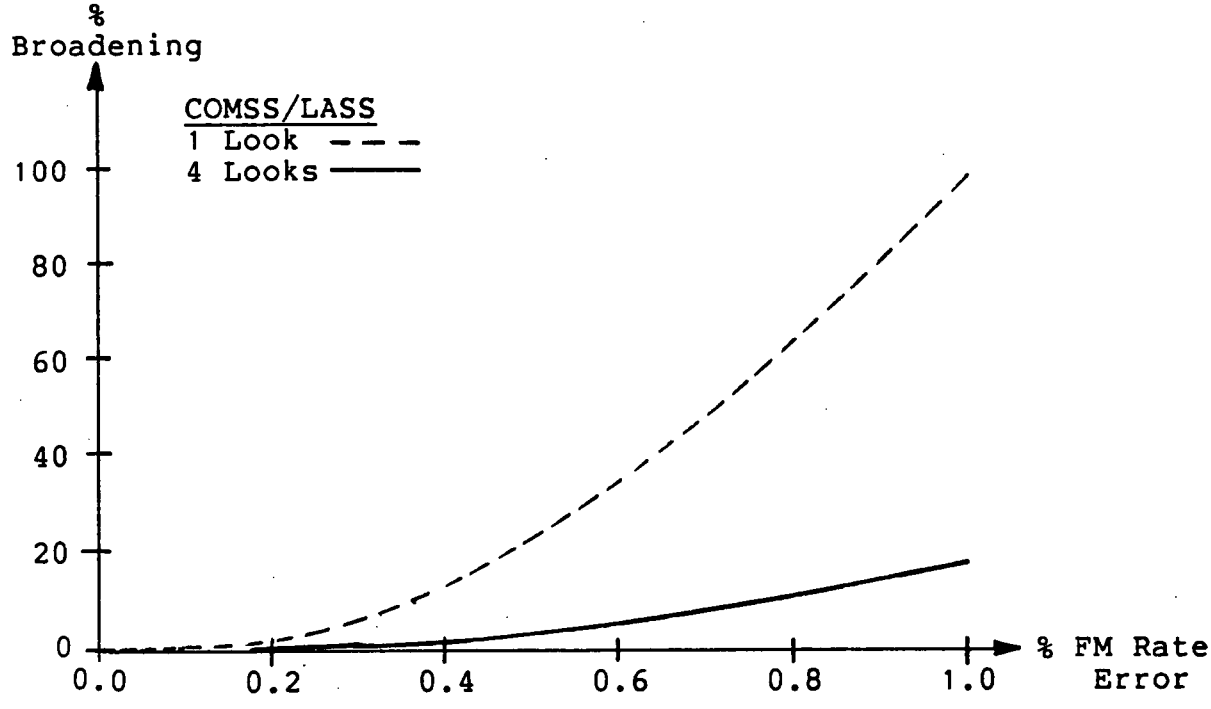

fine resolution aperture data has some additional effects. Since each look covers only a portion of the aperture, the data in each look does not cover as broad a portion of the frequency spectrum as for the single-look case. Therefore, the % broadening within each look is less than for the single-look case. However, the centre frequency of the individual looks is displaced causing misregistration of the output pulses between individual looks. This contributes to the broadening of the final output pulse when the looks are summed together. The effect is illustrated in Figure 12. Because the resolution of the final output image is decreased for the multi-look situation, the actual % broadening of the output pulse is significantly less for that case.

The next most striking fact about the results obtained is that there is a great variation between the three SAR systems used. This can be attributed to the variation in the extent of the processed signal aperture in terms of the number of samples, T/Δ. Due to the exact time-frequency correspondence of the linear FM signal, the actual frequency displacement of the azimuth signal at the ends of the aperture is much greater for the JPL Nominal system than for the COMMS/LASS system. Therefore, a given % FM rate error has a much more severe impact on the image quality obtained from the JPL Nominal system. FM rate error effects can be more easily studied analytically using the BPF SPECAN pulse compression approach as a vehicle and this has been done by MacDonald, Dettwiler and Associates [24]. Because the BPF SPECAN and step transform techniques essentially

Figure 12 - Effect of FM Rate Error on Addition of Looks for SEASAT Case

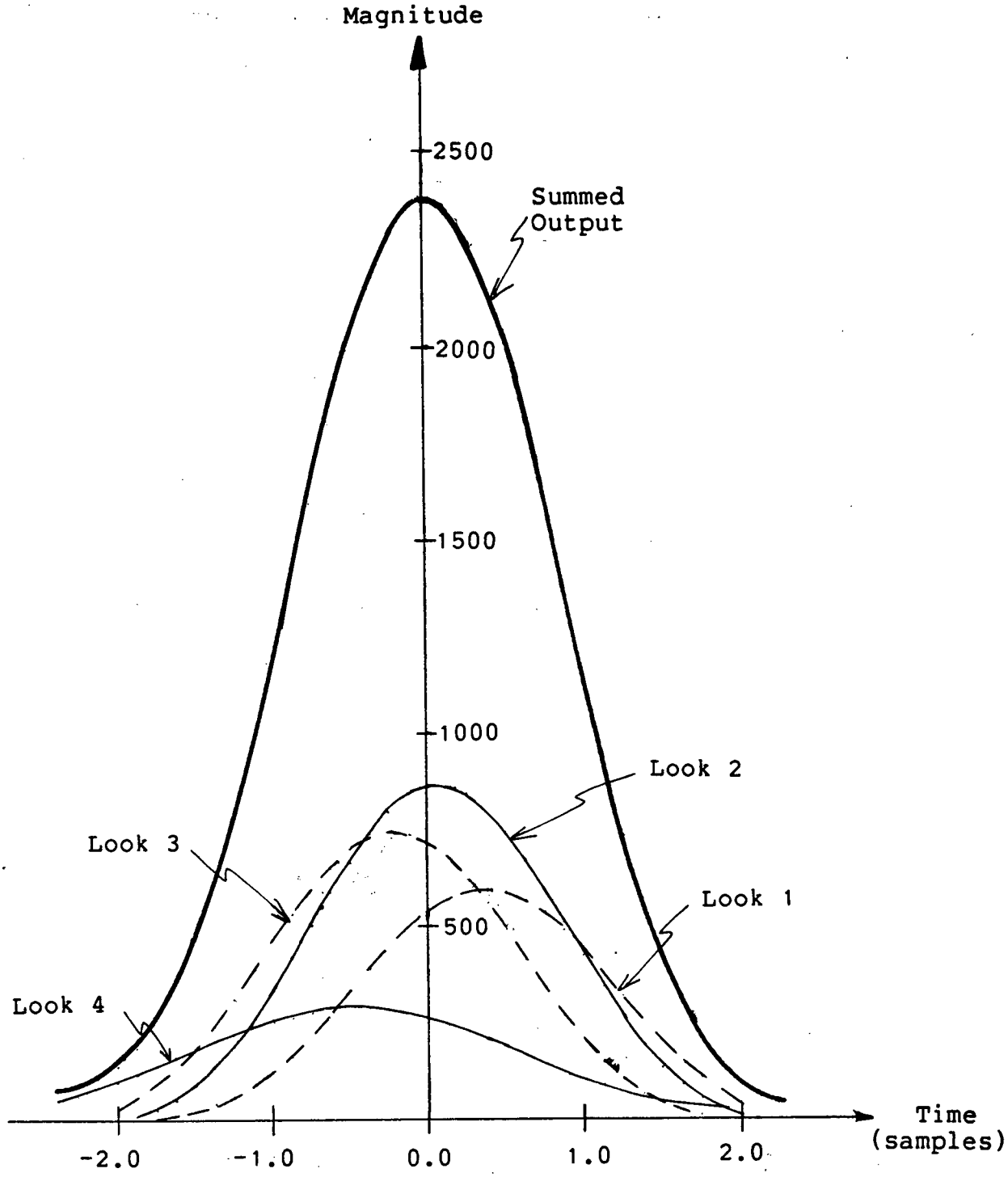

perform the same transformation on an input signal, it is expected that FM rate errors would have very similar effects on the output images of both. Although the results presented here and in [24] cannot be compared exactly, because different data windows were used and different approaches were taken to the measurement and analysis of the data, similar trends are demonstrated.

6.1.2 Frequency Step Mismatch

Another factor which must be considered when examining the effects of FM rate error, is that the step transform processing parameters may need to be changed as well. In particular, as the FM rate changes, the value of H or the frequency stepping between coarse resolution apertures will change as well. As was noted in Chapter III, it is necessary to maintain these steps close to an integer number of output bins. The principle means of making adjustments to compensate for this error is by adjusting the time, $N\Delta$, between successive coarse resolution apertures. However, this adjustment can only be made in increments of the sampling period (determined by the PRF) or integer values of N. For efficient FFT operation, the number of samples in the coarse resolution aperture must be a power of 2 and, therefore, cannot be used to do this finetuning.

The principle question which must be asked is whether adjustment of $N\Delta$ by integer values of N provides a sufficient degree of accuracy. In Sec. 3.1, it was shown that the stepping

between coarse resolution apertures is

$$H = \frac{BT'\Delta N}{T} \quad \text{output bins.}$$

Substituting the FM rate $K = B/T$, $H = KT'\Delta N$ output bins. For two different coarse resolution aperture separations

$$N_1 - N_2 = \frac{H}{K_1 T'\Delta} - \frac{H}{K_2 T'\Delta}$$

$$= \frac{H}{T'\Delta}\left(\frac{K_2 - K_1}{K_1 K_2}\right) \qquad (8)$$

As explained before, the minimum adjustment for N is 1, and, therefore the minimum value of $N_1 - N_2$ is 1. Thus

$$K_2 - K_1 = \frac{K_1 K_2 T'\Delta}{H}$$

Assuming $K_2 \cong K_1$ and substituting $K_1 = K_2 = K$ on the righthand side,

$$\frac{K_2 - K_1}{K} = \frac{KT'\Delta}{H}$$

$$= \frac{KT'\Delta}{H} \cdot 100\ \%\ \text{change in FM rate.}$$

Noting that $H = KT'\Delta N$ and assuming $N_1 \cong N_2 = N$, the % change in FM rate can also be expressed by the following equation

$$\frac{K_2 - K_1}{K} \cong \frac{1}{N} \cdot 100\ \%$$

Using the data in Appendix C, we see that the change in FM rate is

1) for SEASAT, 2.4 %

2) for JPL Nominal, 1.7 %

3) for COMSS/LASS, 6.3 %.

It can be seen that incrementing N by 1 does not provide a fine enough adjustment for FM rate change compensation. In order for this method to be used, the value of N would have to be on the order of 1000. (For N=1000, $(K_2-K_1)/K \cong 0.1\%$). This is clearly not feasible, since it is required that $(T'/N\Delta) > 2$ to prevent aliasing effects. For example, in the COMSS/LASS case, $T/\Delta = 1081$ samples. There are also upper limits on the value of T' imposed by the RCMC requirements, as is discussed in the following section. Thus it is apparent that, at least for the three satellite SAR systems described here, it is not possible to rely on this simple method of parameter adjustment for FM rate errors.

An alternative method might be provided as follows. It is possible to give the appearance of non-integer values of N by recalculating the reference function for each new position so that the ramp occupies a slightly displaced time segment, but still has its zero frequency at the proper time position. In this way, the reference ramps are spaced at non-integer values of N and, thereby, achieve the correct value of H. This would not affect the theoretical analysis of Chapter III, since one end of the ramp is being extended and the other end deleted. The important phase factors, i.e. the linear FM factor for input to the fine resolution FFT and the quadratic phase correction term, are still present. Perry and Martinson, in their theoretical analysis of the step transform [29], suggest that such an adjustment may be necessary in some cases.

However, a significant price is paid for this solution in that the reference must be recalculated for each instance or a number of different reference ramps must be stored. For example, if the required value of N is 38.2, there would be 4 possible reference ramp positions between samples and 5 different reference functions would be required. Therefore, the accuracy required of N must be determined in order to get some idea of the number of reference functions which must be used. Thus, returning to equation (8),

$$N_1 - N_2 = \frac{H}{T'\Delta}\left(\frac{K_2-K_1}{K^2}\right)$$

$$= N\left(\frac{K_2-K_1}{K}\right)$$

The inverse of this value is the number of reference functions required. In the previous section, it was demonstrated that, for a given % broadening of the main lobe, the three SAR systems exhibit very different FM rate accuracy requirements. If it is assumed that 10% broadening is the most that can be tolerated, the following results are obtained for the 4-look case:

1) for SEASAT, 0.06 % FM rate accuracy or approximately 17 different reference functions,
2) for JPL Nominal, 0.04 % FM rate accuracy or approximately 17 different reference functions,
3) for COMSS/LASS, 0.8 % FM rate accuracy or approximately 8 different reference functions.

6.2 Range Cell Migration

The range cell migration problem arises due to the fact that the azimuth signal does not lie in a single range cell, as shown in equation (5) of Sec. 5.1. Depending on the extent of the migration, it may not be possible to complete the step transform processing without some corrections. Ideally, each target would be corrected individually in situations where RCMC is required. However, this results in excessive amounts of processing. Therefore, ways of isolating groups of targets which can be corrected at the same time are sought.

In the step transform process, groups of targets are isolated by the coarse resolution FFT. Each FFT output bin contains phase and magnitude information relating to a certain number of targets which are closely grouped together. Furthermore, this information is isolated to a known segment of the azimuth signal because of the unique time-frequency relationship of the linear FM signal. It may be possible to move the data in each FFT output bin by an appropriate number of range cells to achieve the desired correction. Admittedly, this will not correct each target exactly. However, if the errors are sufficiently small so that image quality remains acceptable, the computation savings will certainly make it worthwhile.

In order to determine the feasibility of performing RCMC in such a manner, it is first necessary to analyze the range cell migration phenomenon in greater depth. Often for satellite systems, there is no mechanism to adjust the alignment of the antenna beam centre with respect to the zero Doppler line.

However, it is possible to determine the offset of the beam. Equation (5) of Sec. 5.1 may be modified to express target range as a function of azimuth time with respect to the beam centre crossing. Substituting $\eta = \eta_{BX} + \eta_0$ into equation (5) we obtain

$$r(\eta_{BX}) = r_0 + \frac{V^2}{2r_0}\eta_0^2 + \frac{V^2}{r_0}\eta_0\eta_{BX} + \frac{V^2}{2r_0}\eta_{BX}^2$$

where η_{BX} = azimuth time referenced to beam centre crossing

η_0 = azimuth time offset of beam centre from zero Doppler

The first two terms represent the target range to the beam centre. Since the time offset of the beam centre, η_0, remains constant over relatively long periods of time, both these terms can be considered to be constant. The third term is known as range walk and represents a linear offset which can be corrected by a simple skewing operation prior to step transform processing. This process has been described in detail for a BPF SPECAN implementation of a SAR processor [24]. The same considerations apply to the step transform and the skewing operation is equally applicable, since it can be done prior to any other processing. Perry and Kaiser [28] briefly describe a similar RCMC method for their step transform processor. Since the application is an airborne SAR system, no further RCMC is required in that case.

The fourth term represents the quadratic component of RCM and must be considered more closely. In deciding whether it would be possible to correct for quadratic RCM after processing the coarse resolution FFT, there are two major issues which must

be considered. Firstly, within any one coarse resolution aperture, there must be enough signal from the point target so that the FFT can adequately filter the signal. Therefore, the QRCM should never be so severe that the azimuth signal migrates across more than one range cell in a single coarse resolution aperture. This implies that there is a maximum length for the coarse resolution aperture. Secondly, each coarse resolution FFT output bin contains data on targets at various range and azimuth positions in the same general area. In reality, each target follows its own path through signal memory and should be corrected individually. The errors introduced by applying the same correction to all targets in an output bin must be determined. This places an upper limit on the frequency range covered by each coarse resolution output bin and effectively places a lower limit on the length of the coarse resolution aperture in terms of the number of samples. Each of these limits will now be derived in a quantitative fashion.

The most severe QRCM occurs at the ends of the processed aperture, where $\eta_{BX} = T(1-\beta)/2$. Thus, QRCM at that point may be expressed as

$$QRCM_1 = \frac{V^2}{2r_o} (T(1-\beta)/2)^2$$

$$= \frac{V^2T^2}{8R_o} (1-\beta)^2$$

At the other end of that coarse resolution aperture $\eta_{BX} = T(1-\beta)/2 - T'$ and

$$QRCM_2 = \frac{V^2}{2r_o}(T(1-\beta)/2 - T')^2$$

$$= \frac{V^2}{2r_o}(T^2(1-\beta)^2/4 - T'T(1-\beta) + T'^2)$$

Therefore the extent of QRCM over that single aperture is

$$QRCM_1 - QRCM_2 = \frac{V^2T'}{2r_o}(T(1-\beta) - T') \quad m$$

$$= \frac{V^2T'}{2r_o\rho}(T(1-\beta) - T') \quad \text{range cells}$$

Assuming $T' << T(1-\beta)$,[12]

$$T' \cong (QRCM_1 - QRCM_2) \cdot \frac{2r_o\rho}{V^2T(1-\beta)}$$

To prevent undue pulse broadening in the range direction, the QRCM should be kept to less than 1 range cell over a coarse resolution aperture. Therefore, $QRCM_1 - QRCM_2 < 1$ and

$$T' < \frac{2r_o\rho}{V^2T(1-\beta)} \quad s$$

or

$$\frac{T'}{\Delta} < \frac{2r_o\rho}{V^2T(1-\beta)\Delta} \quad \text{samples}$$

Now, an expression for the lower limit on T' will be derived. There are T'/Δ coarse resolution FFT output bins, each covering a bandwidth of $KT\Delta/T'$ Hz or target information over a time period $T\Delta/T'$. Again, the situation where the QRCM is the

---

[12] The effects of this and another similar approximation are demonstrated at a later point.

most severe must be considered, i.e. the time $\eta_{BX} = T(1-\beta)/2$ to $\eta_{BX} = T(1-\beta)/2 - T\Delta/T'$. Therefore,

$$QRCM_1 = \frac{V^2T^2}{8r_o}(1-\beta)^2$$

and

$$QRCM_3 = \frac{V^2T^2}{2r_o}((1-\beta)^2/4 - (1-\beta)\Delta/T' + \Delta^2/T'^2)$$

so that,

$$QRCM_1 - QRCM_3 = \frac{V^2T^2\Delta}{2r_oT'}(1 - \beta - \Delta/T') \quad m$$

$$= \frac{V^2T^2\Delta}{2r_o\rho T'}(1 - \beta - \Delta/T') \quad \text{range cells}$$

Assuming $\Delta/T' << 1 - \beta$

$$QRCM_1 - QRCM_3 = \frac{V^2T^2\Delta(1-\beta)}{2r_oT'} \quad m$$

$$= \frac{V^2T^2\Delta(1-\beta)}{2r_oT'\rho} \quad \text{range cells}$$

Again, for $QRCM_1 - QRCM_3 < 1$ range cells,

$$T' > \frac{V^2T^2\Delta(1-\beta)}{2r_o\rho} \quad s$$

or

$$\frac{T'}{\Delta} > \frac{V^2T^2(1-\beta)}{2r_o\rho} \quad \text{samples}$$

The permissible range of values for T' for some typical SAR systems is presented in Table VIII. Since some appoximations were made to obtain the range of values for T', the actual QRCM

Table VIII - RCM Limits on Coarse Resolution Aperture Size

	Units	SEASAT	JPL Nominal	COMSS/LASS
Slant range	km	860	550	636
Minimum - T'	s	0.0246	0.0139	0.00122
Minimum - T'/Δ	samples	40	36	2
QRCM in sample for minimum T'	range cells	0.97	0.96	0.47
Maximum - T'	s	0.0801	0.0806	0.324
Maximum - T'/Δ	samples	132	210	535
QRCM over aperture for maximum T'	range cells	0.97	0.96	0.41

corresponding to each limit has been calculated. As can be seen from the figures, the approximations actually produce somewhat conservative estimates.

There are some situations where it may not be possible to accept the above restrictions placed on the value of T' including:

1) the two ranges of values specified for T' by the above calculations do not intersect,
2) the amount of uncorrected RCM produces unacceptable degradation of image quality,
3) the range of values for T'/Δ does not include a power of two (for efficient FFT computation).

In the above situations, a greater frequency resolution is required for a given amount of target return data. This

resolution can be obtained by padding the aperture with zeros. Note that the coarse resolution FFT output pulses will be broadened by using this technique. Care must be taken to provide sufficient overlapping of the apertures so that there are no aliasing problems with the fine resolution FFT data.

As an extension of this concept, an attempt could be made to define an optimum value of T' using the criterion that the product $(QRCM_1 - QRCM_2)(QRCM_1 - QRCM_3)$ be a minimum. It turns out that there is no absolute minimum for that product as a function of T'. However, it does have a negative slope and, therefore, lesser values are found for larger values of T'.

VII. IMPLEMENTATION ON SOME SATELLITE SAR SYSTEMS

In this chapter, an attempt will be made to draw together the conclusions which have been made about how individual factors affect the step transform technique. The process of parameter selection for the step transform will be described and the solutions arrived at for some typical SAR systems will be examined. Using that data, some observations are made about the performance of the step transform in terms of computation and memory requirements. This information allows us to make quantitative comparisons with other pulse compression techniques. Finally, some ideas are presented on what an implementation of a step transform SAR processor might look like.

7.1 Summary Of Processing Parameter Restrictions

The first parameter chosen is the length of the coarse resolution aperture. Table VIII specifies upper and lower limits on its value, in terms of time units and number of samples for the three SAR systems considered, based on RCMC considerations. For efficient FFT processing, the restriction that the number of samples must be a power of 2 is added. This still leaves several different values which can be chosen. Counterbalancing this is the consideration that there must be no significant aliasing between FFT output samples because the FFT is too short. This applies to the fine resolution FFT as well and, in that case, the number of looks, L, must be taken into

account. For this reason, $T'/\Delta L$ should be 16 or greater. A secondary consideration is that the value of T' indirectly affects the number of reference functions which must be stored by determining the value of N. The relationship between N and the number of reference functions is described in Sec. 6.1.2.

Once a value of T' has been chosen, it is possible to determine the spacing between the reference ramps using the formula $H = BT'\Delta N/T$, noting that H must be an integer. The number of possible values for N is reduced by noting that the overlap ratio $T'/N\Delta$ should be sufficiently large to prevent any significant aliasing of the coarse resolution FFT output data. However, it is desirable to minimize $T'/N\Delta$ since it plays a very significant role in determining the computation rates and memory requirements.

After choosing the value of N, and thereby specifying the overlap ratio $T'/N\Delta$, it is possible to choose an optimal window for the coarse resolution aperture using data such as that presented in Table II. Note that Table II gives only a partial selection of possible windows since some, eg. Kaiser-Bessel, actually offer a continuum of choices using the parameter α. The data window for the fine resolution aperture is determined by the requirements of the final output pulse in terms of the mainlobe width and sidelobe levels.

7.2 Parameters Chosen For Typical SAR Systems

Since each of the example SAR systems chosen for consideration is somewhat unique in its properties and the challenges it presents, they will be discussed on an individual basis. In each case, the slant range was reduced to obtain parameters which would result in an integer value of N for use in the simulation program. The slant range was not increased since Appendix C specifies the maximum slant range for each system.

SEASAT

The most challenging problem posed by the SEASAT SAR system for any azimuth correlation algorithm is the significant amount of QRCM. As can be seen from Table VIII, the coarse resolution aperture size is basically limited to two choices, 64 and 128 samples. Both choices permit four-look processing, which is what SEASAT is designed for. To determine the spacing of the reference ramps at the maximum slant range, the formula $H = BT'\Delta N/T$ is used and shows that for $T'/\Delta = 128$ samples, $N = 41.7$ and $H = 1$. The system parameters were modified as specified in Appendix C to allow an integer value of N to be used in the simulation program. A 64 sample aperture cannot be used because it results in a situation where $H < 1$ and there is aliasing of the data in the fine resolution FFT's.

JPL Nominal

This system is quite similar to the SEASAT SAR, except that the RCM problem turns out to somewhat less severe, as demonstrated in Table VIII. On the other hand, the FM rate changes much more quickly than in the other cases. Also the data rate is greater, which has a significant effect on the processing rate. There are still only two different choices for the size of the coarse resolution aperture. Using the system parameters for the maximum slant range, for T'/Δ = 128 samples, N = 58.9 and H = 1. The modified system and processing parameters for this case are specified in Appendix C. Once again, the 64 sample aperture cannot be used because of aliasing effects.

COMSS/LASS

The COMSS/LASS system is the least demanding of the three systems, in that the RCM problem is not nearly as great as in the other two systems. This means that much less overlapping of the processing swaths is required, with a corresponding decrease in the excess computation capacity and memory requirements.

Using the same method as for the previous two systems, the following results apply at the maximum slant range:

1) for T'/Δ = 128 samples, N = 33.5 and H = 4,

2) for T'/Δ = 64 samples, N = 16.8 and H = 1.

Again the case where H = 1 is chosen, since the fine resolution aperture contains 64 samples versus 32 for the other case. This allows greater flexibility in choosing the number of looks.

Note from Appendix C that the chosen processing parameters for the COMSS/LASS system result in a high overlap ratio. Because of the limited choice of values for H, the next smallest overlap ratio which could be used was approximately 1.9. From Table II, it will be seen that there are no windows listed except the boxcar which can be used with such a small overlap ratio. From the data presented, it is surmised that any such window would have sidelobe levels of 25 - 30 dB. The step transform would produce processing artifacts at those levels and the image quality would not be acceptable. This decision has a significant effect on the computation rates and memory requirements discussed in the next section.

7.3 Computation Rates And Memory Requirements

The information presented in Chapters V and VI reveals that there are some additional considerations which must be taken into account in addition to those presented in Sec. 4.2 and 4.3 when determining the computation and memory requirements.

One of the significant aspects of SAR signal processing is that the output is a two dimensional image. Thus the calculations made previously in Chapter IV must be expanded to take account of those aspects. Because of the RCM phenomenon, it is necessary to have several azimuth lines of data stored in memory in order to compress even a single point target. In practice, azimuth processing is done in range subswaths which are of a manageable size in terms of memory storage

requirements, yet allow azimuth processing to be completed for a significant number of azimuth lines. Thus, the amount of overlapping of the range subswaths does not become a significant burden. In order to produce a standardized comparison, the computation rates, calculated for the three SAR systems specified in Appendix C, will be expressed quantitatively in terms of the number of complex multiplications per second (cmps) required to produce an image of 128 azimuth lines in real time. The specific computational stages considered will be those relating to the pulse compression operation itself. Linear RCMC and look summation requirements will not be considered since they are the same for all approaches. The requirement to correct QRCM will be considered quantitatively only in the amount of overlapping required in the range subswaths.[13] Thus, processing is performed over (128 + QRCM) azimuth lines before RCMC and 128 azimuth lines after RCMC.

Another factor which must be considered is the azimuth time extent of the image to be produced. It will be necessary to validate or reject the assumption made in Chapter IV that the processed portion of a point target return signal is small in comparison to the full time extent of the processing region, i.e. the assumption that the regions of rejected data in Figure 5 are small. This will be done by computing the number of data points not used and the amount of processing done on them.

---

[13] In general, it is necessary to perform some sort of interpolation to reduce pulse broadening sufficiently in the range direction. This must be done for each input point to the fine resolution FFT.

Thus, the processing requirements at each stage are as follows:

1) Reference Function Multiply - $F\cdot(128 + QRCM)\cdot(T'/N\Delta)$ cmps,

2) Coarse Resolution FFT - $F\cdot(128 + QRCM)\cdot(T'/N\Delta)\cdot\log_2\{T'/\Delta\}/2$ cmps,

3) Quadratic Phase Correction - $F\cdot(128 + QRCM)\cdot(T'/N\Delta)$ cmps,

4) Fine Resolution FFT Window - $64F\cdot(T'/N\Delta)\cdot(1-\beta)$ cmps for the single look case and $64F\cdot(T'/N\Delta)$ cmps for the multi-look case,

5) Fine Resolution FFT - $64F\cdot(T'/N\Delta)\cdot\log_2\{T'/\Delta L\}$ cmps,

6) Scaling - $64F/L$ cmps.

The amount of rejected data is essentially equal to the time extent of the processed signal aperture, T/Δ. The coarse resolution aperture FFT and reference function multiply are the only computations which must be performed on this data. Therefore, the number of complex multiplications is $(128 + QRCM)(T/\Delta)(T'/N\Delta)$ for the multiply operation and $(128 + QRCM)TT'\cdot\log_2\{T'/\Delta\}/2N$ for the FFT.

Memory requirements may be computed as follows, assuming that each complex number occupies 1 word of memory. A single coarse resolution aperture must be stored ahead of the reference function multiply requiring $(128 + QRCM)T'/\Delta$ words of memory. For all of the systems considered here, processing parameters have been chosen such that $H = 1$. The reorder memory, therefore, requires approximately $T'^2/2\Delta^2$ words per range line or $(128 + QRCM)T'^2/2\Delta^2$ words per swath. Look summation memory requirements are not included since they are the same for all

Table IX - Memory Requirements and Computation Rates

	SEASAT		JPL Nominal		COMSS/LASS	
Looks	1	4	1	4	1	4
Computation Rates (x 10^6 cmps)						
Reference Function Multiply	0.7	0.7	0.8	0.8	0.9	0.9
Quadratic Phase Correction	0.7	0.7	0.8	0.8	0.9	0.9
Coarse Resolution FFT	2.5	2.5	2.8	2.8	2.6	2.6
Fine Resolution Aperture Window	0.3	0.3	0.3	0.4	0.4	0.4
Fine Resolution FFT	2.3	1.7	2.6	1.8	2.5	1.7
Scaling	0.1	-	0.2	-	0.1	-
Total	6.6	5.9	7.5	6.6	7.4	6.5
Complex Multiplies on Rejected Data (x 10^6)						
Reference Function Multiply	2.3	2.3	2.3	2.3	0.6	0.6
Coarse Resolution FFT	8.1	8.1	8.1	8.1	1.7	1.7
Total	10.4	10.4	10.4	10.4	2.3	2.3
Memory (x 10^6 words)						
Coarse Resolution Aperture	0.02	0.02	0.02	0.02	0.01	0.01
Reorder Memory	1.1	1.1	1.1	1.1	0.3	0.3
Total	1.12	1.12	1.12	1.12	0.31	0.31

approaches.

Examining Table IX, it can be seen that the computation requirements are amazingly similar for all three systems, in spite of the wide disparity in sampling rate and number of samples in the processed signal aperture. This is due, in large part, to the moderating effect of the overlap ratio. Note that there is a significant disparity in memory requirements, which are determined by the number of samples in the coarse resolution aperture. In calculating the amount of computation on the rejected data, it is seen that the JPL Nominal and SEASAT systems exhibit similar requirements, due to the effect of the overlap ratio. However, for the COMSS/LASS situation, the processed aperture is much shorter and is the overwhelming influence.

7.4 Comparison With Other Techniques

The results of the previous section demonstrate that the hardware requirements to perform step transform pulse compression do not always turn out as one would expect for a given set of system parameters, but are also heavily influenced by the processing parameter requirements of the step transform. In order to arrive at some general conclusions, it is necessary to derive some results which demonstrate a general trend and to support those results with some specific examples. Comparisons will be made with three other pulse compression techniques described in Chapter II; time-domain convolution, fast

convolution and bandpass filter spectral analysis. Initially, a generalized comparison will be done to show the major trends. Then, the computation rates will be calculated for the three systems specified in Appendix C, using the same assumptions as in the previous section for the step transform.

7.4.1 General Comparison

Computation rates will be expressed as the number of complex multiplications required to produce a single point of output data. RCMC requirements are not taken into account, since a specific system is not considered. The results are expressed as a function of the number of samples in the processed signal aperture, M, and the number of looks, L, and are displayed graphically in Figure 13. FFT processing efficiency is assumed to be equivalent to that achieved for power of 2 FFT lengths.

Time-Domain Convolution

The time-domain convolution approach is generally characterized as having large computation rates and small memory requirements. For multi-look processing, frequency translation and lowpass filtering must be done to extract data for the individual looks. For satellite systems, the antenna may not always be pointing broadside. Therefore, the beam centre may not always be aligned with the zero Doppler frequency and we will assume that these two stages must be performed for

single-look processing as well. Frequency translation requires 1 complex multiplication per point (cmpp) for each look or L cmpp in total. Lowpass filtering is done using a 16-point non-recursive digital filter which requires the equivalent of 2 complex multiplies per point or 2L cmpp. The filter output can be subsampled by a factor L. Therefore, the correlation function is M/L^2 complex words for each look and the azimuth correlator requires M/L cmpp. Therefore, the total number of computations per point is

$$CP = 3L + M/L \quad \text{cmpp.}$$

Fast Convolution

If it is assumed that the forward FFT's are overlapped by 50% [14], each FFT is 2M/L samples long. $M \cdot \log_2\{2M/L\}/L$ complex multiplications are required for each FFT aperture. The matched filtering stage requires 2M/L complex multiplications. The inverse FFT's are of length $2M/L^2$ and require $M \cdot \log_2\{2M/L^2\}/L^2$ complex multiplications each or $M \cdot \log_2\{2M/L^2\}/L$ complex multiplications per aperture. Processing of each aperture produces M/L valid output points. Therefore,

$$CP = \log_2\{2M/L\} + 2 + \log_2\{2M/L^2\}$$

$$= 4 + 2 \cdot \log_2\{M\} - 3 \cdot \log_2\{L\} \quad \text{cmpp.}$$

---

[14] The FFT overlap determines the tradeoff between computation and memory requirements. If the overlap is reduced to 25%, the computation rate is decreased by approximately 20 - 25 % and the memory requirements are doubled. The 50% value was chosen here, since it results in comparable memory requirements for the step transform and fast convolution methods. This is demonstrated for some specific SAR systems in the next section.

Figure 13 - Generalized Computation Requirements as a Function of Signal Aperture Extent

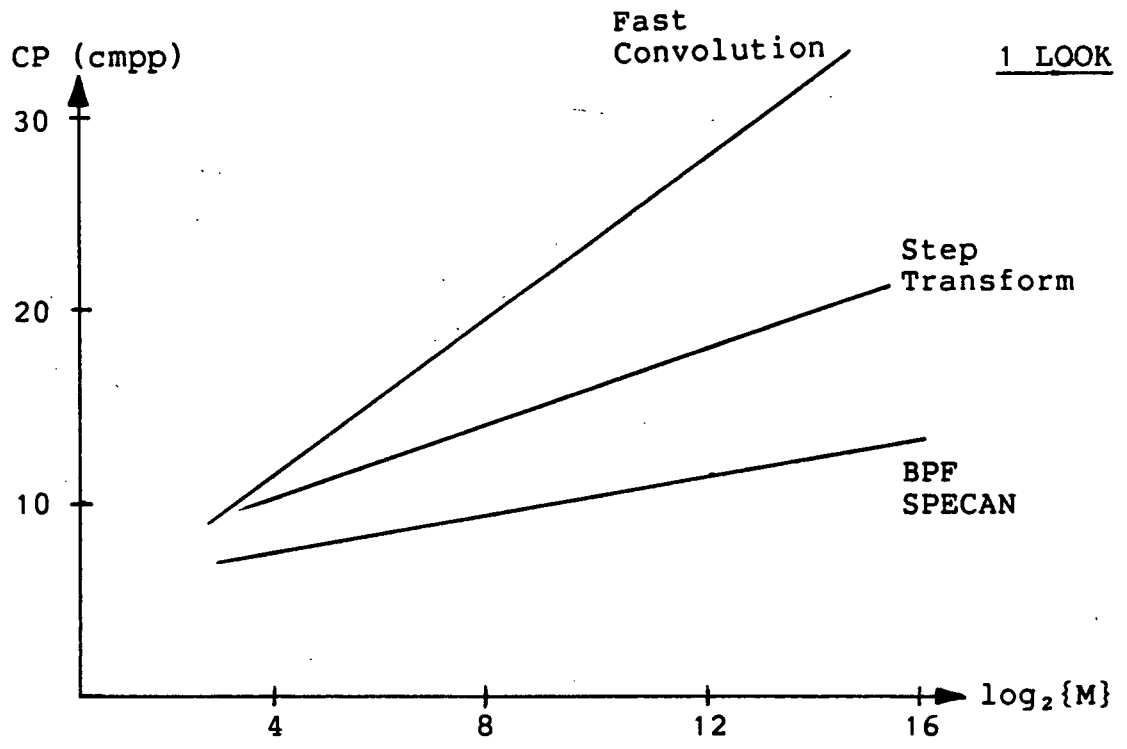

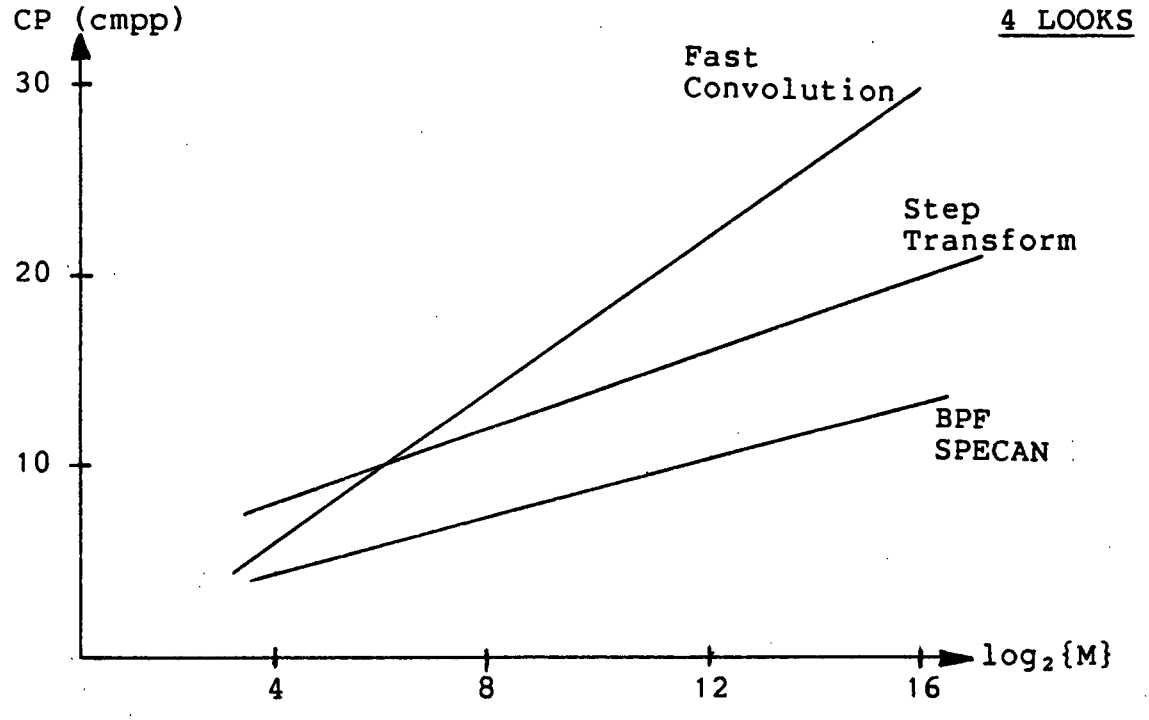

Bandpass Filter Spectral Analysis

The bandpass filter spectral analysis technique requires that the number of bandpass filter channels be chosen. The major considerations which determine the number of channels required are based on the extent of QRCM. For the purposes of this discussion, it is assumed that 16 channels are required. The first stage is the reference function multiply which requires 1 cmpp. Bandpass filtering and subsampling are performed as a single operation and requires 6 cmpp [24]. The FFT's are approximately M/16L samples long and each require $M \cdot \log_2\{M/16L\}/32L$ complex multiplications. There are 16L FFT's for every M points requiring $\log_2\{M/16L\}/2$ cmpp. The FFT input data must also be windowed, requiring 0.5 cmpp. Therefore,

$$CP = 7.5 + \log_2\{M/16L\}/2$$
$$= 5.5 + (\log_2\{M\} - \log_2\{L\})/2 \quad \text{cmpp.}$$

Step Transform

For the step transform, it is necessary to make some assumptions about the processing parameters to be used in order to show a general result, as for the previous approaches. Therefore, the following values are specified:

$$T'/N\Delta = 2 \text{ and}$$
$$H = BT'\Delta N/T = 1.$$

For convenience, assume $B = 1$, $T = M$ and $\Delta = 1$.

Therefore, $M = T'\Delta N$

$$\doteq T'^2/2.$$

The number of samples in each coarse resolution aperture is

SQRT{2M}. Therefore, using the expression for CP as derived in Sec. 4.2, with appropriate modifications for multi-look processing,

$$CP = 6 + \log_2\{M\} - \log_2\{L\} + 1/4L \quad \text{cmpp.}$$

7.4.2 Comparisons For Specific SAR Systems

In this section, computation rates and memory requirements are computed for three SAR systems, using the same criteria as for the step transform in Sec. 7.3. The number of samples in the signal aperture is $T(1-\beta)/\Delta$. Results are presented in Table X.

Time-Domain Convolution

For this approach, quadratic RCMC is done during the convolution operation. Range swaths are overlapped for frequency translation and lowpass filtering. Therefore, computation rates may be calculated as follows:

1) Frequency Translation - (128 + QRCM)FL cmps,
2) Lowpass Filtering - 2FL(128 + QRCM) cmps,
3) Convolution - $128F \cdot T(1-\beta)/\Delta L$ cmps.

Memory requirements are one look extent for each range cell or $128T(1-\beta)/\Delta L$ words. Memory requirements for the filter and correlator are negligible.

Fast Convolution

The fast convolution approach requires an appropriate

Table X - Memory Requirements and Computation Rates for Alternative Approaches

	SEASAT		JPL Nominal		COMSS/LASS	
Looks	1	4	1	4	1	4
Computation Rate (x 10^6 cmps)						
Time-Domain Convolution	956	62	2134	137	195	14.7
Fast Convolution	6.9	6.4	8.2	7.7	4.6	4.2
Bandpass Filter Spectral Analysis	2.4	2.2	4.4	4.0	2.2	2.0
Step Transform	6.6	5.9	7.5	6.6	7.4	6.5
Memory (x 10^6 words)						
Time Domain Convolution	0.7	0.17	1.0	0.24	0.14	0.03
Fast Convolution	1.1	0.3	2.3	0.6	0.26	0.07
Bandpass Filter Spectral Analysis	0.4	0.4	0.6	0.6	0.08	0.08
Step Transform	1.1	1.1	1.1	1.1	0.31	0.31

choice of FFT length to achieve an adequate compromise between computation and memory requirements. Here, the FFT length P is chosen to be approximately double the length of the matched filter $T(1-\beta)/\Delta L$. For efficient processing, the closest power of 2 is chosen. The single-look FFT lengths used are 8192 samples for SEASAT, 16384 samples for JPL Nominal and 2048 samples for COMSS/LASS. The computational requirements may be computed by considering that $T(1 - \beta)/\Delta L$ data points must be

rejected. Thus, the computation rate is calculated as follows:

1) Forward FFT - $P \cdot \log_2\{P\}/2$ complex multiplications per FFT or $F \cdot (128 + QRCM) \cdot P \cdot \log_2\{P\}/2(P - T(1-\beta)/\Delta L)$ cmps,

2) Matched Filter - P complex multiplications per aperture or $128FP/(P - T(1-\beta)/\Delta L)$ cmps,

3) Inverse FFT's - L FFT's of length P/L per aperture requiring $P \cdot \log_2\{P/L\}/2L$ complex multiplications each or $64P \cdot \log_2\{P/L\}/(P - T(1-\beta)/\Delta L)$ cmps.

Memory requirements are 1 full FFT aperture per range bin or (128 + QRCM)P words per range swath.

Bandpass Filter Spectral Analysis

Computation rates are as follows:

1) Reference Function Multiply - $F \cdot (128 + QRCM)$ cmps,

2) Bandpass Filtering - $6F \cdot (128 + QRCM)$ cmps,

3) FFT's - the length, P, of the FFT's is 64, 256 and 512 samples respectively for the single-look COMSS/LASS, SEASAT and JPL Nominal cases respectively. There are 16L FFT's every T seconds, requiring $128 \cdot 16P \cdot \log_2\{P/L\}/2T$ cmps per range swath.

4) Window - each FFT aperture must be windowed, requiring $128 \cdot 16P/2T$ cmps.

The main memory requirements are determined by the input buffer requirements for the FFT's. A similar scheme to that employed for the step transform may be used so that only a triangular region of data must be stored [24]. Since the outputs of the bandpass filters are oversampled by a factor of 1.33, the memory

requirements are $1.33(128 + QRCM) \cdot T(1 - \beta)/2\Delta$.

7.4.3 Remarks On Computation Rates

The most significant conclusions can be drawn from the general results presented in Sec. 7.4.1. Figure 13 demonstrates that, for the vast majority of systems, the BPF SPECAN approach is the most efficient. It is evident that the crossover point with the fast convolution technique moves to the right as the number of looks is increased. Thus, there are certain situations, when a large number of looks is required, where the fast convolution technique is more efficient than both the BPF SPECAN and the step transform. But, the step transform virtually never has an advantage over the BPF SPECAN approach in terms of these criteria. These conclusions are generally supported by the data in Table X. It is interesting to note that the ratio of the step transform to BPF SPECAN computation rates for those three systems is very close to the overlap ratio required in the step transform process for each of the systems.

A major additional consideration is the method of performing RCMC. This is particularly critical for systems which have a significant QRCM component, i.e. SEASAT and JPL Nominal. In this regard, time-domain convolution becomes extremely difficult to implement, since there is no way of separating groups of point targets to achieve some sort of block processing efficiency as part of the pulse compression algorithm. The fast convolution technique presents a viable

alternative in this regard, in that when the forward FFT is performed, all of the targets are superimposed on each other in signal memory and they can all be corrected at the same time. In the BPF SPECAN approach, the filters are used to separate groups of targets in close proximity and block processing efficiency is achieved by correcting the groups together. As was explained in Chapter IV, there are parallels between the step transform and BPF SPECAN approaches, in that they both separate out groups of targets. However, for cases of severe RCM, the BPF SPECAN technique holds certain advantages in flexibility. As shown in Table VIII, for the SEASAT case, there is basically one choice for the length of the coarse resolution aperture without making significant sacrifices in computation and memory requirements. In the BPF SPECAN technique, the equivalent choice which must be made is the number of bandpass filter channels. There tend to be less restrictions on the number of channels than on the coarse resolution aperture length.

For each of the systems, there are additional considerations which affect the complexity of the control logic. The variable antenna pointing angle of satellite SAR systems poses some significant complications for the fast convolution approach, in that the matched filter output function must be recalculated as the angle changes. For the step transform, the control logic must deal with the requirement for multiple reference functions. The BPF SPECAN approach is affected by the fact that the output sample rate varies with the FM rate and,

thus, slant range [24]. Considerable effort must be expended computationally to compensate for this effect.

The above discussion gives some indications of the hardware requirements of the step transform for azimuth SAR processing relative to some popular alternative approaches. As can be seen from the results, it is more efficient than general convolution algorithms in many situations, but is not competitive with bandpass filter spectral analysis, which is also specifically designed to filter linear FM signals.

7.5 Step Transform Processor Architecture

The basic design concept of the processor which will be proposed is similar to that of Martinson [25], in that both use a pipeline architecture. However, some adjustments must be made for the SAR situation. It is assumed that processing is done in range subswaths which correspond approximately to the FM rate error which can be tolerated. As was demonstrated in Sec. 6.1.1, this varies greatly for the three systems we have considered. Each range cell would essentially be processed by a separate pipeline and the pipelines would converge at certain points such as the reorder memory where RCMC must be performed. The pipeline processors would be grouped in range subswaths, each group being controlled by a separate control processor. Such an architecture bears similarities to a SIMD (single instruction stream, multiple data stream) machine, in terms of the usual classification system for multiprocessor

architectures. Alternatively, there could be only one group of processors which would process each subswath in turn. The control processor would be responsible for calculating the reference functions and determining the processing parameters and other variables such as rotation of the coarse resolution FFT outputs according to the beam centre offset. Figure 14 illustrates this configuration.

This approach has a reasonable degree of modularity. Therefore, it should be amenable to the design of basic system components which could be used in slightly different configurations for the different SAR systems and still retain basically the same computational rates as calculated previously for all of the systems.

Figure 14 - Step Transform Processor Architecture

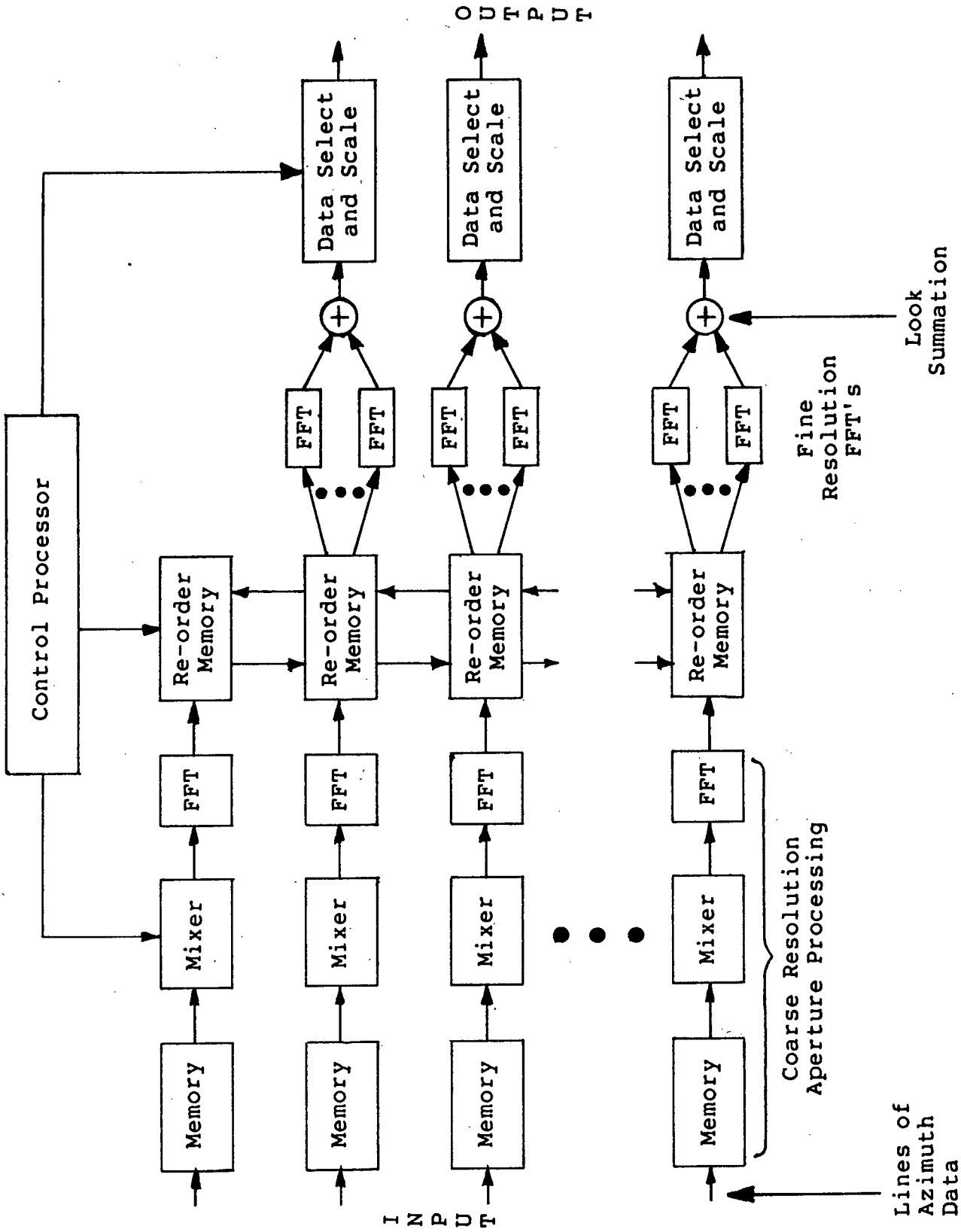

VIII. CONCLUSIONS

The step transform process has been described in great detail in the preceding chapters. In this chapter, the results which have been obtained will be summarized and some comments will be made about further work which must be done before the step transform could be implemented in actual applications, such as the SAR systems described in Appendix C.

8.1 Discussion

The step transform was originally developed for signal processing applications which present much less stringent demands than some of the SAR systems considered here. Perry and Kaiser consider use of a step transform processor in both conventional and synthetic aperture airborne radar applications [28]. Martinson describes some specifications of a step transform processor implementation which has only three different SAR focussing modes [25], indicating that the FM rate must only be adjusted to three different values over the full range swath. This is far different from the JPL Nominal SAR system, which is extremely sensitive to FM rate errors because of the large time extent of the processing aperture. These requirements significantly complicate the step transform as has been described in previous chapters.

Table X and Figure 13 show that the step transform is competitive with the fast convolution method in terms of computational requirements. In addition, its major use of the

very basic concepts of digital signal processing such as FFT's, data windows, and mixers should make the design of a step transform processor relatively straightforward, since all of the components have been studied in depth before. The major potential design problem is probably the design of the re-order memory, which is also used to correct QRCM when required. The challenge here is to ensure that both operations can be carried out efficiently without creating a major bottleneck in the process. The actual memory requirements should also be minimized in order for the step transform to be at all competitive, since Table X shows that the step transform has close to the highest memory requirements of any of the approaches considered.

Most other pulse compression applications present less stringent requirements. For example, in normal radar systems, the pulse generator is part of the same system and could be designed partly for optimum step transform processing. Essentially, the designer only needs to have control over one of the system parameters, such as the sampling frequency or the FM rate. Therefore, one would not have to worry about problems such as frequency step mismatching as described in Sec. 6.1.2. However, it is possible that other approaches to pulse compression would also be simplified in such applications and it would be necessary to perform some analysis of the individual application to make some judgment on the relative merits of each approach. No attempts are made to do that here. It should be noted, however, that in Chapters III and IV, the fundamental

concepts of the step transform are presented without regard to any particular application and would be useful in such an analysis.

8.2 Directions For Further Research

Many of the results presented in this thesis were derived using analytical methods. A computer simulation program was written to perform the step transform on a linear FM signal. This was useful in gaining a better understanding of how the step transform works and in confirming the analytical results. It was also used to examine FM rate error effects.

However, a SAR processor produces a two dimensional output image and the system must produce acceptable pulse compression in both azimuth and range directions. The major cause of image degradation in the range direction is inadequate RCMC, so that not all of the energy from a single point target is contained within a single range cell when the azimuth pulse compression operation is performed. In Sec. 6.2, some analysis was done on the basic limitations which must be placed on step transform processing parameters to allow RCMC to be performed efficiently. However, the actual RCMC technique proposed was not implemented in a simulation program. Therefore, the next major step in the study of the step transform would be to extend the simulation program to compress a point target with significant QRCM in two dimensions applying the RCMC techniques described previously. Examining the side lobe levels and main lobe width in the range

direction, it could be determined whether or not the limitations imposed on the step transform processing parameters are adequate. If not, the alternative of padding the coarse resolution aperture with zeros would have to be implemented. This could seriously affect the computation rate and memory requirements and would have some effect on the competitiveness of the step transform relative to other approaches.

Before implementation of the step transform as a SAR processor, it would also be useful to obtain some further analytical results on the error effects. In particular, it is useful to use error budgeting techniques to indicate the degree of precision required of the processing algorithm. There are certain fixed errors which remain constant such as the FM rate estimation error. Deducting errors such as this from the total permissible FM rate error gives an indication of the maximum allowable error contribution from the pulse compression algorithm.

Because of the high computation rates required by satellite SAR systems, it is generally considered that hardware requirements for a SAR processor are dominated by the actual data processing function. Control functions are assumed to play a less significant role in determining the viability of a particular algorithm. Efforts to implement algorithms which de-emphasize control requirements, eg. the JPL work on the time-domain convolution technique [1] [37], have not been very successful. In this case, it was largely due to the slower-than-predicted advancement of VLSI technology. Control

structures are often implemented in software and the increasing dominance of software costs in most development projects makes it dangerous to ignore this facet of processor design. In previous chapters, some issues related to the control structure have been mentioned, but further work on this aspect is required.

8.3 Summary

The step transform process and its application to SAR azimuth processing has been examined in some detail. The requirements placed on the processing parameters and the selection of parameters for efficient computation have been described. Some of the restrictions placed on the parameters are fairly stringent and lead to similar hardware requirements for SAR systems which exhibit large disparities in their requirements for most other approaches. It was demonstrated that the step transform approach is more efficient than general matched filtering algorithms if it is possible to use crucial processing parameter values, such as the overlap ratio $T'/N\Delta$, which are close to the optimal for the step transform. This point is illustrated most clearly by the three SAR systems used to perform a quantitative analysis of the step transform relative to other approaches. The JPL Nominal system, with $T'/N\Delta = 2.21$, and the COMSS/LASS system, with $T'/N\Delta = 4.0$, exhibited approximately the same computational requirements. Yet, other approaches cut their computational requirements in

half for the COMSS/LASS system.

The step transform can be seen, therefore, as a significant step forward from general algorithms for the processing of linear FM signals. This breakthrough is made even more significant in light of the advent of satellite SAR systems, whose high computation rates make it extremely attractive to seek specialized processing techniques. The step transform is representative of a class of algorithms which perform the matched filtering operation on a continuous stream of data, rather than processing distinct blocks of data as in the fast convolution method. However, since the introduction of the step transform, a large amount of work has been done on the spectral analysis concept, including the development of the BPF SPECAN technique. Some parallels have been drawn between the step transform and the BPF SPECAN approaches in this paper.

In terms of the amount of computation, the step transform lies somewhere in between the fast convolution and BPF SPECAN approaches. For the design of multi-look SAR processors, both the BPF SPECAN and step transform have the advantage that multi-look processing is a relatively minor consideration in most cases, and only impacts one stage of the algorithm. This provides an added degree of flexibility over the fast convolution technique.

In comparing the BPF SPECAN and step transform, the major issue besides computation rates is the processing of the output data. The BPF SPECAN requirement to process the output data to obtain a uniform data rate over the full range swath brings it

somewhat more in line with the step transform, which has greater computational requirements and control complexity within the algorithm itself.

BIBLIOGRAPHY

1. Arens, W. E. "Real Time Synthetic Aperture Radar Processing for Space Applications", Real-time Signal Processing, Proc. Soc. Photo-Opt. Instr. Eng. 154, 14-21(1978).

2. Barcilon, V., and G. C. Temes. "Optimum Impulse Response and the van der Maas Function", IEEE Trans. on Circuit Theory, vol. CT-19, no. 4, pp. 336-342, July 1972.

3. Bennett, J. R., and I. G. Cumming. "Digital SAR Image Formation Airborne and Satellite Results", 13th Int. Symposium on Remote Sensing of Environment, Ann Arbor, Michigan, April 1979.

4. ———. "Digital Processing of SEASAT SAR Data", Int. Conference on Acoustics, Speech and Signal Processing, Washington, D.C., April 1979.

5. Bennett, J. R., I. G. Cumming, and R. A. Deane. "The Digital Processing of SEASAT Synthetic Aperture Radar Data", IEEE International Radar Conference, April 1980, pp. 168-175.

6. Bennett, J. R., I. G. Cumming, and R. M. Wedding. "Algorithms for Preprocessing of SAR Data", Proc. ISPRS Commission II Symposium, Ottawa, Canada, August 1982.

7. Bennett, J. R., et al. "A Fast, Programmable Hardware Architecture for Spaceborne SAR Processing", Spaceborne Imaging Radar Symposium, JPL, Pasadena, Calif., January 1983.

8. Bennett, J. R., and P. R. McConnell. "Considerations in the Design of Optimal Multilook Processors for Image Quality", in Proc. of the 3rd SEASAT-SAR Workshop on 'SAR Image Quality', Frascati, Italy, December 1980, paper ESA SP-172.

9. Brown, W. M., and L. J. Porcello. "An Introduction to Synthetic-Aperture Radar", IEEE Spectrum, vol. 6, no. 9, pp. 52-62, September 1969.

10. Cutrona, L. J. "Synthetic Aperture Radar", in Radar Handbook, ed. M. I. Skolnik, pp. 23.1-23.25, New York: McGraw-Hill, 1970.

11. Dainty, J. C. Laser Speckle and Related Phenomena, Berlin:Springer-Verlag, 1970.

12. Darby, B. J., and J. M. Hannah. "Frequency Hop Synthesizers Based on Chirp Mixing", Int. Specialist

Seminar on Case Studies in Advanced Signal Processing, Institution of Electrical Engineers, pp. 97-101, September 1979.

13. Elachi, C., et al. "Spaceborne Synthetic-Aperture Imaging Radars: Applications, Techniques, and Technology", Proceedings of the IEEE, vol. 70, no. 10, pp. 1174-1209, October 1982.

14. Ellis, A. B. E. "A Proposed Method for Digitally Processing SAR Data from a Satellite", Int. Specialist Seminar on Case Studies in Advanced Signal Processing, Institution of Electrical Engineers, pp. 155-160, September 1979.

15. Ford, J. P. "Resolution Versus Speckle Reduction Relative to Geologic Interpretability of Spaceborne Radar Images: A Survey of User Preference", IEEE Trans. on Geoscience and Remote Sensing, vol. GE-20, no. 4, pp. 434-444, October 1982.

16. Harris, F. J. "On the Use of Windows for Harmonic Analysis with the Discrete Fourier Transform", Proceedings of the IEEE, vol. 66, no. 1, pp. 51-83, January 1978.

17. Helms, H. D. "Digital Filters with Equiripple or Minimax Responses", IEEE Trans. on Audio and Electroacoustics, vol. AU-19, no. 1, pp. 87-93, March 1971.

18. Helms, H. D. "Nonrecursive Digital Filters: Design Methods for Achieving Specifications on Frequency Response", IEEE Trans. on Audio and Electroacoustics, vol. AU-16, no. 3, pp. 336-342, September 1968.

19. Hidayet, M., and P. A. McInnes. "On the Specification of an Antenna Pattern for a Synthetic Aperture Radar", Radar-77 International Conference, Institution of Electrical Engineers, October 1977, pp. 391-395.

20. Kirk, J. C. "A Discussion of Digital Processing in Synthetic Aperture Radar", IEEE Trans. on Aerospace and Electronic Systems, vol. AES-10, no. 3, pp. 326-337, May 1975.

21. Kuhler, D. "Application and Limitation of Very Large Scale Integration in SAR Azimuth Processing", Proceedings of the 1978 Synthetic Aperture Radar Technology Conference, New Mexico State University, Las Cruces, N.M., March 1978, paper V-7.

22. Lee, J. S. "A Simple Speckle Smoothing Algorithm for Synthetic Aperture Radar Images", IEEE Trans. on Systems, Man, and Cybernetics, vol. SMC-13, no. 1, pp. 85-89, January/February 1983.

23. Lynch, D. "Signal Processor for Synthetic Aperture Radar", Real-time Signal Processing II, Proc. Soc. Photo-Opt. Instr. Eng. 180, 225-229(1979).

24. MacDonald, Dettwiler and Associates. The Design of a Digital Breadboard Processor for the ESA Remote Sensing Satellite Synthetic Aperture Radar Final Report, European Space Agency Report No. 276, Doc. No. 00-0636, July 1981.

25. Martinson, L. W. "A Programmable Digital Processor for Airborne Radar", IEEE International Radar Conference, April 1975, pp. 186-191.

26. Martinson, L. W., and J. A. Lunsford. "A CMOS/SOS Pipeline FFT Processor - Construction, Performance, and Applications", IEEE National Aerospace and Electronics Conference, May 1977, pp. 574-579.

27. Moore, C. UBC CURVE - Curve Fitting Routines, Computing Centre, University of British Columbia, Vancouver, B.C., September 1981.

28. Perry, R. P., and H. W. Kaiser. "Digital Step Transform Approach to Airborne Radar Processing", IEEE National Aerospace and Electronics Conference, May 1973, pp. 280-287.

29. Perry, R. P., and L. W. Martinson. "Radar Matched Filtering" in Radar Technology, ed. E. Brookner, ch. 11, pp. 163-169, Dedham, MA: Artech House, 1977.

30. Porcello, L. J., et al. "Speckle Reduction in Synthetic-Aperture Radars", Journal of the Optical Society of America, vol. 66, no. 11, pp. 1305-1311, November 1976.

31. Purdy, R. J. "Signal Processing Linear Frequency Modulated Signals", in Radar Technology, ed. E. Brookner, ch. 10, pp. 155-162, Dedham, MA: Artech House, 1977.

32. Søndergaard, F. "A Dual Mode Digital Processor for Medium Resolution Synthetic Aperture Radars", Radar-77 International Conference, Institution of Electrical Engineers, October 1977, pp. 384-390.

33. Tomiyasu, K. "Tutorial Review of Synthetic-Aperture Radar with Applications to Imaging of the Ocean Surface", Proceedings of the IEEE, vol. 66, no. 5, pp. 563-583, May 1978.

34. Tyree, V. C. "Custom Large Scale Integrated Circuits for Space-Borne SAR Processors", Proceedings of the 1978 Synthetic Aperture Radar Technology Conference, New Mexico State University, Las Cruces, N.M., March 1978, paper V-4.

35. van de Lindt, W. J. "Digital Technique for Generating Synthetic Aperture Radar Images", IBM Journal of Research and Development, vol. 21, no. 5, pp. 415-432, September 1977.

36. Wu, C. "Considerations on Real-Time Processing of Spaceborne Synthetic Aperture Radar Data", Real-time Signal Processing III, Proc. Soc. Photo-Opt. Instr. Eng. 241, 11-19(1980).

37. ———. "Electronic SAR Processors for Space Missions", Proceedings of the 1978 Synthetic Aperture Radar Technology Conference, New Mexico State University, Las Cruces, N.M., paper V-3.

38. Wu, C., et al. "SEASAT Synthetic-Aperture Radar Data Reduction Using Parallel Programmable Array Processors", IEEE Trans. on Geoscience and Remote Sensing, vol. GE-20, no. 3, pp. 352-358, July 1982.

39. Wu, C., K. Y. Lu and M. Jin. "Modeling and a Correlation Algorithm for Spaceborne SAR Signals", IEEE Trans. on Aerospace and Electronic Systems, vol. AES-18, no. 5, pp. 563-574, September 1982.

APPENDIX A - DEFINITION OF DATA WINDOWS

The following window definitions are taken from the survey paper by Harris [16].

Rectangle - $w(n) = 1.0$, $n = 0 , 1 , 2 \ldots N - 1$

Hamming - $w(n) = 0.54 - 0.46 \cos\{2\pi n/N\}$,
$n = 0 , 1 , 2 \ldots N - 1$

Blackman-Harris

$w(n) = a_0 - a_1 \cdot \cos\{2\pi n/N\} + a_2 \cdot \cos\{4\pi n/N\} - a_3 \cdot \cos\{6\pi n/N\}$,
$n = 0 , 1 , 2 \ldots N - 1$

	Min 3-Term	3-Term	Min 4-Term	4-Term
a_0	0.42323	0.44959	0.35875	0.40217
a_1	0.49755	0.49364	0.48829	0.49703
a_2	0.07922	0.05677	0.14128	0.09392
a_3	0.0	0.0	0.01168	0.00183

4-sample Kaiser-Bessel

For $\alpha = 3.0$, use Blackman-Harris window with the following coefficients: $a_0 = 0.40243$
$a_1 = 0.49804$
$a_2 = 0.09831$
$a_3 = 0.00122$

Exact Blackman

Use Blackman-Harris window, with the following coefficients:

$$a_0 = \frac{7938}{18608} \doteq 0.42659071$$

$$a_1 = \frac{9240}{18608} \doteq 0.49656062$$

$$a_2 = \frac{1430}{18608} \doteq 0.07684867$$

$$a_3 = 0.0$$

Blackman

Use Blackman-Harris window with the following coefficients:

$a_0 = 0.42$
$a_1 = 0.50$
$a_2 = 0.08$
$a_3 = 0.0$

Gaussian - $w(n) = \exp\{-2(\alpha n/N)^2\}$

Kaiser-Bessel

$$w(n) = \frac{I_0\{\pi\alpha \ \mathrm{SQRT}\{1.0 - 4(n/N)^2\}\}}{I_0\{\pi\alpha\}}, \quad 0 \le n \le N/2$$

where I_0 is the zero-order modified Bessel function of the first kind.

Dolph-Chebyshev

$$W(k) = \frac{\cos\{N \cos^{-1}\{\beta \cos\{\pi k/N\}\}\}}{\cosh\{N \cosh^{-1}\{\beta\}\}}$$

where $\beta = \cosh\{\cosh^{-1}\{10^{\alpha}\}/N\}$

For the time-domain samples w(n), perform an inverse DFT on the samples W(k) and scale appropriately.[15]

[15] Harris [16] specifies that a DFT be performed to obtain Dolph-Chebyshev window coefficients. Actual computation showed this to be in error. Results were confirmed by consulting the original paper by Helms [18].

Barcilon-Temes

$$W(k) = \frac{A\cos\{y\{k\}\} + B(y\{k\}\sin\{y\{k\}\}/C)}{(C + AB)((y\{k\}/C)^2 + 1.0)}$$

where $A = \sinh\{C\}$

$B = \cosh\{C\}$

$C = \cosh^{-1}\{10^{a}\}$

$\beta = \cosh\{C/N\}$

$y\{k\} = N\cos^{-1}\{\beta\cos\{\pi k/N\}\}$

For the time-domain samples, w(n), perform a DFT on the samples W(k) and scale appropriately.[16]

---

[16] Harris [16] specifies that an inverse DFT be performed to obtain Barcilon-Temes window coefficients. Actual computation showed this to be in error. Results were confirmed by consulting the original paper by Barcilon and Temes [2].

APPENDIX B - SYMBOLS AND ACRONYMS USED

a = coarse resolution aperture number

B = Bandwidth of signal

BPF SPECAN = BandPass Filter SPECtral ANalysis

cmpp = complex multiplies per point

cmps = complex multiplies per second

CP = Number of computations per point

Δ = Sampling period = $1/F$

η = Azimuth time variable relative to zero Doppler line

η_{BX} = Azimuth time variable relative to beam-centre crossing

η_0 = Azimuth time offset of beam centre from zero Doppler

F = Pulse repetition frequency

H = Frequency step between coarse resolution apertures in FFT output bins

$j^2 = -1$

K = Azimuth FM rate

L = Number of looks

λ = Radar wavelength

M = Number of samples in signal aperture

N = Time displacement between successive coarse resolution apertures in samples

PRF = Pulse Repetition Frequency

QRCM = Quadratic component of RCM

RCM = Range Cell Migration

RCMC = Range Cell Migration Correction

r_0 = Slant range at closest approach

SAR = Synthetic Aperture Radar

SPECAN = SPECtral ANalysis

SQRT{x} = the square root of x

T = Time extent of SAR signal in azimuth direction

T' = Time extent of coarse resolution aperture

V = Velocity of radar platform

W = Width of main lobe of window

W_1 = Data window for coarse resolution aperture

W_2 = Data window for fine resolution aperture

APPENDIX C - RADAR PARAMETERS

System Parameters at Maximum Slant Range

System Parameters	Units	SEASAT	JPL Nominal	COMSS/LASS
Maximum slant range of closest approach - r_o	km	860	550	636
Pulse repetition frequency - F	Hz	1647	2600	1650
Wavelength - λ	m	0.235	0.235	0.057
Slant range cell width - ρ	m	6.59	10.43	5.73
Effective platform velocity - V	m/s	7170	7600	6800
Azimuth FM rate (at max. r_o) - K	Hz/s	508	894	2550
Time period - T of signal - T/Δ	s samples	3.24 5330	2.90 7540	0.65 1081
Extent of QRCM	m range cells	78.4 11.9	110.4 10.6	3.84 0.67

Adjusted System Parameters and Step Transform Processing Parameters

System Parameters	Units	SEASAT	JPL Nominal	COMSS/LASS
Azimuth FM rate - K	Hz/s	517	911	2659
Time period of signal - T	s	3.19	2.86	0.62
- T/Δ	samples	5248	7424	1024
Slant range of closest approach - r_0	km	846	540	610
Processing Parameters				
Coarse resolution aperture - T'	s	0.0783	0.0493	0.0338
- T'/Δ	samples	128	128	64
Time between coarse resolution apertures - NΔ	s	0.0249	0.0223	0.0097
- N	samples	41	58	16
Overlap ratio - T'/NΔ		3.12	2.21	4.00
Coarse resolution aperture data window - W_1		Kaiser-Bessel a=2.5	Dolph-Chebyshev a=2.0	Kaiser-Bessel a=3.5
Guardband - β		0.15	0.15	0.15
No. of samples rejected		20	20	10
Bandwidth of processed signal	Hz	1390	2194	1392
Frequency stepping of apertures - H		1	1	1
Fine resolution aperture - T'/ΔH	samples	128	128	64

APPENDIX D - COMPUTER SIMULATION OF THE STEP TRANSFORM

The program is written in FORTRAN IV and uses single precision arithmetic. Source code for each subroutine is stored in a separate file named as follows: routine.fs. The program is run by using the following MTS command:

```
$RUN STEPTRAN 1=outputfile
```

or

```
$RUN STEPTRAN+*IG 1=outputfile
```

(the latter if output of filter is to be plotted on the terminal).

Initially the user controlled parameters are set to some arbitrary values. The user is then prompted to enter a parameter name from a list of possible choices and is given the opportunity to change the value of that parameter. If a name is spelled wrong, the user is requested to re-enter the name. This process continues until the user types a carriage return only, which indicates that all parameters are set to the user's satisfaction. Step transform processing is then performed. When processing is completed, a plot of the output may appear on the screen, depending on the value of the parameter YESPLT. The user can manipulate the plot by entering IG commands. When this portion of the processing has been completed, the user is asked if another run is to be performed. If the answer is affirmative, changes to parameter values are again requested. At this stage, the parameter values are set to the values to which they had been changed for the previous run.

Parameter names, types and meanings are specified in the accompanying table at the end of the appendix. The parameter values are passed to the appropriate subroutines in which they are used by the use of named COMMON blocks.

The major procedural subdivisions of the program are the following subroutines:

MAIN - the main procedure of the program. It declares the major data structures and initializes them. Subroutines INIT, PARAM, STEPT and DATAM are called.

INIT - sets initial values of parameters which are user controlled. This subroutine is usually written so that parameter values correspond to the particular SAR system being studied. All named common blocks are used in this routine.

PARAM - controls user selection of parameter values. All named common blocks are used in this routine.

STEPT - oversees step transform data processing. It calculates the processing parameters not directly controlled by the user, such as the length of the fine resolution FFT, the frequency steps between coarse resolution output pulses,

and recalculates the spacing of the coarse resolution apertures, taking into consideration the user requested value. It calls FORMST, MULT, FFT1, ORDER and FFT2.

FORMST - forms the target return signal (with antenna profile as requested) and reference function (with coarse resolution aperture window as requested). It calls WINDOW.

MULT - performs multiplication of target return by reference function.

FFT1 - performs coarse resolution FFT operation, quadratic phase correction, clearing of guardband data.

ORDER - reorders coarse resolution FFT output data into fine resolution apertures.

FFT2 - performs fine resolution FFT operation on 10 apertures surrounding the pulse peak. Look summation, data selection and output scaling are also performed. It calls WINDOW.

DATAM - converts filter data to real values. It determines the position of the peak of the output pulse and interpolates the data to determine the 3 dB width. A plot is produced if specified by the user.

WINDOW - performs a window operation on complex data passed to it in an array. The data window to be used is also passed as a parameter.

The major data structures used are as follows:

SIGNAL - complex array of 32000 elements. FORMST uses this data structure to store the initial target return signal. ORDER uses it to store the fine resolution apertures.

UNORD - complex array of 32000 elements. The output of the multiply operation is stored in this array and the coarse resolution FFT's and associated processing are performed in-place in this data structure.

FILTER - complex array of 512 elements used to store the reference ramp.

PDATA, XDATA - real arrays of 8192 elements used to store the y- and x-coordinates respectively of the filter output. They are used mainly for interpolation and plotting of the output function.

Data Output Parameters

Parameter Name	Type and Range of Values	Meaning
PLTWDH	Integer	Specifies the number of abscissae values around the peak of the output pulse which are to be plotted.
POUT	Logical T or F	If TRUE, final output data from filter is printed on unit 1.
PRINT0	Logical T or F	If TRUE, output data from multiply operation is printed on unit 1.
PRINT1	Logical T or F	If TRUE, output data from coarse resolution FFT's is printed on unit 1.
PRINT2	Logical T or F	If TRUE, output data from reordering operation, i.e. input data to fine resolution FFT's is printed on unit 1.
PRINT3	Logical T or F	If TRUE, output data from fine resolution FFT's is printed on unit 1.
PRNTER	Logical T or F	Controls values of PRINT0, PRINT1, PRINT2, PRINT3, and POUT. If FALSE, none of above may be set to TRUE.
TENSHN	Real ≥ 0.	Specifies tension parameters for interpolation of final output. 0. = cubic spline interpolation 0.+ = mixed exponential interpolation (almost polygonal for large values)
YESPLT	Logical T or F	If TRUE, plot is produced - on screen if *IG is concatenated to $RUN command - in unit 9 if *IG is not used

SAR System and Processing Parameters

Parameter Name	Type and Range of Values	Meaning
ACCURA	Power of 2 ≥ 1	Specifies factor by which fine resolution FFT's are expanded for data interpolation.
ALPHA1	Real > 0.	Specifies value of parameter α for appropriate coarse resolution aperture windows.
ALPHA2	Real > 0.	Specifies value of parameter α for appropriate fine resolution aperture windows.
FFTCNT	Integer > 0	Specifies point in first fine resolution FFT at which data selection is to start. Value is determined empirically.
GUARD	Real 0.-1.	Specifies guardband, β, or amount of rejected data from coarse resolution FFT's. Number of points zeroed at each end of FFT is GUARD*REFWID/2 + 0.5
NLOOKS	Integer	Specifies number of looks.
RATERR	Real	Specifies percentage rate error to be used in formation of target return signal.
REFWID	Power of 2 < 512	Specifies number of samples in reference ramp.
SRATE	Real	Specifies factor by which target return is oversampled.
START	Integer |START| ≤ 1000	Specifies position of target return pulse.
STPSIZ	Integer	Specifies sample spacing between successive coarse resolution apertures.

SAR System and Processing Parameters (cont.)

Parameter Name	Type and Range of Values	Meaning
SYSTEM	Integer	Specifies antenna profile to be used on target return signal. 1 = SEASAT 2 = JPL Nominal 3 = COMSS/LASS For all other values, no profile is applied.
WIDTH	Integer ≤ 8000	Specifies number of samples in target return pulse.
WIND1	Integer	Specifies type of window used on coarse resolution aperture.
WIND2	Integer	Specifies type of window used on fine resolution aperture.